UNIVERSITAT POLITÈCNICA DE VALÈNCIA

Improved Spectrum Usage with Multi-RF Channel Aggregation Technologies for the Next-Generation Terrestrial Broadcasting

Departamento de Comunicaciones
Universitat Politècnica de València

A thesis for the degree of
PhD in Telecommunications Engineering
Valencia, June 2015

Author:
Jordi Joan Giménez Gandia

Supervisors:
Dr. David Gómez Barquero
Prof. Narcís Cardona Marcet

Abstract

Next-generation terrestrial broadcasting targets at enhancing spectral efficiency to overcome the challenges derived from the spectrum shortage as a result of the progressive allocation of frequencies – the so-called *Digital Dividend* – to satisfy the growing demands for wireless broadband capacity. Advances in both transmission and video coding technologies are paramount to enable the progressive roll-out of high video quality services such as HDTV (High Definition Televison) or Ultra HDTV. The transition to the second generation European terrestrial standard DVB-T2 and the introduction of MPEG-4/AVC video coding already enables the transmission of 4-5 HDTV services per RF (Radio Frequency) channel. However, the impossibility to allocate higher bit-rate within the remaining spectrum could jeopardize the evolution of the DTT platforms in favour of other high-capacity systems such as the satellite or cable distribution platforms. Next steps are focused on the deployment of the High Efficiency Video Coding (HEVC) standard, which provides up to 50% coding gain with respect to AVC, with the next-generation terrestrial transmission standards. This could ensure the competitiveness of the DTT.

Broadcasting standardization bodies are planning the technical evolution of the standards. The North American standard ATSC (Advanced Television Systems Committee) is being evolved to the ATSC 3.0 standard. DVB is also evaluating the convenience of an evolution beyond DVB-T2. The proposed techniques in this fora focus on shortening the gap to Shannon limit through more efficient modulation and coding schemes, the combined provision of fixed and mobile services, the introduction of spatial diversity, or the aggregation of the capacity of multiple RF channels, among others.

This dissertation addresses the use of multi-RF channel aggregation technologies to increase the spectral efficiency of future DTT networks. The core of the Thesis are two technologies: *Time Frequency Slicing (TFS)* and *Channel Bonding (CB)*. TFS and CB consist in the transmission of the data of a TV service across multiple RF channels instead of using a single channel. CB spreads data of a service over multiple classical RF channels (RF-Mux). TFS spreads

the data by time-slicing (slot-by-slot) across multiple RF channels which are sequentially recovered at the receiver by frequency hopping. Transmissions using these features can benefit from capacity and coverage gains. The first one comes from a more efficient statistical multiplexing (StatMux) for Variable Bit Rate (VBR) services due to a StatMux pool over a higher number of services. Furthermore, CB allows increasing service data rate with the number of bonded RF channels and also advantages when combined with SVC (Scalable Video Coding). The coverage gain comes from the increased RF performance due to the reception of the data of a service from different RF channels rather that a single one that could be, potentially, degraded. Robustness against interferences is also improved since the received signal does not depend on a unique potentially interfered RF channel.

TFS was firstly introduced as an informative annex in DVB-T2 (not normative) and adopted in DVB-NGH (Next Generation Handheld). TFS and CB are proposed for inclusion in ATSC 3.0. However, they have never been implemented. The investigations carried out in this dissertation employ an information-theoretical approach to obtain their upper bounds, physical layer simulations to evaluate the performance in real systems and the analysis of field measurements that approach realistic conditions of the network deployments. The analysis report coverage gains about 4-5 dB with 4 RF channels and high capacity gains already with 2 RF channels.

The improved RF performance could be translated into a network planning gain by means of the combined effect of a tighter frequency reuse and a modified capacity per RF channel. As discussed in this Thesis, this effect can also be enhanced by the introduction of Advanced Network Planning (ANP) strategies within the existing network topologies. The results indicate the feasibility to retain a similar number of RF channels within the remaining spectrum after the 700 MHz digital dividend by the reduction of the frequency reuse factor from 7 to 4.

This dissertation also focuses on implementation aspects. Channel bonding receivers require one tuner per bonded RF channel. The implementation of TFS with a single tuner demands the fulfilment of several timing requirements. However, the use of just two tuners would still allow for a good performance with a cost-effective implementation or the sharing of existing architectures with dual tuner operation such as MIMO (Multiple Input Multiple Output).

The implementation of multi-RF channel aggregation technologies would provide next-generation DTT systems with a spectrum flexibility capability unprecedented in any DTT technology.

Resumen

La televisión digital terrestre (TDT) de última generación está orientada a una necesaria mejora de la eficiencia espectral con el fin de abordar los desafíos derivados de la escasez de espectro como resultado de la progresiva asignación de frecuencias – el llamado *Dividendo Digital* – para satisfacer la creciente demanda de capacidad para la banda ancha inalámbrica. Los avances tanto en los estándares de transmisión como de codificación de vídeo son de suma importancia para la progresiva puesta en marcha de servicios de alta calidad como la televisión de Ultra AD (Alta Definición). La transición al estándar europeo de segunda generación DVB-T2 y la introducción de la codificación de vídeo MPEG-4/AVC ya permite la transmisión de 4-5 servicios de televisión de AD por canal RF (Radiofrecuencia). Sin embargo, la imposibilidad de asignar una mayor tasa de bit sobre el espectro restante podría poner en peligro la evolución de las plataformas de TDT en favor de otros sistemas de alta capacidad tales como el satélite o las distribuidoras de cable. El siguiente paso se centra en el despliegue del reciente estándar HEVC (High Efficiency Video Coding), que ofrece un 50 % de ganancia de codificación con respecto a AVC, junto con los estándares terrestres de próxima generación, lo que podría garantizar la competitividad de la TDT en un futuro cercano.

Los foros de estandarización ya están planeando la evolución de sus normas. El ATSC (Advanced Television Systems Committee) americano se encuentra desarrollando el ATSC 3.0. DVB también está evaluando la conveniencia de una evolución más allá de DVB-T2. Las técnicas propuestas se centran en acortar la brecha al límite de Shannon a través de esquemas de codificación y modulación más eficientes, la transmision conjunta de servicios fijos y móviles, la introducción de diversidad espacial, o la agregación de múltiples canales RF.

Esta tesis aborda el uso de tecnologías de agregación de canales RF que permitan incrementar la eficiencia espectral de las futuras redes. La tesis se centra en torno a dos tecnologías: emph Time Frequency Slicing (TFS) y emph Channel Bonding (CB). TFS y CB consisten en la transmisión de los datos de un servicio de televisión a través de múltiples canales RF en lugar de utilizar

un solo canal. CB difunde los datos de un servicio a través de varios canales RF convencionales formando un RF-Mux. TFS difunde los datos a través de ranuras temporales en diferentes canales RF. Los datos son recuperados de forma secuencial en el receptor mediante saltos en frecuencia. La implementación de estas técnicas permite obtener ganancias en capacidad y cobertura. La primera de ellas proviene de una multiplexación estadística (StatMux) de servicios de tasa variable (VBR) más eficiente. Además, CB permite aumentar la tasa de pico de un servicio de forma proporcional al número de canales así como ventajas al combinarla con codificación de vídeo escalable. La ganancia en cobertura proviene de un mejor rendimiento RF debido a la recepción de los datos de un servicio desde diferentes canales en lugar uno sólo que podría estar degradado. Del mismo modo, es posible obtener una mayor robustez frente a interferencias ya que la recepción o no de un servicio no depende de si el canal que lo alberga está o no interferido.

TFS fue introducido en primer lugar como un anexo informativo en DVB-T2 (no normativo) y posteriormente fue adoptado en DVB-NGH (Next Generation Handheld). TFS y CB han sido propuestos para su inclusión en ATSC 3.0. Aún así, nunca han sido implementados. Las investigaciones llevadas a cabo en esta Tesis emplean diversos enfoques basados en teoría de la información para obtener los límites de ganancia, en simulaciones de capa física para evaluar el rendimiento en sistemas reales y en el análisis de medidas de campo. Estos estudios reportan ganancias en cobertura en torno a 4-5 dB con 4 canales e importantes ganancias en capacidad aún con sólo 2 canales RF.

Estas mejoras podrían traducirse en una ganancia en planificación de red por medio del efecto combinado de un reuso de frecuencias más estrecho y una capacidad por canal adecuada. Como se discute en esta Tesis, este efecto puede verse amplificado con la introducción de estrategias de planificación de red avanzadas (ANP) sobre las topologías de red existentes. Los resultados indican que es factible retener un número similar de canales RF en el espectro que queda libre tras la liberación de la banda de 700 MHz con una reducción del factor de reuso de frecuencias de 7 a 4.

Esta tesis también se centra en los aspectos de implementación. Los receptores para CB requieren un sintonizador por canal RF agregado. La implementación de TFS con un solo sintonizador exige el cumplimiento de requisitos temporales. Sin embargo, el uso de dos sintonizadores permitiría un buen rendimiento con una implementación más rentable o su introducción junto con las arquitecturas existentes que operan con un doble sintonizador tales como MIMO (Multiple Input Multiple Output).

La aplicación de tecnologías de agregación de canales RF proporcionaría a los sistemas de TDT de última generación de unas capacidades y una flexibilidad espectral sin precedentes en tecnologías de TDT.

Resum

La televisió digital terrestre (TDT) d'última generació està orientada a una necessària millora de l'eficiència espectral a fi d'abordar els desafiaments derivats de l'escassetat d'espectre com a resultat de la progressiva assignació de freqüències – l'anomenat *Dividend Digital* – per a satisfer la creixent demanda de capacitat per a la banda ampla sense fil. Els avanços tant en els estàndards de transmissió com de codificació de vídeo són de la màxima importància per a la progressiva posada en marxa de serveis d'alta qualitat com la televisió d'Ultra AD (Alta Definició). La transició a l'estàndard europeu de segona generació DVB-T2 i la introducció de la codificació de vídeo MPEG-4/AVC ja permet la transmissió de 4-5 serveis de televisió d'AD per canal RF (Radiofreqüència). No obstant això, la impossibilitat d'assignar una major taxa de bit sobre l'espectre restant podria posar en perill l'evolució de les plataformes de TDT en favor d'altres sistemes d'alta capacitat com ara el satèlÂ·lit o les distribuïdores de cable. El següent pas se centra en el desplegament del recent estàndard HEVC (High Efficiency Vídeo Coding), que oferix un 50 % de guany de codificació respecte a AVC, junt amb els estàndards terrestres de pròxima generació, la qual cosa podria garantir la competitivitat de la TDT en un futur pròxim.

Els fòrums d'estandardització ja estan planejant l'evolució de les seues normes. L'ATSC (Advanced Televisió Systems Committee) americà es troba desenvolupant l'ATSC 3.0. DVB també està avaluant la conveniència d'una evolució més enllà de DVB-T2. Les tècniques propostes se centren a acurtar la bretxa al límit de Shannon a través d'esquemes de codificació i modulació més eficients, la transmissió conjunta de serveis fixos i mòbils, la introducció de diversitat espacial, o l'agregació de múltiples canals RF.

Aquesta tesi aborda l'ús de tecnologies d'agregació de canals RF que permeten incrementar l'eficiència espectral de les futures xarxes. La tesi se centra entorn de dues tecnologies: *Time Frequency Slicing (TFS)* i *Channel Bonding (CB)*. TFS i CB consistixen en la transmissió de les dades d'un servei de televisió a través de múltiples canals RF en compte d'utilitzar un sol canal. CB difon

les dades d'un servei a través d'uns quants canals RF convencionals formant un RF-Mux. TFS difon les dades a través de ranures temporals en diferents canals RF. Les dades són recuperades de forma seqüencial en el receptor per mitjà de salts en freqüència. La implementació d'aquestes tècniques permet obtindre guanys en capacitat i cobertura. La primera d'elles prové d'una multiplexació estadística (StatMux) de serveis de taxa variable (VBR) més eficient. A més, CB permet augmentar la taxa de pic d'un servei de forma proporcional al nombre de canals així com avantatges al combinar-la amb codificació de vídeo escalable. El guany en cobertura prové d'un millor rendiment RF a causa de la recepció de les dades d'un servei des de diferents canals en lloc de només un que podria estar degradat. De la mateixa manera, és possible obtindre una major robustesa enfront d'interferències ja que la recepció o no d'un servei no depén de si el canal que l'allotja està o no interferit.

TFS va ser introduït en primer lloc com un annex informatiu en DVB-T2 (no normatiu) i posteriorment va ser adoptat en DVB-NGH (Next Generation Handheld). TFS i CB han sigut proposades per a la seva inclusió en ATSC 3.0. Encara així, mai han sigut implementades. Les investigacions dutes a terme en esta Tesi empren diverses vessants basades en teoria de la informació per a obtindre els límits de guany, en simulacions de capa física per a avaluar el rendiment en sistemes reals i en l'anàlisi de mesures de camp. Aquestos estudis reporten guanys en cobertura entorn als 4-5 dB amb 4 canals i importants guanys en capacitat encara amb només 2 canals RF.

Aquestes millores podrien traduir-se en un guany en planificació de xarxa per mitjà de l'efecte combinat d'un reús de freqüències més estret i una capacitat per canal adequada. Com es discutix en esta Tesi, este efecte pot veure's amplificat amb la introducció d'estratègies de planificació de xarxa avançades (ANP) sobre les topologies de xarxa existents. Els resultats indiquen que és factible retindre un nombre semblant de canals RF en l'espectre que queda lliure després de l'alliberament de la banda de 700 MHz amb una reducció del factor de reús de freqüències de 7 a 4.

Esta tesi també se centra en els aspectes d'implementació. Els receptors per a CB requerixen un sintonitzador per canal RF agregat. La implementació de TFS amb un sol sintonitzador exigix el compliment de diversos requisits temporals. No obstant això, l'ús de dos sintonitzadors permetria un bon rendiment amb una implementació més rendible o la seua introducció junt amb les arquitectures existents que operen amb un doble sintonitzador com ara MIMO (Multiple Input Multiple Output).

L'aplicació de tecnologies d'agregació de canals RF proporcionaria als sistemes de TDT d'última generació d'unes capacitats i una flexibilitat espectral sense precedents en tecnologies de TDT.

Acknowledgements

I would like with these few lines to express my gratitude to those who made this thesis possible.

First and foremost, I offer my sincerest gratitude to my supervisors, Dr. David Gómez Barquero and Prof. Narcís Cardona, for their guidance, support and motivation. I really appreciate their dedication and commitment along these years and for giving me the opportunity to conduct this thesis within their research group.

It is also my pleasure to thank Erik Stare and Staffan Bergsmark from Teracom for inviting me to visit their company, for all the valuable discussions on TFS and terrestrial broadcasting and the support received during my two stays in Sweden. Thanks also to Prof. Jens Zander and Dr. Ki Won Sung for the opportunity they gave me to work within their great team at Kungliga Tekniska Högskolan (KTH).

I am very grateful to Dr. Roland Brugger from the Institut für Rundfunktechnik (IRT) and Dr. Javier Morgade from the Fraunhofer Institute for Integrated circuits (IIS) for serving as reviewers of this thesis. Special thanks also to Dr. Yiyan Wu from the Communications Research Center (CRC) for serving as reviewer of this thesis and for acting as member of the committee. I thank Prof. Pablo Angueira and Prof. Alberto González for also being members of the committee. I really appreciate the time they dedicated to review this thesis.

I would like to thank all the people at the Mobile Communications Group (MCG) of the Institute of Telecommunications and Multimedia Applications (iTEAM) with whom I shared my working days: David Vargas, Edu, Manuel, Charlie, Gerardo, Damián Ruiz, Conchi, Josetxo, Jorge, Sonia, Miguel, Tere, Juanan, Irene, Alicia, Carlos, Alejandro, Dani, Sandra and many others. A special mention also to David Gozálvez and Jaime López.

I finalment, i no per això menys important sinó més bé tot el contrari, voldria donar les gràcies als meus pares, Juanfa i Conxa, pel seu recolzament incondicional al llarg de tots aquestos anys d'intensa feina.

ACKNOWLEDGEMENTS

Contents

List of Abbreviations

2DRC Two-Dimensional Rotated Constellations

4DRC Four-Dimensional Rotated Constellations

ANP Advanced Network Planning

ATSC Advanced Television Systems Committee

AWGN Additive White Gaussian Noise

BCH Bose Chadhuri Hocquenghem

BI Block Interleaving

BICM Bit Interleaved Coded Modulation

bps bits per second

CBR Constant Bit Rate

CCI co-channel interference

CDF Cumulative Distribution Function

CI Convolutional Interleaving

CNR Carrier to Noise Ratio

COFDM Coded Orthogonal Frequency-Division Multiplexing

DDS Direct Digital Synthesizer

DAB Digital Audio Broadcasting

DTMB Digital Terrestrial Multimedia Broadcast

DTT Digital Terrestrial TV

DVB Digital Video Broadcasting

DVB-H Digital Video Broadcasting (DVB) – Handheld

DVB-NGH DVB – Next Generation Handheld

DVB-T DVB – Terrestrial

DVB-T2 DVB – Terrestrial 2^{nd} Generation

ERP Effective Radiated Power

EPG Electronic Program Guide

FEC Forward Error Correction

FER Frame Error Rate

FI frequency interleaving

GE06 Geneva Plan 2006

GI Guard Interval

HDTV High Definition TV

HEVC High Efficiency Video Coding

HPHT High-Power High-Tower

ICI Inter-Carrier Interference

IMT International Mobile Telecommunications

ISDB-T Integrated Services Digital Broadcasting - Terrestrial

ISI Inter-Symbol Interference

ITU International Telecommunications Union

LDM Layer Division Multiplexing

LDPC Low Density Parity Check

LoS Line-of-Sight

LPLT Low-Power Low-Tower

LTE Long Term Evolution

pdf probability density function

MAP Maximum A Posteriori

MFN Multiple Frequency Network

MFRP Multiple Frequency Reuse Patterns

MIMO Multiple-Input Multiple-Output

MODCOD Modulation and Coding

MPN Mixed Polarization Network

NSE Network Spectral Efficiency

OFDM Orthogonal Frequency-Division Multiplexing

PLP Physical Layer Pipe

PP Pilot Pattern

PVR Personal Video Recorder

QAM Quadrature Amplitude Modulation

RC Rotated Constellations

RF Radio Frequency

SDTV Standard Definition TV

SFN Single Frequency Network

SHVC Scalable High Efficiency Video Coding

SISO Single-Input Single-Output

SNR Signal to Noise Ratio

SSD Signal-Space Diversity

StatMux Statistical Multiplexing

TDM Time Division Multiplexing

T-DMB Terrestrial - Digital Multimedia Broadcasting

TFS Time Frequency Slicing

TI Time Interleaving

UHDTV Ultra-High Definition TV

UHF Ultra High Frequency

UWB Ultra Wide Band

VBR Variable Bit Rate

VHF Very High Frequency

WRC12 World Radiocommunications Conference 2012

XPD Cross Polarization Discrimination

Chapter 1

Introduction

1.1 The Evolution towards Next-Generation Terrestrial Broadcasting

Digital Terrestrial TV (DTT) has experienced a big success during the last 15 years. DTT has been designed for the efficient delivery of video and audio content to mass audiences by means of point-to-multipoint transmission. This system can provide a wide range of services without any limitation in the number of viewers [1]. DTT is the main TV platform in the majority of the European markets (43% of European households receive terrestrial TV) [2]. Worldwide, many countries have developed DTT networks to replace the former analogue TV systems. The DTT platform has held a privileged position for years since it allows the cost-effective transmission of multiple TV services over the same spectrum resource needed to deliver a single program in analogue TV. Moreover, the reuse of existing analogue infrastructure (e.g. aerials already installed in many households) ensures a rapid penetration of this technology. DTT also permits to provide high video and audio quality as well as the delivery of value-added services such as an Electronic Program Guide (EPG) or interactive services, subtitles or multi-lingual audio tracks.

Several broadcast technologies are in place around the world to provide DTT services: the Advanced Television Systems Committee (ATSC) in the United States of America, the Integrated Services Digital Broadcasting - Terrestrial (ISDB-T) in Japan, the Terrestrial - Digital Multimedia Broadcasting (T-DMB) in South Korea, the Digital Terrestrial Multimedia Broadcast (DTMB) in China, or the DVB family of standards in Europe. DVB – Terrestrial (DVB-T) has become the most widely adopted DTT standard in the world

since it provides a wide set of configuration parameters that can be optimized according to specific network and transmission requirements providing payload capacities ranging around 4 to 30 Mbps [3]. Though the main standards, including DVB-T, are based on the multi-carrier Orthogonal Frequency-Division Multiplexing (OFDM) modulation [3], ATSC relies on a single-carrier modulation that enables a unique configuration that provides 19 Mbps. However, these standards are still far from the theoretical Shannon capacity limit[1] so that further development is possible.

The second generation of DTT standards reaches its greatest exponent with DVB – Terrestrial 2^{nd} Generation (DVB-T2) [5]. DVB-T2 outperforms DVB-T spectral efficiency by 50%, expands the set of configuration parameters and provides advanced coding and modulation techniques. To date, DVB-T2 has been adopted or trialled in many countries in Europe, Asia and Africa. DVB-T2 is also based on OFDM and introduces, among other advancements, Low Density Parity Check (LDPC) combined with Bose Chadhuri Hocquenghem (BCH) error correction coding offering a very robust signal, the concept of Multiple Physical Layer Pipes which confers service-specific capacity and robustness, and extended interleaving by means of cell, time and frequency interleavers to increase signal robustness. Rotated Constellations (RC) is also a distinctive technique of DVB-T2 which exploits the concept of Signal-Space Diversity (SSD) to improve the robustness of the signal against the loss of data [6]. A novel technique known as Time Frequency Slicing (TFS) is also introduced in the DVB-T2 specification as an informative annex (i.e. not mandatory). This technique breaks with the existing concept of transmitting services by means of isolated Radio Frequency (RF) channels and opens the door to the multiple aggregation of RF channels into a high-capacity multiplex that could potentially exploit capacity gains and enhanced frequency diversity.

Although the evolution of the DTT standards has mainly been addressed to provide high capacity for fixed roof-top reception, standardization bodies have also progressed on the development of mobile broadcast systems to expand the market niche of the DTT [7]. Although the lack of a strong market and the required investment to update current networks have hindered the deployment of such systems, DVB – Next Generation Handheld (DVB-NGH) is the state-of-the-art standard providing the most advanced transmission techniques to cope with the transmission characteristics of the mobile channel [8]. Some of the most relevant techniques included in this standard are Multiple-Input Multiple-Output (MIMO), which is used to transmit two signals from different antennas at the same time using the existing frequency resource, and TFS, which was adopted as a way to increase the robustness of the signal against the

[1]Shannon capacity determines the theoretical maximum information transfer rate in a channel for a given noise level [4].

degradation of some RF channels and to cope with the lack of enough time diversity for slow time-varying channels. Although not yet deployed, DVB-NGH provides an extensive tool-box which can be the basis of new standards.

The development of the DTT standards is focused towards increasing spectral efficiency by closing the gap to Shannon limit and enabling a more efficient network planning. On the one hand, the implementation and transition to DTT provides improved co-channel interference (CCI) and adjacent channel interference (ACI) performance which permits. On the other hand, it enables the deployment of Single Frequency Networks (SFNs) [9], where adjacent transmitters can deliver the same signal using the same frequency. TV services are packed in multiplexes and transmitted over single RF channels. The use of several RF channels (one per multiplex) per station allows the delivery of the complete service offering. DVB-T, using MPEG-2 video coding, allowed the transmission of about 4 to 7 Standard Definition TV (SDTV) services per multiplex using about 20 to 24 Mbps for fixed roof-top reception conditions. The evolution of video coding standards and the demand for high quality services allowed the launch of High Definition TV (HDTV) using MPEG-4/AVC (Advanced Video Coding), which provides more than 50% coding gain with respect to MPEG-2. DVB-T2 with MPEG-4/AVC enables the transmission of 4-5 HDTV services using about 36-40 Mbps. The joint evolution of transmission and video coding standards permits the improvement of video quality while retaining a similar number of services in the DTT platform.

The spectral efficiency increase offered by DTT attracts emerging technologies such as International Mobile Telecommunications (IMT) to request part of the DTT spectrum surplus. The International Telecommunications Union (ITU) reached a decision to release frequencies allocated to the broadcast service (the so-called *digital dividend* [10]). Terrestrial broadcasting service has traditionally been allocated in the Ultra High Frequency (UHF) and Very High Frequency (VHF) bands. The range of frequencies and channelization differs depending on each ITU Region[2]. Table 1.1 shows the ranges of frequencies assigned to DTT in each ITU region.

The first digital dividend affects the 800 MHz band (790-862 MHz) in ITU Region 1, and the 700 MHz band (698-806 MHz) in ITU Regions 2 and 3. The major beneficiary of these regulatory policies is IMT in its goal to satiate the demand for mobile data. Mobile communications data demand will dramatically increase in the next years [11, 12], requiring more spectrum. Broadcast bands are specially optimum for these services due to their excellent propagation conditions. In fact, the World Radiocommunications Conference 2012 (WRC12)

[2]In order to manage spectrum, ITU divides the world into three ITU regions. Region 1 comprises Europe, Africa, the Middle East and the north of Asia. Region 2 mainly covers the Americas. Region 3 covers the rest of Asia and most of Oceania.

Table 1.1: Frequency band allocated to terrestrial broadcasting services

Band	ITU Region 1	ITU Region 2	ITU Region 3
VHF Band III	174 - 230 MHz	174 - 216 MHz	174 - 230 MHz
UHF Band IV/V	470 - 790 MHz	470 - 694 MHz	470 - 790 MHz

already assigned the 700 MHz band (694-790 MHz) in Region 1 to broadcasting and IMT on a co-primary basis. This band is currently allocated on a co-primary basis in North America (Region 2) and Asia (Region 3) and selected for IMT in North America and in some countries of Region 3 [13, 14]. The WRC-15 will make a decision on the convenience of releasing the 700 MHz band (also known as the second digital dividend). In Europe, some countries (e.g., Sweden, Finland, France, United Kingdom or Germany) have already decided or announced their intentions to assign the band to IMT. The European Commission is also studying this point with a proposal to release the 700 MHz band by 2020 and guarantee regulatory stability for broadcasting in the band 470-694 MHz until 2030 [15].

A second digital dividend will reduce the amount of spectrum by 30% - more than the reduction by the first digital dividend. Under this situation, DTT needs to evolve towards new high-quality formats such as HDTV and even Ultra-High Definition TV (UHDTV) to remain competitive against other transmission media such as cable, satellite or fixed broadband that are able to provide a higher amount of services with a reduced cost. Note also that the traditional linear TV market is threatened by the changing viewer habits to IP-based service consumption and video-on-demand services. From the network perspective, the new situation of the spectrum may require an update of the inter-country frequency allocation. The Geneva Plan 2006 (GE06) defines the current frequency coordination between countries to guarantee an efficient use of the spectrum and minimize the interferences among stations using the same frequencies. This plan currently defines, in average, a frequency reuse factor of 7 [16]. The remaining spectrum after the second digital dividend will only keep 4 RF channels to be used per station, what seems to be a strong limitation.

Next-generation terrestrial broadcasting involves the use of new digital standards along with more efficient video coding standards that will guarantee an efficient use of the remaining DTT spectrum. High Efficiency Video Coding (HEVC) [17] is the new video coding standard which outperforms MPEG-4/AVC by up to 50% [18]. This will permit to move the complete offer to HDTV and later to UHDTV which will require a considerably big amount of spectrum. Broadcasting standardization bodies are already planning the technical evolu-

tion of the standards. The latest attempt has come from ATSC. DVB is also evaluating the convenience of an evolution beyond DVB-T2. The proposed techniques in this fora focus on shortening the gap to Shannon limit through more efficient modulation and coding schemes, the combined provision of fixed and mobile services, the introduction of spatial diversity, or the aggregation of the capacity of multiple RF channels, among others. This latter feature could allow for increasing spectrum flexibility as well as providing important gains in service data rate and signal robustness. The study and evaluation of the multi-RF channel aggregation are the core of this dissertation.

1.2 Problem Formulation

The needs for an efficient use of the broadcast spectrum requires the investigation of new technologies to guarantee an increased spectrum usage. The development of the next-generation DTT standards arises as a key opportunity to implement such new technical approaches. The aggregation of multiple RF channels into a high capacity multiplex could provide DTT with an unprecedented spectrum flexibility to allocate TV services in a DTT system. The concept of multi-RF channel aggregation is developed by *Time Frequency Slicing (TFS)* and *Channel Bonding (CB)*.

Both techniques consist in the transmission of the data of a TV service across multiple RF channels instead of using a single channel. TFS spreads the data by time-slicing (slot-by-slot) across multiple RF channels which are sequentially tuned at the receiver by frequency hopping. CB simply spreads service data over several RF channels which are directly tuned at the receiver (one tuner per RF channel).

A proper distribution of the service data across the RF channels potentially allows two main network gains:

- Improved RF performance. Spreading service data across multiple RF channels by inter-RF frequency interleaving (FI) improves frequency diversity beyond that achieved over a single RF channel. This confers increased robustness against eventually degraded RF channels due to propagation features or potential interferences.

- Capacity gain. An increased global capacity to allocate services allows for a more efficient statistical multiplexing (StatMux) for Variable Bit Rate (VBR) services due to a StatMux pool over a higher number of services. Furthermore, receiving multiple RF channels at the same time permits increasing service data rate with the number of bonded RF channels.

Additionally, these gains could be exploited to achieve a higher network spectrum efficiency by means of the combined effect of a tighter frequency reuse, due to the increased interference immunity and a modified capacity per RF channel.

TFS was firstly introduced as an informative annex in DVB-T2 (not normative) and adopted in DVB-NGH. CB has been adopted in ATSC 3.0. However, these techniques have never been implemented. Their potential network gains have not been either evaluated or measured due to the non-existence of real deployments. The bounds of these gains need to be assessed as well as their advantages to allocate high-demanding data rate services in the next-generation DTT. The further exploitation of such gains to allow an increased network spectral efficiency that could hypothetically reduce the necessary frequency reuse between stations also requires to be explored.

The implementation aspects of these technologies should be investigated from the point of view of transmitter and receiver sides. Whereas classical reception is performed by tuning the RF channel carrying the wanted services. Reception when there is more than one RF channel carrying service data could involve the necessity to allocate more than one tuner or a proper scheduling in order to use a single tuner, if feasible. The technical compatibility of these technologies with existing DTT network deployments and any additional requirements, if it is the case, also need to be evaluated.

1.3 Objectives and Thesis Scope

The main research topic of the dissertation is the aggregation of multiple RF channels in broadcast transmission. In particular, two technical solutions are investigated for such implementation:

- Time Frequency Slicing (TFS).
- Channel Bonding (CB).

The **main objective** of this dissertation is to **investigate and assess the potential for an efficient spectrum use by the aggregation of multiple RF channels in the next-generation DTT networks**. In particular, the following are the partial objectives of the dissertation:

- **Study the potential advantages of inter-RF frequency interleaving (FI).** Current DTT systems transmit service conveyed over single RF channels. To receive a particular service, the tuner must be locked to a fixed frequency. When degradation occurs in one RF channel, it is not possible to demodulate the services transmitted in it. Operators should

design the network to satisfy the requirements for the worst case, with the consequent loss in efficiency. Users are also affected since they are not able to receive the full set of services when one RF channel cannot be received. Inter-RF FI would average the signal imbalances between RF channels providing a common signal quality for all services. This study raises the following secondary objectives:

  - Quantify the theoretical performance bounds of the extended FI by inter-RF FI.
  - Evaluate the performance over real systems by means of physical layer simulations.
  - Identify the potential causes of signal imbalances between RF channels on the link budget.
  - Evaluate and model the potential coverage gains derived from the improved RF performance.

- **Assess and quantify the potential capacity gains.** The bundling of multiple RF channels may provide capacity gains derived from the more efficient Statistical Multiplexing (StatMux) as well as the potential for increasing service data rate with CB. The analysis focuses on the next topics:

  - Identify the potential capacity gains when operating TFS or CB.
  - Analyse the gains derived from the StatMux of VBR services as a function of the aggregated RF channels.

- **Investigate potential synergies with network planning for a potential increased spectral efficiency.** The potential increased RF performance could be exploited as a higher network spectrum efficiency, thanks to the combined effect of a modified capacity per RF channel and a tighter frequency reuse. The implementation of Advanced Network Planning (ANP) strategies could lead to an effective reduction of the signal levels interfering the receiver that could be translated into an increased spectral efficiency. The following secondary objectives are posed:

  - Evaluate the application of ANP to current network not implementing inter-RF FI.
  - Evaluate the network spectral efficiency gains provided when implementing inter-RF FI.
  - Evaluate the network spectral efficiency gains achieved with the combined use of multi-RF technologies and ANP strategies.

- **Identify and investigate the implementation requirements of the TFS and CB systems and their potential restrictions and limitations on service performance and network deployment.** The implementation of multi-RF technologies in DTT networks requires a proper study of the implications at the transmitter, receiver as well as network sides. One of the main impacts is the required number of tuners to allow reception of the services. Whereas single-tuner operation is desirable in order not to add more tuners to the current receiver devices, CB can only work with two or more tuners. TFS can work with a single tuner provided that time gaps are allocated to allow re-tuning for frequency hopping. The possible impact on transmission and performance needs to be assessed. The network implementation requirements as well as the regulatory framework to allow spectrum flexibility for the bundling of RF channels require to be studied.

The advantages of the implementation of these techniques in DTT networks are currently unknown due to the non-existence of prototypes or field measurements. The research presented in this dissertation aims to contribute to the international consortia developing the next-generation terrestrial broadcasting systems. In particular, the DVB task group working on the requirements for an evolved terrestrial broadcasting system and the ATSC 3.0 standardization process.

1.4 Thesis Outline and Main Contributions

The thesis is organized in six main chapters as follows: Chapter 2 describes techniques proposed to implement RF channel aggregation for terrestrial broadcasting: TFS and CB. The fundamentals of both techniques are studied as well as their envisaged operation modes. Chapter 2 also introduces the main advantages of such implementations regarding improved RF performance and capacity gains. Chapter 3 presents the potential gains from the point of view of coverage, capacity and increased robustness against interferences. This chapter evaluates the coverage gains from an information-theoretic point of view as well as based on physical layer simulations and field measurements. Capacity gains are evaluated according to the known performance of statistical multiplexing as well as by computing the potential service data rate increase with CB. The potential robustness against interferences is evaluated according to the number of interfered RF channels. Chapter 4 focusses on ANP strategies to allow for a potential reduction of the current frequency reuse factors that lead to an increased spectral efficiency to counteract the release of spectrum by the digital dividend. Chapter 5 is centred on the implementations aspects of TFS and CB

from the point of view of the transmitter, receiver and network deployment. Transmitter issues mainly focus on the required blocks to distribute data across multiple RF channels as well as the necessary framing and scheduling processes to adequate the transmission of the data that will be recovered by less tuners than the actual number of bonded RF channels. Reception mainly focusses on the tuning process and its relation with data scheduling. Network aspects deal with the requirements for implementing TFS and CB in the current network topologies. This section also investigates the compatibility with the regulatory framework on the allocation of RF channels and services. Finally, Chapter 6 summarizes the results obtained in previous chapters and discusses a number of recommendations for the use of the related techniques in the next-generation broadcasting systems.

The methodology approach of the investigations is partially covered in each of the chapters of the dissertation. Three appendices at the end of this document explain the main concept regarding simulations, measurement campaign and other details.

The key contribution of the core chapters of this Thesis are summarized next. Notice that Chapter 2 presents the fundamentals of the technologies which do not represent an original contribution of this Thesis. The reader should refer to Section 1.5 for a complete reference of the publications originated from the work carried out in the dissertation.

Chapter 3. Network Advantages by Multiple RF Channel Aggregation

The main contributions of this chapter are the evaluation of the improved RF performance and capacity gains offered by TFS and CB. Information-theoretic capacity of Bit Interleaved Coded Modulation (BICM) as well as physical layer simulations, based and validated according to DVB-T2 and DVB-NGH standards, are used to assess the bounds of the potential performance of inter-RF FI. Furthermore, the performance of rotated constellations with inter-RF FI is also investigated since their combined use with TFS and CB together with an appropriate component interleaver can extend diversity gains. The nature of the imbalances in the current DTT networks is theoretically analysed and evaluated from field measurements in outdoor and indoor scenarios. Statistical models are developed from measurements to estimate the imbalances between RF channels as a function of the frequency and to calculate the potential coverage gain given the frequencies of the bundled RF channels. The analysis is completed with the study of the coverage gain based on state-of-the-art propagation models. Capacity gains are evaluated from different perspectives. The gains derived from the increased RF performance are translated into capacity gain

by selecting a transmission configuration that offers reduced robustness but increased capacity. Statistical multiplexing gains for VBR services are evaluated for the UHDTV services according to the foreseen data rates next-generation DTT will offer using HEVC. Finally, the robustness against interferences by inter-RF FI is assessed as a function of the potentially interfered RF channels within an RF-Mux.

Chapter 4. Advanced Network Planning (ANP) with Inter-RF Frequency Interleaving

This chapter investigates how the increased interference immunity may drive to a spectral efficiency increase from the point of view of network planning. Different scenarios are evaluated considering current network deployments as well as the use of inter-RF FI. The potential tighter frequency reuse is very interesting since it can increase the overall capacity per transmitter station. The implementation of ANP strategies is also discussed by the selection of a proper horizontal or vertical polarization at the different co-channel stations and the use of multiple frequency reuse factors per each frequency so that the interferences on a given frequency become effectively decreased. Potential gains are evaluated according to different frequency reuse factors and taking into account the current DTT topologies based on MFNs and SFNs. Finally, gains are compared to the existing network deployments based on GE06.

Chapter 5. Implementation Aspects of TFS and CB

The work presented in this chapter investigates the requirements for the implementation of TFS and CB. Transmitter aspects deal with the required steps to distribute the data of a service across multiple RF channels. In particular for the TFS case the use of a time interleaver to spread data across the RF-Mux is discussed taking into consideration its trade-offs regarding optimum performance and implementation requirements. The use of less tuners than RF channels in the RF-Mux makes it necessary to account for a proper scheduling of data in frames so that reception can be performed by frequency tuning. Scheduling is approached for single-tuner and dual-tuner operation. The investigation particularly emphasizes the necessary time gaps to allow tuner operation. Potential capacity overheads derived from the limited amount of memory for time de-interleaving as well as the tuning gaps are computed considering different parameters as well as the number of bonded RF channels. The main operations that need to take place at the receiver for tuning, synchronization and channel estimation are analysed also in this chapter. Efficient implementations aimed to reduce the tuning gaps are discussed. Finally, net-

work deployment is investigated and recommendations are provided in order to allow for an efficient implementation of the techniques. In particular, this section deals with the operator capacity to aggregate and allocate services in the broadcasting band to obtain the desired gains, the generation and distribution of the data to transmitter sites and how ANP affect the current network topologies and user equipment. Finally, regulatory aspects are discussed focussed on the potential for an effective sharing of RF resources among all broadcasters.

Appendix A. Measurement Campaigns Details

This first appendix provides details on the measurement campaign in outdoor and indoor environments. These measurements are processes and analysed to compute the potential coverage gains of TFS and CB. The field strength variations between RF channels as a function of the frequency are evaluated. These measurements are also the basis of the models developed to estimate the field strength imbalances between RF channels and the coverage gain with multiple RF channels.

Appendix B. Physical Layer and Network Planning Simulations

This appendix covers the main issues regarding the physical layer simulations based on the DVB-T2 and DVB-NGH standards. Besides the simulations details this appendix also covers the emulation of the RF-Mux channel based on the models developed for the outdoor measurements. An approach to the network planning simulations to asses the inter-RF FI advantages with ANP is also included in this annex.

Appendix C. VHF and UHF Propagation Models

The characteristics of the state-of-the-art propagation models in the UHF and VHF bands are described. In particular, details of the ITU-R P.525, ITU-R P.529 and ITU-R P.1546 recommendations as well as brief references to other models are provided.

1.5 List of Publications

International Journals

[IJ1] **J. J. Giménez**, D. Gozálvez, D. Gómez-Barquero, and N. Cardona, "A statistical model of the imbalance between RF channels in a DTT network," *Electronics Letters*, vol. 48, no. 12 pp. 731-732, June 2012.[3]

[IJ2] D. Gozálvez, J. López-Sánchez, D. Gómez-Barquero, **J. J. Giménez** and N. Cardona, "Combined time and space diversity for mobile reception in DVB-T and DVB-T2 systems," *IEEE Vehicular Technology Magazine*, vol. 7, no. 4, pp. 114-121, December 2012.

[IJ3] D. Gozálvez, **J. J. Giménez**, D. Gómez-Barquero, and N. Cardona, "Rotated constellations for improved time and frequency diversity in DVB-NGH," *IEEE Transactions on Broadcasting*, vol. 59, no. 2, pp. 298-305, June 2013.

[IJ4] **J. J. Giménez**, E. Stare, S. Bergsmark, and D. Gómez-Barquero, "Time Frequency Slicing for Future Digital Terrestrial Broadcasting Networks," *IEEE Transactions on Broadcasting*, vol. 60, no. 2, pp. 227-238, June 2014.

[IJ5] **J. J. Giménez**, E. Stare, S. Bergsmark, and D. Gómez-Barquero, "Advanced Network Planning for Time Frequency Slicing (TFS) Toward Enhanced Efficiency of the Next-Generation Terrestrial Broadcast Networks," *IEEE Transactions on Broadcasting*, vol. 61, no. 2, June 2015.

[IJ6] E. Garro, **J. J. Giménez**, S.I. Park, and D. Gómez-Barquero, "Layered Division Multiplexing (LDM) with Multi-RF Channel Aggregation Technologies," to be submitted to *IEEE Transactions on Broadcasting*.

[IJ7] L. Stadelmeier, D. Schneider, Jan Zöllner, and **J. J. Giménez**, "Channel Bonding for ATSC 3.0," to be submitted to *IEEE Transactions on Broadcasting*.

Book Chapters

[S1] **J. J. Giménez**, D. Gómez-Barquero, S. Bergsmark, and E. Stare, "Chapter 13: Time-Frequency Slicing for DVB-NGH," *Next Generation Mobile Multimedia Broadcasting*, D. Gómez Barquero (Ed.), CRC Press, 2013.

[3] This paper was also presented in the European cooperation network for scientific and technical research COST IC1400 (www.ic1004.org)

[S2] **J. J. Giménez**, A. Mourad, and D. Gómez-Barquero, "Chapter 14: DVB-NGH Logical Frame Structure and Bundling DVB-T2 Future Extension Frames (FEF)," *Next Generation Mobile Multimedia Broadcasting*, D. Gómez Barquero (Ed.), CRC Press, 2013.

International Conferences

[IC1] **J. J. Giménez**, D. Gómez Barquero, S. Bergsmark, and E. Stare, "Time Frequency Slicing for the Next Generation Mobile Broadcasting Standard DVB-NGH," in *International Broadcasting Convention (IBC'13)*, Amsterdam, The Netherlands, 2013.

[IC2] **J. J. Giménez**, D. Gómez Barquero, C. García Pardo, and N. Cardona, "Time Frequency Slicing Coverage Gain Modeling for the Future Broadcasting Networks," in *IEEE International Conference on Telecommunications (ICT'14)*, Lisbon, Portugal, 2014.

[IC3] E. Garro, **J. J. Giménez**, S. Park, and D. Gómez-Barquero, "Performance Evaluation of Layer Division Multiplexing (LDM) combined with Time Frequency Slicing (TFS)," in *IEEE International Symposium on Broadband Multimedia Systems and Broadcasting (BMSB)*. Ghent, Belgium, 2015.

National Conferences

[NC1] D. Gómez-Barquero, D. E. Vargas, P. F. Gómez, J. Llorca, C. Romero, J. Puig, **J. J. Giménez**, J. López, D. Gozálvez and N. Cardona, "DVB-NGH, la nueva generación de televisión digital móvil" in *XXI Jornadas Telecom I+D*, Santander, Cantabria, 2011.

Contributions to Standardization Activities

[ST1] 3 contributions to the Framing Sounding and Synchronization task force in the standardization process of DVB-NGH.

[ST2] 8 contribution to the DVB Technical Module MIMO Study Mission and contribution to the clause 9: Time Frequency Slicing (TFS) and Advanced Network Planning (ANP), in the DVB Technical Module MIMO Study Mission Report.

[ST3] 2 contributions to the TG3/S32-3 Ad-hoc Group on Waveform in the standardization process of ATSC 3.0.

Chapter 2

Multi-RF Technologies in the Next-Generation DTT Systems

2.1 Introduction

DTT platforms require increased spectral efficiency to allocate the current service offering within the remaining spectrum after the digital dividends. This becomes even more important with the roll-out of HDTV services or even the start-up of Ultra HDTV services in the near future, which require higher bit-rates compared to the classical SDTV. The evolution of the broadcasting standards is a key point to increase the payload capacity per RF channel. New strategies on network planning can also contribute to increase the overall capacity of the networks by means of reducing the needs of guard channels and enabling the use of more RF channels per station.

Terrestrial broadcasting services are located in the VHF and UHF bands. These frequency ranges provide advantageous features such as good propagation characteristics in outdoor environments and the ability to penetrate into buildings enabling indoor reception. Fixed roof-top reception is the most important use case of digital terrestrial broadcasting. Indoor reception may be possible for those users close to transmitter stations, due to the severe propagation conditions of the indoor channel. Contrary to other wireless systems where there exist a return channel that enables the delivery of a particular capacity according to the reception quality reported back to the transmitter, broadcasting systems are designed to fulfil the quality requirements for a given

(high) percentage of locations within the target coverage area. Delivered capacity per RF channel is the same for those users within that area, regardless of the received signal quality.

The given set of services to be delivered are packed and multiplexed before being transmitted over the air. Each multiplex conveys a small group of services which are allocated to single RF channel. According to the selected transmission parameters — mainly Modulation and Coding (MODCOD) and bandwidth — the available data rate per RF channel is set. The selected MODCOD also fixes the minimum required Carrier to Noise Ratio (CNR) to enable error-free reception. In practice, this limits the amount of services that can be allocated per multiplex and also the maximum service bit-rate, which is linked to the quality and format of the TV service. Following this approach, each multiplex has its own coverage area, according to the frequency as a result of the propagation characteristics. This requires that the network is planned to satisty the coverage requirements in the worst case. Furthermore, reception of all services in a given location may be sometimes difficult, specially when a particular channel is degraded by fading or interference.

The next-generation terrestrial broadcasting standards envisage to overcome the capacity limitations and increase the system flexibility to allow the transmission of high data rate services within the remaining bandwidth. The combination of multiple RF channels (N_{RF}) to transmit services is a cost-effective technique to create a high-capacity multiplex (RF-Mux) that allows for a wider space to allocate services rather than being restricted to the capacity of a single RF channel.

This chapter presents the fundamentals of two transmission techniques making use of multi-RF channel aggregation: Time Frequency Slicing (TFS) and Channel Bonding (CB). Each one uses a different methodology to transmit data across the multiple RF channels. With TFS, services are transmitted both in the time and frequency domains by means of time-slicing (slot-by-slot transmission) and frequency-hopping (RF channel switching). CB consist of the bonding of multiple RF channels and the combination of the data sent across them. TFS allows for an increased RF performance when encoded data is interleaved across different slots (and in different RF channels). CB can also exploit this feature when inter-RF FI is implemented. However, data of a service can be transmitted over multiple RF channels but not necessary interleaved. In both CB cases, capacity gain (derived from the aggregation of the capacity per RF channel and efficient StatMuxing) can still be exploited. TFS cannot exploit this data rate increase but the StatMux capacity gain, instead.

The chapter is organized as follows: Section 2.2 presents an overview about the transmission of services in the current DTT systems. Section 2.3 and Section 2.4 explain the concepts of TFS and CB, respectively. Section 2.5 in-

Figure 2.1: Simplified transmitter chain in current OFDM-based DTT systems.

troduces the potential network gains of multi-RF channel aggregation. Finally, conclusions are presented in Section 2.6.

2.2 An Overview to Data Transmission in Current DTT Systems

Figure 2.1 depicts a simplified transmitter block chain of the current OFDM-based DTT systems:

The basic components of the system are the BICM, Frame Builder and OFDM Generation.

The input of the system depicted here are data streams which can be packed into the so-called Physical Layer Pipes (PLPs) which are physical layer TDM channels containing service data (e.g. an MPEG-TS stream with audio and video data of one or more TV services and/or associated service data).

BICM block provides the data with necessary protection to enable error-free reception in noisy channels. Forward Error Correction (FEC) mechanism inserts redundant data into the transmitted sequence of information which allow receivers to detect and correct a certain number of errors occurs during transmission. LDPC codes have been included in the physical layer of DVB-T2 and DVB-NGH and ATSC 3.0 because they can closely approach the Shannon's capacity bound in Additive White Gaussian Noise (AWGN) channels with reasonable decoding complexity. Information is processed as slots of data that are sequentially encoded into message blocks of k source bits. The encoder transforms each block into a codeword of n bits.

FEC performance is generally improved by means of interleaving to spread the codewords in the time and frequency domains in order to randomize the codeword components [19]. This is done to cope time and frequency selectivity due to the relative speed between transmitter and receiver (mainly affecting mobile reception) and multipath and impulsive noise (mainly affecting fixed roof-top reception).

OFDM already provides robustness against frequency selectivity by dividing the band of an RF channel in multiple orthogonal sub-carriers. With this, each sub-carrier experiments a flat frequency channel. OFDM in combination with

FEC allows the distribution of the FEC codewords across multiple sub-carriers so that frequency diversity can be achieved. The combination of FEC and OFDM is usually referred to as Coded Orthogonal Frequency-Division Multiplexing (COFDM) [20]. It is desirable that the interleaving in the frequency domain is longer than the *coherence bandwidth* of the channel. The coherence bandwidth can be defined as the bandwidth over which the channel is assumed constant, so that sub-carriers separated longer than the coherence bandwidth experiment independent fading. The coherence bandwidth of the channel is inversely proportional to the *delay spread*, which defines the multipath nature of the channel as a function of the relative delays and powers of the most relevant contributions (taps)[1]. In addition to the frequency selectivity caused by multipath propagation, large differences in the received signal strength can be found across frequency channels. Strong variations with the position of the receive antenna relatively to the transmitter and imbalances due to the frequency-dependent behaviour of antenna systems and propagation are found, in practice, in the broadcasting bands. However, this cannot be coped when interleaving is restricted to a single RF channel.

Time diversity is achieved by means of Time Interleaving (TI) [22]. With TI, multiple codewords are interlaced so that parts of each codeword are transmitted over an extended period of time (interleaving duration). The DVB-T2, DVB-NGH and ATSC 3.0 standards implement Block Interleaving (BI) and Convolutional Interleaving (CI) interleavers operating on a cell level[2]. The BI can be seen as a matrix with N_r rows and N_c columns which is written column-by-column and read row-by-row. The CI is based on a cascade of buffers which sequentially delay the inputs so that consecutive cells are spread in time at the output.

The diversity order of BICM systems can be enhanced by the concept of SSD. The main idea behind this is to apply a certain rotation to the information symbols so that each resultant component can experience independent fading. RC [23], which where firstly introduced in DVB-T2, exploit this concept at the expense of a higher demodulation complexity but with the same transmitter power and bandwidth. With regular, non-rotated constellations, each Quadrature Amplitude Modulation (QAM) symbol consist of real in-phase (I) and quadrature (Q) components carrying half of the binary information. These two components are transmitted in the same channel and suffer identi-

[1]The coherence bandwidth of the channel for a classical Doppler spectrum [21] of all components and a correlation of 0.5 is $B_c = \sqrt{3}/(2\pi\tau_{RMS})$, where τ_{RMS} is the delay spread. In turn, the delay spread is given by $\tau_{RMS} = \sqrt{(1/P_t)\sum P_i\tau_i^2 - \tau_0^2}$ where P_t is the total power in the channel and P_i and τ_i are the power and delay of each tap, respectively.

[2]Cells are complex symbols carrying modulated data that constitute a FEC codeword. A FEC codeword of 64800 consist of 8100 cells if modulated using 256QAM

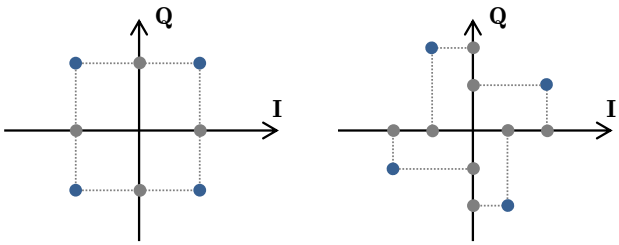

Figure 2.2: Regular QPSK (left) and Rotated QPSK (right). If the Q-axis is lost, two points are projected to the same I-axis position with a normal QAM and to different positions with the Rotated QAM.

cal degradation. Thus, the symbol suffers an irreparable loss since full information cannot be retrieved. When implementing Two-Dimensional Rotated Constellations (2DRC) (see Figure 2.2), each I and Q component holds all the symbol information. When each component suffers independent fading, information can still be decoded even if the symbol is deeply faded or erased. For this purpose it is necessary that each component is transmitted in a different time and/or frequency resource (e.g. a different subcarrier). DVB-NGH also introduced the concept of Four-Dimensional Rotated Constellations (4DRC) for QPSK and code rates below 1/2 [24]. In these cases, rotation is applied to pair of symbols, generating four different components. Increasing the rotation order implies additional complexity since all components must be demodulated together.

Once service data has been protected, the frame builder is the responsible of organizing data into frames. A scheduler is a core element when data of several PLPs (services) must share the same frame in a Time Division Multiplexing (TDM) manner or when e.g. time-slicing (discontinuous data transmission) is implemented. This way the frame is composed by all the service data according to their required bit-rate.

The OFDM generation block is in charge of producing an appropriate time domain signal from the frequency domain coefficients generated in the earlier stages. It also inserts reference information (pilots[3]) which allow the receiver to estimate the channel impulse response in order to compensate for the distortions during transmission.

[3]OFDM systems usually employ pilot-aided channel estimation. The channel state is estimated using the pilot sub-carriers and afterwards is interpolated in the time and/or frequency domains across the other sub-carriers and OFDM symbols. The use of pilots decreases the available sub-carriers for data transmission. Thus, it generates a capacity overhead.

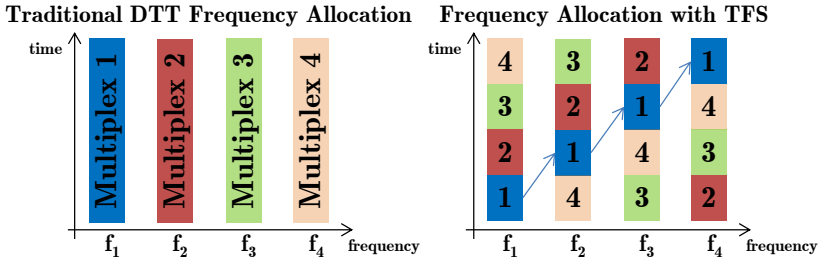

Figure 2.3: Classical allocation of services (left) and allocation with TFS (right). The arrows show the sequential hopping to recover service data.

2.3 Time Frequency Slicing (TFS)

2.3.1 Concept

Time Frequency Slicing (TFS) consists in transmitting the data of each TV service across several RF channels by means of time-slicing and frequency hopping. With this, time slots containing the data of a service are sequentially transmitted over different RF channels, breaking with the tradition of sending each service using a particular RF channel. Whereas traditional reception is simply performed by tuning the RF channel which carries the desired service, with TFS, the slots of a service are sequentially recovered by tuning the RF channel that carries the data slot at a given instant in a sequential manner (frequency hopping) [25].

Figure 2.3 depicts a basic scheme of the traditional allocation of services without TFS and when using TFS. As an example, whereas the services in multiplex 1 are uniquely transmitted in the RF channel with frequency f_1, with TFS the services previously contained in this multiplex are split and transmitted also across f_2, f_3 and f_4. In the first case the tuner is fixed to f_1. In the TFS case, frequency hopping enables the sequential collection of the data.

The concept of TFS is not only linked to the simple distribution of data across multiple RF channels. The core of the system relies on a proper error correction and interleaving which makes possible to spread the data of a codeword across the different RF channels. A proper framing and scheduling may enable the allocation of the data slots into the time and frequency domains so that service data slots are transmitted one after another and each one on a different RF channel. Figure 2.4 depict the basic scheme to perform TFS. It can be seen that the BICM process is performed for each service. The framer generates one frame per RF channel containing data of all services.

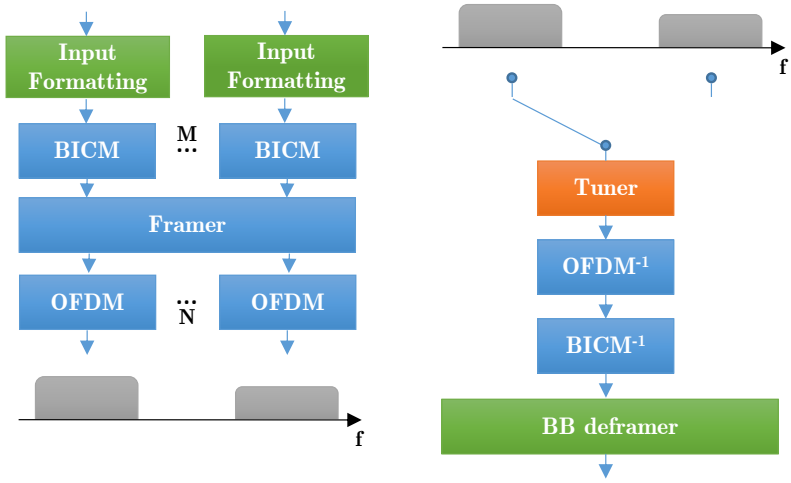

(a) Transmitter (b) Receiver

Figure 2.4: Transmitter and receiver chains for TFS operation. Single-tuner reception approach.

Data allocation in each frame is directly linked to receiver operation. Two slots of the same services are not transmitted at the same time over different RF channels. This allows reception by means of frequency hopping when there are less tuners than RF channels in the RF-Mux. Reception with a single tuner may be even possible as soon as framing and scheduling consider the need of guard times between two consecutive slots so that it is possible to perform the switch from one frequency to another. The faster the switching is produced, the less the required guard times. Note that increasing the guard times involve consuming time where service data cannot be allocated, what leads to a data rate overhead. The use of more than one tuner could eliminate the need of guard times and allow the ideal TFS operation without restricting data rate. The drawback is the need to introduce additional tuners at the receiver unit.

TFS was originally proposed and informatively specified within the standardization process of DVB-T2 [26] to be operated using two tuners. Single-tuner TFS was fully adopted in the mobile broadcasting standard DVB-NGH (Next Generation Handheld)[27, 28]. However, it has never been implemented since DVB-NGH has not been yet deployed in any country. The concept of TFS, however, may be applied to any other new terrestrial broadcasting standard since it defines a physical layer technique.

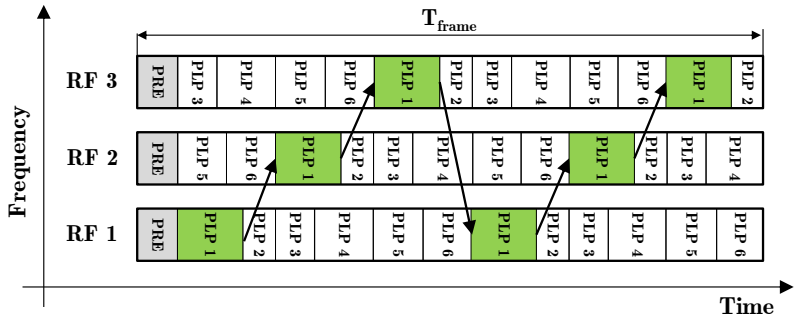

Figure 2.5: Intra-frame TFS within slots of each PLPs within a frame.

These two standards introduce TFS being operated intra-frame or inter-frame, depending on the operator requirements. Intra-frame TFS operates internally within the same frame. Data slots of the service are sequentially allocated at different positions within the frames that are transmitted in each RF channel. A frame containing slots of all the services is transmitted in each RF channel. In such case, interleaving duration does not exceeds frame duration. Figure 2.5 shows an example of an intra-frame TFS transmission with 3 RF channels and one frame per RF channel. In this case each RF channel carries information of all the services (PLPs). The reception of a given PLP is performed sequentially within the frame duration. For the given configuration each frame duration involves two TFS cycles (2 tuning rounds over the 3 RF channels), what could also be achieved with inter-frame TFS.

Frame-by-frame operation (inter-frame TFS) is also possible by allocating the slots only from frame to frame or directly using short frames. With this, data of a particular service is totally transmitted in a different RF channel during frame duration. Figure 2.6 shows an example of a transmission of 3 frames per RF channel. PLP slots are allocated frame-by-frame. The figure depicts one TFS cycle involving 3 slots of the PLP.

2.3.2 Background

The concept of TFS in terrestrial broadcasting is investigated in [29, 30] considering its potential realization within the DVB-T2 standard. According to this, the data of each service is carried into one of the so-called Physical Layer Pipe (PLP). Data is coded, modulated and time-interleaved so that a codeword can be split and evenly distributed across the RF channels that constitute the RF-Mux. By means of physical layer simulations the potential performance of

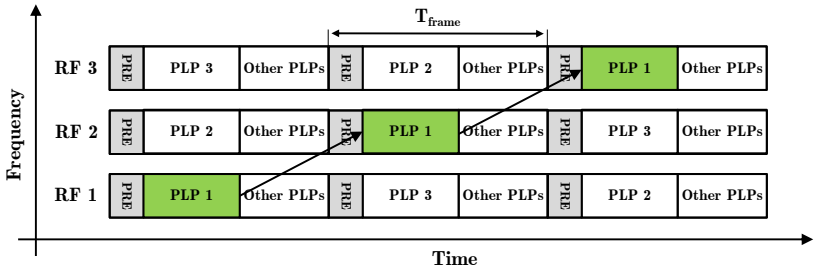

Figure 2.6: Inter-frame TFS within slots allocated in different frames.

TFS is evaluated. When a RF-Mux built of 2 RF channels is considered, a weak channel can be compensated by means of a strong channel. However, the performance is limited when there is a high attenuation on one channel and a high coderate is used. The study also introduces the potential of TFS combined with the RC feature of the DVB-T2 standard, using an idealized component interleaver, which evenly distributes the in-phase and quadrature components of each coded symbol across the two RF channels. If one RF channel is lost, the symbol can still be recovered by means of the information sent in the good RF channel.

The use of time-slicing and frequency hopping is also investigated in [31]. A framing structure consisting on the fragmentation of the transmission bandwidth is proposed in the context of mobile reception to increase the flexibility of the system and the power efficiency. The idea consists in dividing the full bandwidth of a traditional transmission into sub-bands where time slicing and/or frequency hopping among the sub-bands is performed. Although for static channels there exit a loss due to the reduced frequency diversity, mobile reception can benefit from increased diversity in fast fading channels or portable outdoor reception.

Though the TFS approach is new in the context of broadcasting, a TFS-like system was already introduced in [32] as a technique that allows multiple users with different data rate requirements access to portions of the spectrum on a slot-by-slot basis. This way the spectrum is used more efficiently than in a traditional time division approach in which users use all the frequency resource but in a time-divided manner. Thus, multiple users can share the time-frequency resource. The implementation aspects of this techniques are, however, not explained and only the benefits on spectral efficiency are assessed.

The concept of TFS has been also developed in connection to Ultra Wide Band (UWB) communication systems. UWB technology traditionally relies on the generation of a series of pulses which occupy a bandwidth of several

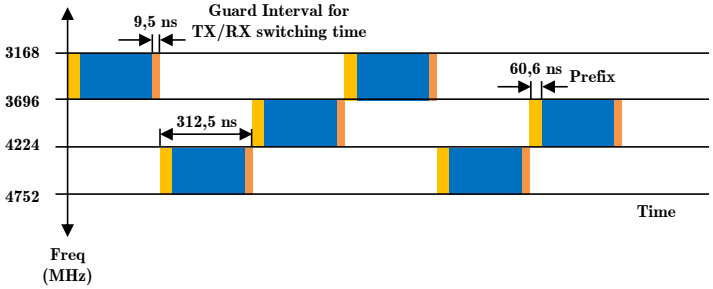

Figure 2.7: Example of the TFI-OFDM system.

GHz. The main drawback of this is the receiver implementation complexity. Multi-band OFDM [33–35], divides the UWB spectrum into smaller sub-bands of hundreds of MHz. OFDM symbols are interleaved across both time and frequency implementing the so-called time frequency interleaving (TFI) OFDM. TFI-OFDM allows reducing receiver design complexity due to the lower receiver bandwidth. As it can be seen from Figure 2.7 a cyclic prefix (CP) and a guard band are appended to the symbol. The guard band is inserted to allow enough time to switch from one band to another. The approach is slightly different to TFS since frequency hopping is performed both at the transmitter and the receiver by a frequency-hopping algorithm to switch between the different sub-bands.

The multi-band OFDM approach was proposed for the IEEE 802.15.3a WPAN (Wireless Personal Area Network) standard [36] and was approved as the UWB standard by the European Computer Manufacturers Association (ECMA) [37]. This standard sets a short guard interval for frequency switching of 9.5 ns.

2.4 Channel Bonding (CB)

2.4.1 Concept

Channel Bonding is introduced in ATSC 3.0 to enable service data rates beyond the capacity of a single RF channel. The strategy consist in sending service data using more than one RF channel simultaneously so that the demodulated data from each channel can be combined as a single signal. In order to reduce modulation and demodulation complexity, the standard operation mode for CB envisages the split of the global capacity of the RF-Mux into as many sub-streams as RF channels. Thus, each stream can be independently modulated

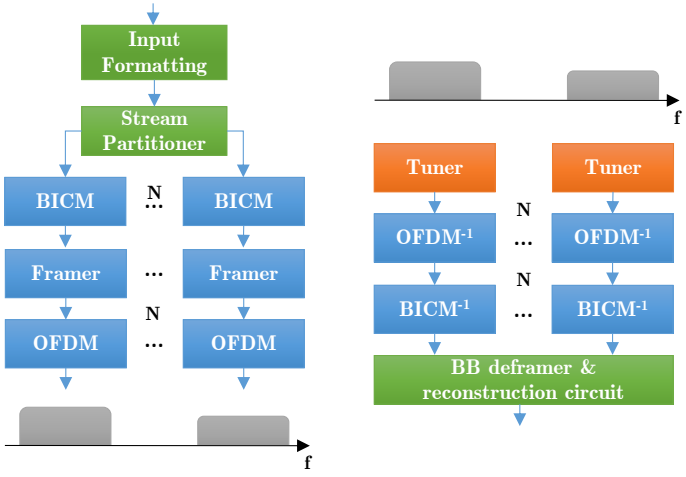

(a) Transmitter (b) Receiver

Figure 2.8: Basic transmitter and receiver chain for CB.

and demodulated. Afterwards, a combination circuit allows to recover the complete stream. From the point of view of frequency diversity, CB cannot directly exploit it since data is encoded independently per stream. A unified data pre-coding or a cell exchange mechanism so that encoded data is sent over the complete RF-Mux may allow for inter-RF FI.

Figure 2.8 depicts a basic schema of the transmission and reception chain for the CB system without inter-RF FI. Basically, the process splits the data into low bit-rate streams that are modulated and transmitter each one in a different RF channel. A set of tuners is in charge of receiving each stream separately. After demodulation, the decoded streams are again combined to global output streams.

The RF channels that are aggregated can be contiguous or non-contiguous. This enables the reuse of standard signals and standard tuner. The RF channel bandwidth remains the same. However, there still exists a band gap between adjacent RF channels, as in a traditional transmission.

It is evident that the number of bonded RF channel has a proportional impact on complexity. An additional tuner is required per aggregated RF channel. For cost and complexity issues, CB is envisaged to operate with 2 tuners in ATSC 3.0.

2.4.2 Background

A similar technique to CB has been developed and included in LTE-Advanced. Carrier aggregation [38] enables a bandwidth extension by aggregating LTE component carriers (CC) — RF channels of 1.4, 3, 5, 10, 15 or 20 MHz. The maximum supported bandwidth is 100 MHz and the aggregated CCs can be contiguous or non-contiguous. Note also that CCs of different bandwidth can be aggregated together. Different CCs can be planned to provide different coverage. In fact, each CC experiences different pathloss, increasing with frequency. The lack of interleaving among the CCs restricts the coverage area to that of the CC with the best propagation conditions. However, the main benefits of carrier aggregation in LTE-Advanced are the increased data rate and the spectrum flexibility and reconfiguration capability.

The concept of CB was previously introduced in [39] in order to enable a throughput increase for small-scale wireless networks. In [40] the authors present measurement results of CB functionality in the IEEE 802.11n standard. The study concludes that the network with bonded channels obtains smaller throughput than a network without CB. To prevent this problem, the authors propose an algorithm to merge the channels depending on the perceived link quality. The study in [41] evaluates a WLAN system with channel width adaptation utilizing OFDM.

The advantages of CB in connection with frequency agility are evaluated in [42], where the network assigns channels after the detection of the available frequency channels. The studies in [43] present the dynamic spectrum allocation for WLAN networks based on CB. Channel bonding is also investigated for IEEE 802.22 networks in [44] based on OFDMA.

CB is also studied in the context of Opportunistic Spectrum Access (OSA) in [45]. The study concludes that CB is generally beneficial but constrained by network features such as its size and the total number of channels available for bonding. Benefits can also be found when adaptively changing the number of channels to be bonded depending on the network conditions.

2.5 Network Gains with Multi-RF Channel Aggregation

The implementation of RF channel aggregation mainly offers two potential benefits: improved reception robustness due to better frequency diversity when inter-RF FI is implemented and increased capacity due to a more efficient statistical multiplexing (with TFS and CB) and increased service data rate (with CB).

The increased frequency diversity by inter-RF FI makes it possible to average the existing signal imbalances between RF channels that are caused by the frequency dependency of the transmitter site, the receiver, and the propagation channel. The signal averaging can be translated to a coverage gain. In a traditional network the coverage of the complete service offering (all multiplexes in a network) is limited by the RF channel with the poorest C/N. Thus, for a given location, the reception of all services is achieved as soon as all RF channels are decodable. If one RF channel cannot be decoded, the services carried within are lost regardless of the better condition of the rest of channels. With inter-RF FI all services are received with the same C/N. This global C/N is larger that the C/N of the worst RF channel in a classical transmission thanks to the achieved signal averaging between the high and low level RF channels. However, the coverage area where at least one multiplex can be received is somewhat reduced with inter-RF FI. For instance, the services allocated in the best received RF channel in a traditional network will have a wider coverage than that of the RF-Mux.

From the point of view of broadcasters and operators the aggregation of RF channels can be beneficial in order to market DTT with an homogeneous coverage area for all the services in the RF-Mux. Consumers will also benefit from getting the complete service pack instead of getting only those services which can be correctly decoded. Moreover, with the pay-TV model implemented in several countries, the whole service offer is delivered by means of several multiplexes which users expect to completely receive, as they pay for them.

Figure 2.9 is an illustrative example of the coverage gain achieved by the distribution of the services across a RF-Mux using inter-RF FI. For instance, some areas receiving RF_4 are unable to receive RF_1, RF_2 and RF_3. On the other hand, when all services are bundled together and transmitted as a unique *virtual* signal the coverage area where all services can be received is the same for all of them. The suppression of data of a service in a particular RF channel does not necessary involve the corruption of the whole service if other parts of data are still good enough to compensate the 'bad' ones. Evidently, whereas some areas in the traditional allocation are able to partially receive some services, the new situation reduced the coverage for such cases. Thus, some areas receiving at least one RF channel are not covered by the global coverage area.

Measurement campaigns collected in [46] reveal a coverage gain with inter-RF FI around 4.5 dB for 6 different areas in Sweden considering RF channel allocations comprising 4 RF channels. However, the gain is presented as an average figure and by means of Cumulative Distribution Function (CDF) but its behaviour with code rate and its dependence with the frequency of the channels in the RF-Mux are not investigated. An extensive measurement campaign in

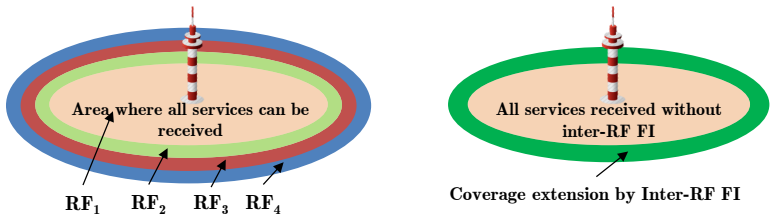

Figure 2.9: Coverage per RF channel in a classical DTT transmission (left) and coverage extension with inter-RF FI for the reception of all services in a RF-Mux.

[47] show achievable gain figures above 5 dB depending on the number of RF channels employed in the RF-Mux. The analysis also shows higher gains in dense urban environments compared to urban or Line-of-Sight (LoS) scenarios.

Regarding RF channels affected by interferences, inter-RF FI can also provide a gain as the interferences from other transmitters are usually frequency dependent and, thus, does not occur in all the channels at the same time. The most important source of interference comes from stations broadcasting in the same RF channel (CCI). Frequency plans for terrestrial broadcasting, such as GE06, are developed in order to limit the interference in the service area when there exist a certain number of networks in the same RF band. The interfering signals coming from a digital TV transmitter also affect the received signal. The wanted signals coming from a specific station, with usually an equal Effective Radiated Power (ERP), show large signal differences for the different frequencies used, as a result of systematic and random, frequency-dependent, variations. The interfering signal level, coming from more distant stations, will, as a result of the same mechanisms, also suffer from these variations. The same type of coverage advantage for the wanted signal can also be applicable to the interfering signal. Moreover, when interferences from other transmitters are statistically independent from the wanted signal, the resulting gain is expected to be significantly larger than that considering field strength of the wanted signal only.

Figure 2.10 shows an illustrative example of an interference limited coverage. The coverage contours of 7 muxes from the station in Örebro, Sweden, are different due since co-channel interferences for each frequency do not come from the same transmitter.

Inter-RF FI can also be beneficial to reduce potential interferences caused by the deployment of 4G Long Term Evolution (LTE) cellular services. LTE uses the upper part of the UHF band as the result of the digital dividend.

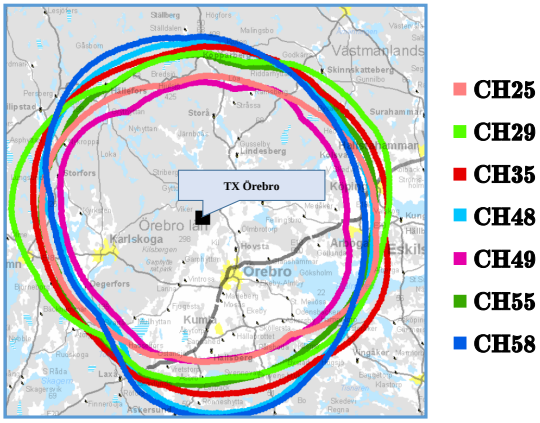

Figure 2.10: Interference limited coverage contours.

These transmissions may have an adverse effect on broadcast reception on RF channels close to LTE [48, 49]. However, using an RF-Mux, only a part of the signal (corresponding to the RF channels close to LTE) would be affected, and reception could still be successful, with only minor degradation in terms of required SNR thanks to the reception of the other parts.

The increased RF performance achieved with these technologies can be directly translated into increased capacity by selecting a less robust transmission mode while keeping coverage. Capacity gain can also be obtained with the transmission of Variable Bit Rate (VBR) services and the utilization of StatMux, as covered in [50]. VBR encoders generate a stream of variable bit rate so that the video quality remains constant. Traditional bit rate allocation with Constant Bit Rate (CBR) accounts for the service peak rate in order to ensure that enough capacity is always available. However, this means that some capacity will be wasted whenever the services are transmitted at a lower bit rate. StatMux relies on the fact that the aggregated peak rate of several VBR services is significantly lower than the peak rate of each individual service. The gain of StatMux depends on the number of channels that are bundled in the same multiplex. In particular, the gain increases with the number of services until reaching a certain saturation point. The utilization inter-RF FI allows for an almost ideal StatMux gain with several HDTV and UHDTV services using VBR encoding. On the other hand, the gain is expected to be much lower with low bit rate services, as a single RF channel may already provide sufficient capacity to approach the saturation point of the StatMux gain. CB allows to double the bit-rate of a single RF channel with the same robust-

ness requirements of a single RF channel since the C/N threshold of each RF channel remains the same. The suppression of the frequency gaps by using a receiver with a wider band and adjacent RF channels would still allow for a further capacity increase.

The benefits of CB in the next-generation DTT standards can be largely exploited in connection with Scalable High Efficiency Video Coding (SHVC). CB with SHVC would make possible to transmit a low data rate (base) layer in one RF channel (e.g. intended for mobile reception) and then increase the quality of the services by means of a high data rate (enhanced) layer transmitted in another RF channel.

2.5.1 Inter-RF FI and Advanced Network Planning (ANP)

Different frequencies are traditionally assigned to multiplexes in each neighbour station in the target service area. At a given reception point, the wanted transmitter provides a certain field strength. Other transmitter stations using the same frequencies provide an interference contribution. Interferences are added so that the total interference power yields a C/(N+I) at the reception point. It is necessary to maintain a sufficiently high C/(N+I) to meet the interference protection requirements of the system. Thus, the RF channels from a transmitter station cannot be reused in a transmitter that is too close to the first one. This minimum separation between co-channel transmitters limits the amount of spectrum that can be used per transmitter station. The amount of spectrum that is distributed among different stations to allocate the services is related to the so-called frequency reuse factor.

The increased robustness achieved by inter-RF FI can be translated into a tighter frequency reuse between stations. This increased interference tolerance may be exploited as a combination of a tighter frequency reuse together with a modified capacity per RF channel when using inter-RF FI.

This effect can be enhanced by the implementation of Advanced Network Planning (ANP) strategies by means of multiple frequency reuse patterns and/or the systematic use of H/V polarizations, as introduced in [51]. The idea of these strategies consist of configuring a different frequency reuse pattern per frequency or using a different transmission polarization so that the interferences in each frequency from co-channel stations reach the receiver with a different direction or with a significantly different level, respectively. These methodology can be applied to the typical DTT network deployments based on pure Multiple Frequency Network (MFN) or medium-scale or large-scale Single Frequency Network (SFN) so that the overall effect is a higher total capacity within a given spectrum.

2.6 Conclusions

This chapter has presented two technologies that implement multi-RF channel aggregation in the framework of the next-generation terrestrial broadcasting systems: Time Frequency Slicing (TFS) and Channel Bonding (CB). These novel technologies permit to transmit services into a high-capacity multiplex rather than doing in on a single RF channel basis.

The benefits of RF channel aggregation depend, basically, on the methodology whereby the services data are sent across the multiple RF channels. Service data rate increase is feasible when data of a particular service is the result of the aggregated capacity of each bundled RF channel. It is theoretically possible to multiply capacity by N_{RF}. However, the bundling of RF channels does not necessary involve increasing service data rate. A *virtual* capacity gain is still achievable when StatMux is used with VBR services thanks to a more efficient distribution of the data rate demands among services, what is translated into more space to allocate more services.

RF channel aggregation may also allow for exploiting increased frequency diversity and thus obtaining an enhanced RF performance, that can lead to a coverage advantage. Frequency diversity is achieved in current broadcasting systems by the spread of the encoded data over different sub-carriers that cover the full signal bandwidth (e.g. 6, 8 MHz), by means of FI. Thanks to this, when frequency selectivity occurs in some carriers (e.g. due to multipath or interferences), a proper error correction can allow complete data decoding. Extending data across the sub-carriers in more than one RF channel by inter-RF FI, allows also compensating potential signal differences between RF channels.

Chapter 3

Network Advantages by Multi-RF Channel Aggregation

3.1 Introduction

The bundling of multiple RF channels into a high-capacity RF-Mux allows for important network gains. Frequency interleaving across multiple RF channels (inter-RF frequency interleaving) increases frequency diversity what leads to an improved RF performance for the reception of the complete set of services in the RF-Mux. By this mechanism, increased robustness against RF channels signal imbalances and interferences is achieved, what can be translated into a *coverage gain* . On the other hand, a *capacity* gain thanks to a more efficient StatMux of the input services and/or a data rate increase beyond that with a single RF channels is also enabled by the aggregation of multiple RF channels.

This chapter assesses the potential network gains by TFS and CB. The generic nature of the investigation make it possible to extend the results to the future evolutions of the standards implementing the concept of RF channel aggregation.

Information theory provides the theoretical bounds of inter-RF FI. By physical layer simulations the performance investigated based on the state-of-the-art DVB-T2 and DVB-NGH standards. Mathematical models to approximately quantify the gains are also developed by the analysis of the frequency-dependent behaviour of propagation in the UHF and VHF bands. Reference propagation models available in the literature and outdoor and indoor field measurements

campaigns are considered for this purpose. Robustness against interferences capability is assessed as a function of the number of interfered RF channels in the RF-Mux. The achievable capacity gains are evaluated according to the number of bundled RF channels, the selected video coding standard and the type of service.

The chapter is organized as follows: Section 3.2 evaluates the potential of inter-RF FI in BICM systems. Section 3.3 deepens on the potential for a coverage gain derived from the increased RF performance with inter-RF FI. Section 3.4 deals with the improved interference robustness. Section 3.5 discusses the way a capacity gain can be obtained by multiple RF channels aggregation. Finally, Section 3.6 presents the conclusions of the studies.

3.2 Performance Evaluation of Inter-RF Frequency Interleaving

This section investigates the potential for an increased RF performance when extending frequency interleaving across multiple RF channels by means of inter-RF FI. The performance is assessed from an information-theoretic perspective based on the limits of BICM systems. Results are presented for 2 RF channels and generalized to more RF channels. The performance with real systems is evaluated by means of physical layer simulations based on the DVB-T2 and DVB-NGH standards. Special attention is paid to the performance with RC to obtain gains beyond the regular QAM mapping.

3.2.1 An Information-Theoretic Approach to Inter-RF Frequency Interleaving

Gains by inter-RF frequency interleaving achieved in broadcasting systems can be modelled as a system in which the codewords are mapped on all the subcarriers in a given bandwidth, across a number of OFDM symbols that is given by the interleaving duration, and across a particular number of RF channels, N_{RF}. The capacity of such a system, C_{RFMux} can be modelled as:

$$C_{\text{RFMux}} = \frac{1}{N_{RF}} \frac{1}{L} \frac{1}{K} \sum_{n=1}^{N_{RF}} \sum_{l=1}^{L} \sum_{k=1}^{K} C_{nlk} \text{ bps/Hz}, \tag{3.1}$$

where C_{nlk} is the capacity of the sub-carrier k of the symbol l which is transmitted in RF channel n.

Note that if the performance is computed solely based on Shannon-Hartley limit, C_{nlk} is given by:

$$C_{Shannon} = \log_2(1+\gamma) \text{ bps/Hz}, \tag{3.2}$$

where γ denotes the Signal to Noise Ratio (SNR).

It should be noted that since Equation (3.1) is based on Shannon limit, the resulting capacity is not conditioned by particular aspects of BICM systems such as the bit labelling, the constellation or the code rate [52].

Equation (3.1) represents the best case scenario for diversity, since the codewords are assumed to be spread across all the subcarriers within the transmission bandwidth, across all the OFDM symbols within the interleaving duration and across all RF channels in the RF-Mux. In real broadcasting systems each codeword is only transmitted in a subset of subcarriers and/or OFDM symbols. Furthermore, it is possible that the transmission using inter-RF FI does not involve the whole set of RF channels. Thus, the values obtained with this model may be considered as upper bounds of the gains that can be achieved in real systems.

Broadcasting systems employ BICM to achieve robust performance over AWGN and fading channels [53]. BICM using OFDM relies on a combination of FEC and interleaving to extend data over the time and frequency domains to exploit diversity. In such systems, a sequence of information bits is encoded using a FEC code and passed through a bit interleaver. After this, a binary labelling maps each block of m coded interleaved bits c_l, $l = 1, \ldots, m$ to a complex data symbol u in a QAM constellation Ψ. The BICM capacity is determined by particular system characteristics such as the bit labelling, the constellation or the code rate. In fact, the BICM capacity is bounded by the employed QAM mapping. Under the assumption of full channel state information (CSI) at the receiver side and ideal infinite interleaving, C_{BICM}, can be computed as the mutual information I between the set of transmitted code bits c_l and the received signal $\mathbf{y}$, conditioned by the channel matrix $\mathbf{H}$. With i.i.d. uniform code bits, this is given by [52][1]:

$$\begin{aligned} C_{\text{BICM}} &= \sum_{l=1}^{m} I(c_l; \mathbf{y}|\mathbf{H}) \\ &= m - \sum_{l=1}^{m} \mathrm{E}_{\mathbf{x},\mathbf{y},\mathbf{H}} \left\{ \log_2 \frac{\sum_{\mathbf{x}' \in \Psi} f(\mathbf{y}|\mathbf{x}', \mathbf{H})}{\sum_{\mathbf{x}' \in \chi_l^b} f(\mathbf{y}|\mathbf{x}', \mathbf{H})} \right\}, \end{aligned} \tag{3.3}$$

[1]For generalization, the transmitted symbol $\mathbf{x} = [x_1, x_2, \ldots, x_D]^\top$ is considered D-dimensional when using a rotated constellation Ψ. $\mathbf{H} = \text{diag}(h_1, h_2, \ldots, h_D)$ is the channel matrix with independent fading coefficients in its diagonal.

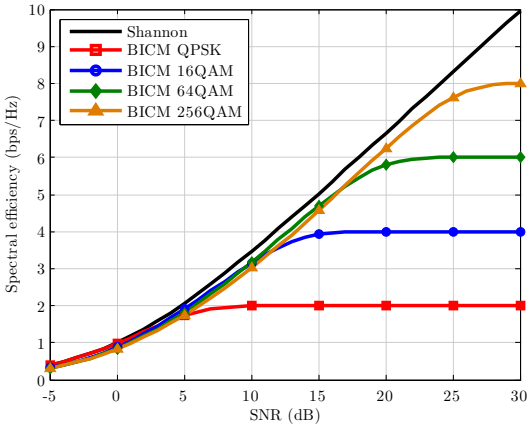

Figure 3.1: BICM capacity of various uniform QAM constellations, compared with the unconstrained Shannon limit. AWGN channel.

where $b \in \{0, 1\}$ is equiprobable and χ_l^b denotes the set of symbols in the constellation Ψ for which the code bit c_l equals b. In the case of the soft-output Maximum A Posteriori (MAP) demodulator, the conditional probability density function (pdf) $f(\mathbf{y}|\mathbf{x}, \mathbf{H})$ corresponds to:

$$f(\mathbf{y}|\mathbf{x}, \mathbf{H}) = \frac{1}{\pi\sigma_w^2} \exp\left(-\frac{||\mathbf{y} - \mathbf{H}\mathbf{x}||^2}{\sigma_w^2}\right), \tag{3.4}$$

Figure 3.1 depicts the normalized channel capacity with AWGN noise according to Shannon limit (Equation (3.2) and BICM (Equation (3.3)) for QPSK, 16QAM, 64QAM and 256QAM, using uniform QAM mappings.

It should be noted that, for any given constellation with spectral efficiency m, the SNR[2] gives a capacity that determines the FEC code rate R_c that is needed in order to achieve error-free communication. In particular, the code rate can be derived from the BICM capacity as $R_c = C_{\text{BICM}}/m$.

BICM capacity is bounded by the maximum efficiency of the QAM mapping, e.g. 2 bps/Hz for QPSK and 8 bps/Hz for 256QAM, respectively. However, the curves are quite close to Shannon limit for the non-saturating areas. In real broadcasting systems each codeword is only transmitted in a subset of subcarriers and/or OFDM symbols. Although perfect FEC codes do not exist, state-of-the-art codes are very close to the theoretic performance.

[2]Under the assumption of normalized transmit symbols $\mathrm{E}[xx^\top] = 1$, the SNR is equivalent to the inverse of the noise variance $\text{SNR} = 1/\sigma_w^2$

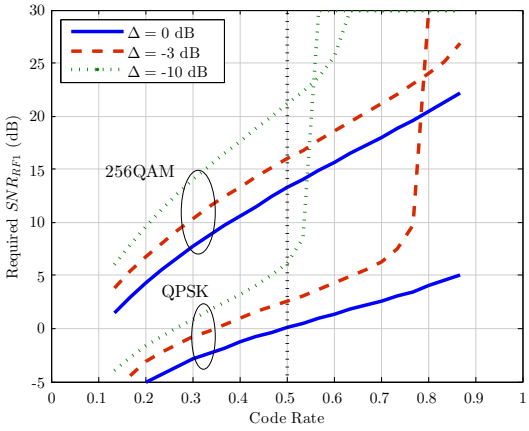

Figure 3.2: Required SNR increase in one of the two RF channels to reach the same spectral efficiency as that achieved without the imbalance.

BICM analysis with 2 RF channels

Ideal inter-RF FI with 2 RF channels (RF_1 and RF_2), allows 50% of the data to be received from RF_1 and the other 50% from RF_2. For emulating the potential field strength differences between RF channels, the CNR of one of the channels is set Δ = -3 and -10 dB below the CNR of the other RF channel. With this situation, the required CNR in RF_1 to achieve a given spectral efficiency (bps/Hz) is computed (see Figure 3.2). The calculation is made according to BICM capacity with 2 different QAM mappings: QPSK and 256QAM. Code rates between 2/15 and 13/15 are selected for each mapping (i.e., the maximum spectral efficiency with QPSK is 1.73 bps/Hz). The curves which spectral efficiency corresponds to that without inter-RF FI are also indicated (Δ = 0 dB).

It is seen that a lower SNR in RF_2 due to the imbalance Δ can be compensated with a significant SNR increase in RF_1. For low imbalances or high imbalances with code rate lower than 1/2, the required increase in one RF channel is less than the actual imbalance in the other. For high imbalances and high code rates the gap increases. For example, it is possible to recover the spectral efficiency for QPSK with code rate 0.55 when one RF channel is affected by an imbalance of -10 dB and the other is at 20 dB. Conversely, it is not possible to achieve the same effect with a -10 dB imbalance and code rate higher than 0.6. For the 256QAM mapping it is possible to exceed code rate

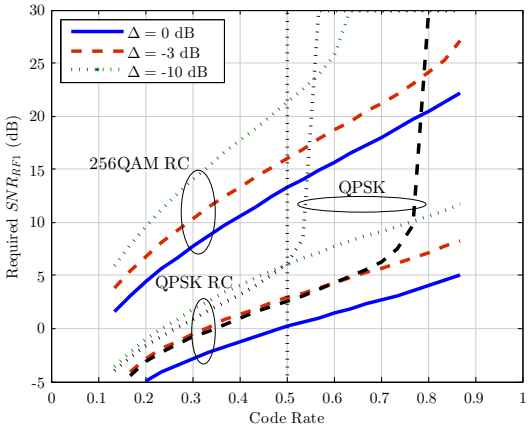

Figure 3.3: RF channel capacity recovery capability with QPSK and 256QAM using RC with 2 RF channels. The regular QPSK case is shown for comparison.

0.6. Moreover, the increase relative to the 0 dB case is higher for the QPSK mode than for the 256QAM mode.

BICM analysis with Rotated Constellations

The potential advantage when using RC is studied following the same methodology. In order to achieve the optimal performance, an I/Q component interleaver is considered after rotation. With it, transmitted rotated symbols are halved so that in RF_1 the I components of one half of symbols are transmitted together with the Q components of the other half. In RF_2 the I components of the second half and the Q components of the first one are transmitted. Figure 3.3 shows the required SNR on RF_1 using QPSK RC and 256QAM RC. The performance for rotated QPSK is compared to the previous curves with regular QPSK.

The use of RC allows extending the SNR range where it is possible to recover the desired capacity. Whereas it was not possible to recover the capacity lost by the imbalance on RF_2 with code rates higher than 1/2 for QPSK, with RC it is possible to recover the lost RF channel for higher CNR values, at the expense of a higher CNR requirement than with the regular QAM constellations. However, the advantage of RC with high-order QAM mappings is null. For code rates below 1/2 there is a loss for QPSK compared to regular QPSK. The loss increases for high imbalances.

The additional diversity introduced by rotated constellations diminishes the information loss caused by erasure events and allows error-free communications with higher code rates. The gain of rotated constellations tends to infinity when the code rate approaches the highest value required with non-rotated constellations.

Extension to multiple RF channels

The behaviour of the BICM capacity as a function of the SNR permits to estimate that, for a given QAM mapping and high code rates, the capacity with inter-RF FI will be bounded. In fact, if the capacity of all RF channels is bounded, the capacity of the RF-Mux equals the capacity of a single RF channel an no gain is achieved. Whereas in real systems each RF channel is received with a different SNR and it is difficult to establish a direct relationship between code rate and the quality of the channels, this relationship can be explained by considering the amount of erased information symbols during transmission. The presence of erasures limits the maximum code rate for which error-free communication is possible. A 10%, 30% and 50% of erasures require code rates lower than 0.9, 0.7 and 0.5 respectively in order to repair the loss of information with regular constellations. In general, the code rate is directly linked to the number of 'erased' RF channels in the RF-Mux. While for 2 RF channels it is possible to recover 1 'erased' channel with code rate 1/2, it is also possible to recover 2 'erased' over 4 RF channels with the same code rate or 1 'erased' channel of 4 RF channels with code rate 3/4, 3 'erased' from 4 channels with code rate 1/4, etc.

The results previously presented show that the capacity comes close to Shannon for a wide range of SNR values and code rates. Furthermore, the use of RC allows extending the potential coverage advantages. Assuming this, the capacity offered by the RF-Mux can be estimated by means of the average Shannon capacity per RF channel, with the following equation:

$$C_{\mathrm{RFMux}} = \frac{1}{N_{RF}} \sum_{n=1}^{N_{RF}} \log_2(1+\gamma_{f_n}) = \frac{1}{N_{RF}} \log_2\Big(\prod_{n=1}^{N_{RF}} (1+\gamma_{f_n})\Big) \text{ bps/Hz}, \quad (3.5)$$

where γ_{f_n} is the SNR at the receiver experienced by each RF channel in a RF-Mux with N_{RF} RF channels.

Approximating capacity by Shannon, it is possible to express the capacity of the RF-Mux as a function of an equivalent SNR as:

$$C_{\mathrm{RFMux}} = \log_2(1+\gamma_{eq}) \quad (3.6)$$

γ_{eq} represents the SNR whereby the average capacity among the RF channels in the RF-Mux is achieved:

$$\gamma_{eq} = (\prod_{l=1}^{N_{RF}} (1 + \gamma_{f_n}))^{1/N_{RF}} - 1 \tag{3.7}$$

A further simplification of (3.7) is possible for high SNR values ($\gamma >> 10$):

$$\gamma_{eq} \approx (\prod_{l=1}^{N_{RF}} (\gamma_{f_n}))^{1/N_{RF}} \tag{3.8}$$

Or, in dB:

$$\Gamma_{eq}[dB] \approx \frac{1}{N_{RF}} (\sum_{l=1}^{N_{RF}} (\Gamma_{f_n}[dB])) \tag{3.9}$$

According to the previous formulation, the potential coverage gain can be defined as:

$$G(dB) = \Gamma_{eq} - \min_{n}(\Gamma_{f_n}) \tag{3.10}$$

where $\min_n(\Gamma_{f_n})$ represents the SNR of the RF channels that limits the reception of the complete service offering

3.2.2 Performance Analysis Based on Physical Layer Simulations

The performance of inter-RF FI is evaluated by means of physical layer simulations. Basic simulation models for the DVB-T2 and DVB-NGH standards are explained in Appendix B. The model for emulating the inter-RF FI transmission is also described.

Performance is studied considering DVB-T2 for fixed roof-top reception (Rician F1 [54] channel). The selected mode is 8 MHz, 32k, 1/4 64QAM. 4 RF channels (474 MHz, 570 MHz, 666 MHz and 762 MHz) are transmitted and their average signal imbalance, given by the model in [55], is used to emulate a transmission in a RF-Mux. Mobile reception in DVB-NGH (TU6 channel [56]) is evaluated considering a fixed Doppler shift for all frequencies ($f_d = 80$ Hz) but the imbalances due to the different signal level per RF channel as in the previous case. Each quarter of the transmitted data is received with a different SNR imbalance according to the model. Figure 3.4 illustrates the performance (in terms of Frame Error Rate (FER)) for different code rates.

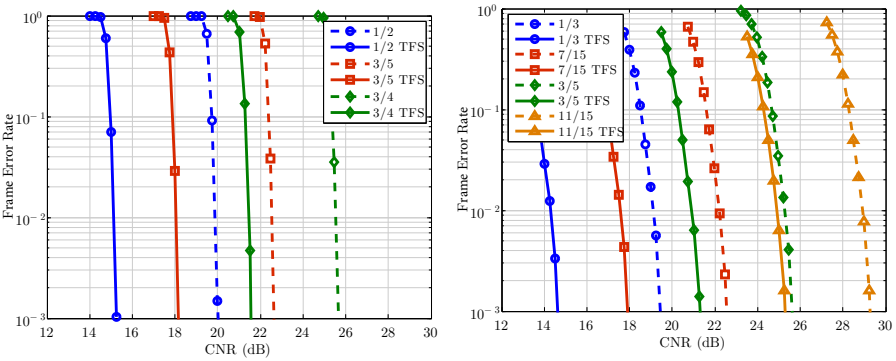

Figure 3.4: Performance of inter-RF FI in the Rician F1 channel for 3 DVB-T2 modes (above) and the TU6 channel ($f_d = 80$ Hz) for 4 DVB-NGH modes (below). FER curves with 64QAM and different code rates according to the standards.

Table 3.1: TFS gain as function of the code rate

Mode	TFS gain	Mode	TFS gain
DVB-T2 Rice 1/2	4.8	DVB-NGH TU6 1/3	4.9
DVB-T2 Rice 3/5	4.5	DVB-NGH TU6 7/15	4.7
DVB-T2 Rice 3/4	4.1	DVB-NGH TU6 3/5	4.4
		DVB-NGH TU6 11/15	4.0

The dashed lines represent the performance of the worst RF channel (the one with the lowest SNR). The difference between solid and dashed lines results in the coverage gain. In this case, the achievable gain is around 4.5 dB for FER 10^{-3} (see Table 3.1). The gain depends on the error-correcting capabilities of the code rate. This effect is more evident in the simulation with DVB-NGH obtaining a difference of 0.9 dB gain between code rate 1/3 and 11/15.

The impact of RC in performance is computed for DVB-NGH and the same channel configuration. Three code rates are selected for QPSK: 1/3, 7/15 and 11/15. In this case, a fixed imbalance of -6 dB in one of the RF channels in the RF-Mux is considered. The imbalance of the other channels is set to 0 dB. Figure 3.5 represents the achieved performance with 2DRC for a RF-Mux of 2 and 4 RF channels. The performance of the worst RF channel is shown with dashed curves.

According to the results, the gain by inter-RF FI decreases with increasing code rates. It can be seen that the difference between the curve corresponding

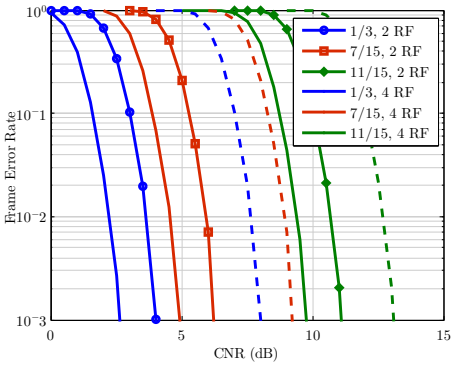

Figure 3.5: Performance of inter-RF FI with rotated constellations for DVB-NGH QPSK 1/3, 7/15 and 11/15. Dashed lines correspond to the performance of the channel with -6 dB imbalance.

to code rate 11/15 is closer to the worst channel than the curve for code rate 1/3 with respect to the worst channel for the same MODCOD.

Inter-RF FI Performance in Slow Time Varying Channels

The previous simulations with the TU-6 channel model have only considered the effect of the RF-Mux imbalances but with a fixed Doppler shift per RF channel. In reality the effect of Doppler shift is present and each RF channel experiences a different behaviour as a function of the frequency. Thus, besides the effect of the imbalance, transmitted data also suffers variations due to Doppler effect.

To illustrate the potential gain of inter-RF FI in such conditions, 4 independent TU-6 channels are generated with a Doppler shift (f_D)[3] according to the frequency as described in Table 3.2 for a receiver speed of 3 km/h (pedestrian reception) and 135 km/h (vehicular reception). In this case, Doppler effect is evaluated isolated and RF channel imbalances are not computed.

Figure 3.6 depicts the simulation results for the NGH mode QPSK 1/4 with a TI duration limited to 100 ms. The Doppler differences at 3 km/h are small, the curves for each RF channel show a similar performance. However, the effect

[3]Doppler shift is defined by

$$f_d\,(\text{Hz}) = v\,(\text{m/s}) \cdot \frac{f_c\,(\text{Hz})}{c\,(\text{m/s})}$$

where v is the receiver speed, f_c is the carrier frequency of the RF channel and c is the light speed.

Table 3.2: Doppler shift f_d (Hz) per RF channel

Speed	RF1 503 MHz	RF2 533 MHz	RF3 563 MHz	RF 4 593 MHz
3 km/h	1,4	1,48	1,56	1,65
135 km/h	62,88	66.63	70,38	74,13

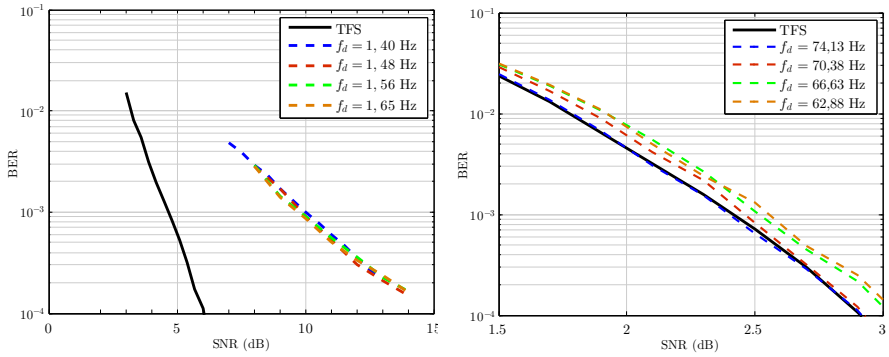

(a) $v = 3$ km/h (b) $v = 135$ km/h

Figure 3.6: Performance of inter-RF FI considering Doppler effect at 3 km/h and 135 km/h for the same RF-Mux. TU-6 channel model.

of the non-correlation between the channels is translated into a significant gain when using inter-RF FI (TFS) that copes with the insufficient TI duration for such slow-varying channel. On the contrary, the gain at higher speed is limited.

3.3 Characterization and Modelling of the Coverage Gain in the VHF and UHF bands

The increased RF performance by inter-RF FI can be translated into a coverage gain where all services can be received with a global SNR thanks to the achieved averaging between the good and bad SNR levels of the different RF channels.

The main features influencing the measured SNR at the receiver are explained next considering the transmitter and receiver sides. The effects of propagation are covered in the next section.

The SNR is a measure of the quality of the received signal. The measured SNR at the receiver conditions the reception or not of a given RF channel. In DTT systems, error-free reception is possible as soon as the measured SNR is higher than a given threshold (set by the selected transmission configuration). The SNR required by the system conditions the required signal level at the receivers at a given percentage of locations, what defines the coverage area of a service. If measured in each RF channel, the SNR experiences differences depending on the degradation the signal suffers in each RF channel. The main sources of imbalances between RF channels involve the transmitter and receiver antenna gains, the propagation loss and the noise figure of the receiver. The received power of a particular RF channel, denoted as P_r, can be calculated taking into account the transmission power of the station delivering the service P_t, the path loss attenuation L_p and the transmitter G_t and receiver G_r antenna gains as:

$$P_r = P_t G_t G_r L_p^{-1} \tag{3.11}$$

Background noise is given by:

$$P_n = kTBF \tag{3.12}$$

where k is the Boltzmann constant, T is the ambient temperature in Kelvin, B is the channel bandwidth, and F is the noise figure of the receiver. The SNR at the receiver, denoted as γ, given in linear scale, is calculated as:

$$\gamma = \frac{P_r}{P_n} = \frac{P_t G_t G_r L_p^{-1}}{kTBF} \tag{3.13}$$

How frequency affects each of the parameters in the equation leads to a different SNR per RF channel, thus, affecting their reception.

Transmitter Characteristics

Stations are usually configured to use the same ERP per RF channel. However, one of the sources for larger differences among the received signal from different frequencies comes from the antenna diagram.

ITU Recommendation BS.1195 [57] provides guidance on the the basic theoretical principles of VHF and UHF antennas and some example of antenna systems at the transmitter stations. VHF and UHF antennas usually consist of an array of elementary radiators (narrow or broadband, linearly or circularly polarized) which conform a panel that enables broadband operation (e.g. the complete UHF bands IV/V in the range 470 MHz - 862 MHz). A compromise exists between the bandwidth and the smoothness of the antenna diagram. The

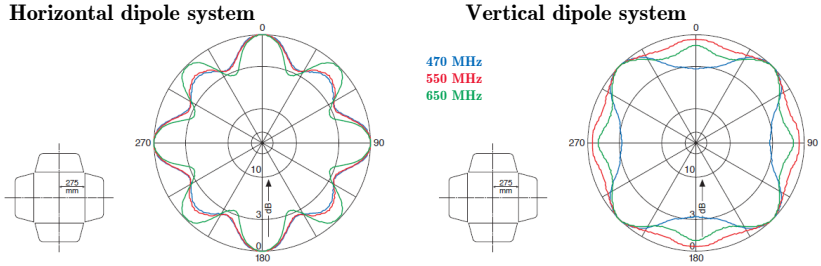

Figure 3.7: Horizontal and Vertical radiation patterns of two commercial UHF antennas. Source: Kathrein.

VHF Band III panels operating in the range 174-230 MHz have gain figures from 10 to 14 dB. A slight gain reduction is produced in case of vertical polarization. At UHF the reduced size of the radiating elements allows the assembly of panels with more directional radiation patterns. Typical gain values are around 10 to 12 dB.

Omni-directional antenna systems are obtained by feeding 4 or more antenna panels with equal power. However, the resulting diagram presents a ripple in azimuth which is proportional to the tower height, in wavelengths. Figure 3.7 shows a commercial panel antenna system design with horizontal and vertical polarization.

In practice, even good UHF antennas have variations in their antenna diagram in the order of 3 to 6 dB [58] at different frequencies as a function of the azimuth angle. Sometimes also very large notches appear for a certain direction and frequency. Furthermore, the physical characteristics of the tower, the coupling effects between antennas, the metallic structure of the platform or even the presence of other antenna systems also influence the performance.

Receiver Characteristics

Reception is typically achieved by directional roof-top antennas pointed towards the main transmitter station. For network planning purposes a reference antenna with a constant antenna gain is used. In reality, gain tends to increase with frequency to compensate the decreasing field strength level due to propagation loss.

In [46], a constant antenna gain of 11 dB_d is recommended for network planning in the UHF band (regardless of the RF channel frequency). It should be noted that whereas ITU-R BT.419 [59] describes a mask for the receiving antenna directivity to be used in network planning, this recommendation

does not provide any requirement on antenna design. ITU Recommendation BT.2138 [60] describes several measurements of the radiation patterns of receiving antennas. Different types of antenna includin Yagi, phased arrays or combinations with different elements are studied. Up to 7 dB gain variations are found between different antenna models. For each antenna, variations are also found between frequencies 620 MHz and 790 MHz. In general gain tends to increase with frequency although in some cases it is kept constant. The maximum difference is 4.3 dB for a Yagi antenna. Three other antennas present differences in the order of 1 to 2 dB. In [61] measurements on UHF antenna gain shows variations of 3-5 dB from the extreme frequencies in the UHF band (after DD1, 470-790 MHz).

In addition to antenna frequency dependency, the noise figure of the receivers can also increase with frequency (1 or 2 dB in the UHF band) as explained in [25] from measurements over 4 different set-top-boxes.

3.3.1 Analysis of the Frequency-Dependent Characteristics of Propagation based on Models

Terrestrial broadcasting networks are traditionally planned for the provision of services to roof-top receivers. Fixed reception is characterised by a fixed directional receiving antenna mounted on the roof of a house (generally at a reference height of 10 m). Portable indoor and outdoor reception are also relevant for terrestrial broadcasting. However, these types of reception are more demanding than roof-top reception due to the lower receiver height (reference height of 1.5 m), the use of omni-directional antennas and the transmission through walls. In some countries, networks are also optimized to provide indoor reception in highly-populated areas.

Propagation at VHF and UHF frequencies is mainly affected by the environment features. The wavelength of these signals is smaller than the size of elements such as buildings, vegetation or terrain features. As a result, propagation is mainly conditioned by the following mechanisms [62]:

- *Diffusion due to distance between transmitter and receiver.*

  Radiated signals suffer a loss in power when they are far away from their sources. This loss does not only increase with distance but also with frequency.

- *Multipath propagation due to reflection from radio-electrical flat surfaces.*

  Reflection cause changes in the phase of the waves, that, in turn also depend on frequency. A reflection cause a secondary path which can

reach the receiver in a constructive or destructive way, thus, affecting the received signal power and generating fading.

- *Scattering from irregular surfaces.*

  Similarly to reflection, scattering is produced at irregular surfaces. In this case reflections are totally incoherent with the main signal. The main effects on the received signal are the appearance of slow fading, which causes large differences on the signal level with small receiver's position changes.

- *Refraction due to changes in the atmosphere.*

  This effect is caused by the variation of the refraction index at different layers of the atmosphere, which changes over time. This variability over time is also distance and frequency-dependent. The highest amount of variability is seen for UHF frequencies over sea path (around 10 dB and 20 dB standard deviation at distances 50 km and 150 km). For UHF land and VHF land and sea, the variability reaches around 4 dB at 50 km and 8 dB at 150 km.

- *Diffraction due to solid obstructions.*

  Diffraction is caused by obstruction in the line of sight between the transmitter and the receiver such as mountains, buildings, etc.

- *Absorption due to objects that attenuate RF energy.*

  Absorption at media such as building materials, vegetation and vehicles have an impact on the received field strength. Again, the properties of the materials may produce frequency-dependent losses.

Several models have been developed to account for these characteristics for network planning and signal level estimation purposes. The frequency-dependent characteristics of propagation are studied next considering the most relevant propagation models available in the literature for path loss estimation in the VHF and UHF bands and considering fixed and outdoor and indoor portable reception. A wide explanation of the models is available in Appendix C.

Fixed Roof-top reception

The ITU-R P.525 recommendation [63] is the basic model which estimates loss as a function of the distance and frequency. In particular, path loss increases as the square of distance and frequency (20 dB/decade). However, this model

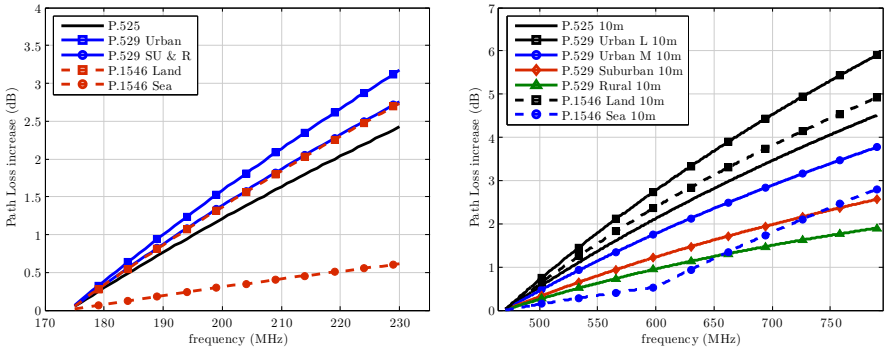

Figure 3.8: Left: Path loss increase with respect to the lower bound of VHF frequency band (174 MHz) for fixed roof-top (10 m) and portable outdoor (1.5 m) reception. Right: Path loss increase with respect to the lower bound of UHF frequency bands (470 MHz) for fixed roof-top (10 m) reception.

does not account for other propagation mechanisms such as those related above. More elaborated models are used instead.

The ITU-R P.529 recommendation [64] provides equations to estimate the path loss for urban areas (medium-small or large cities), suburban and rural areas based on field measurements. The ITU-R P.1546 [65] is the standard propagation model for VHF and UHF for a wide range of parameters and environments. The Longley-Rice model [66] include the properties of the terrain ground curvature, subsoil, and climate.

Figure 3.8 depicts the path loss increase with frequency for P.525, P.529 and P.1546 models with respect to the lower bound of the VHF band and the UHF band.

With P.525, the maximum difference is found for RF channels allocated in the extreme positions of the VHF band (with a maximum imbalance of 2.4 dB) and UHF band. For UHF after DD1 the difference reaches 4.5 dB and 3.5 dB for UHF after DD2. It can be seen that the differences increase more rapidly for VHF than UHF.

All corrections of the P.529 model are frequency-dependent and the frequency differences are also sensitive to receiving antenna height. The frequency behaviour of the model is distance-independent for distances shorter than 20 km but path loss increases with frequency for larger distances. This characteristic can be seen in Figure 3.9 which depicts the path loss difference between two RF channels, one located in the medium part of the UHF band and another in the medium VHF band. The path loss imbalance increases quasi-linearly with distance.

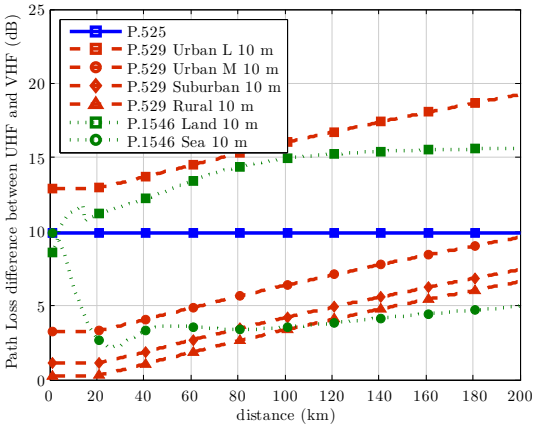

Figure 3.9: Path loss increase with distance between the medium VHF band frequency (202 MHz) and UHF band (630 MHz) for fixed roof-top (10 m) reception.

At 20 km and at VHF, the path loss difference reaches a maximum of 3.2 dB for both large cities and medium-small cities in urban areas. For suburban and rural areas the maximum difference is 2.7 dB. At UHF, large urban areas reach a maximum difference of 5.9 dB whereas for medium-small areas it is 3.8 dB. For suburban areas, the differences reach 2.5 dB whereas they decrease to 1.9 dB in rural areas.

For ITU-R P.1546 at 20 km, the frequency increase is larger for land paths than sea paths. The differences between cold and warm sea are irrelevant. The largest difference for UHF band is 4.9 dB whereas for VHF it is 2.7 dB.

Figure 3.9 illustrates the path loss difference between the centre frequency in UHF (630 MHz) and VHF (202 MHz) bands as a function of path range. For P.529, large urban areas at UHF involve 13 dB more path loss than VHF band, at 20 km.

With the default values of the Longley-Rice model included in [66] and at 20 km distance, Table 3.3 shows the maximum differences in path loss between frequencies in the UHF and VHF bands for different environments and fixed roof-top reception.

It can be seen that the differences increase with the irregularity of the terrain. The extreme frequencies in UHF band lead to a maximum path loss imbalance of 9.2 dB whereas for plain terrain it is around 1.6 dB at VHF and 5.4 dB at UHF.

Table 3.3: Maximum path loss difference between the extreme frequencies in VHF and UHF bands and difference between the path loss at the centre frequency of UHF and VHF bands

Type of environment	VHF (dB)	UHF (dB)	UHF vs VHF (dB)
Flat or Water	0.1	4.5	5.2
Plains 30 m	1.6	5.4	6.9
Hills 90 m	1.5	5.4	3.3
Mountains 200 m	2.1	6.8	8.2
Rugged Mountains 500 m	3.9	9.2	17

Table 3.4: Height loss (dB) for different environments in VHF and UHF bands

Frequency (MHz)	Band III	Band IV/V	Difference
Urban	19	23.5	4.5
SubUrban 30 m	12	17	5
Rural 90 m	12	16.5	4.5

Portable outdoor reception

Portable reception involves receivers at 1.5 m. P.529 explicitly account for the receiver antenna height in its path loss expressions. For the Urban area in large cities, the frequency difference between RF channels in the same band (VHF, below 300 MHz, and UHF, above 300 MHz) do not produce a path loss difference with antenna height. For medium-small cities, the frequency difference between RF channels depends on the receiver height. At VHF, the path loss increase for P.529 is the same as for fixed reception (see Figure 3.8). The maximum path loss increase is found for urban areas in UHF band (5.9 dB), as depicted in Figure 3.10 (left). Regarding suburban and rural areas, the maximum increase is reached in UHF band (4.7 dB and 4 dB, respectively). For portable reception, P.529 for rural areas is optimistic with respect to the Free-Space loss model. Regarding the frequency differences between UHF and VHF band, Figure 3.10 (right) depicts the differences as a function of the distance for this model. It can be seen that the maximum differences are found in the urban areas which can reach more than 15 dB difference at 70 km distance.

Other models such as the ITU-R P.1546 are described for a reference height of 10 m. In order to derive the path loss prediction for portable reception, a correction (height loss) needs to be introduced based on a receiving antenna near ground floor level, at 1.5 m. This correction is specified for different types of environments in [67] which are shown in Table 3.4.

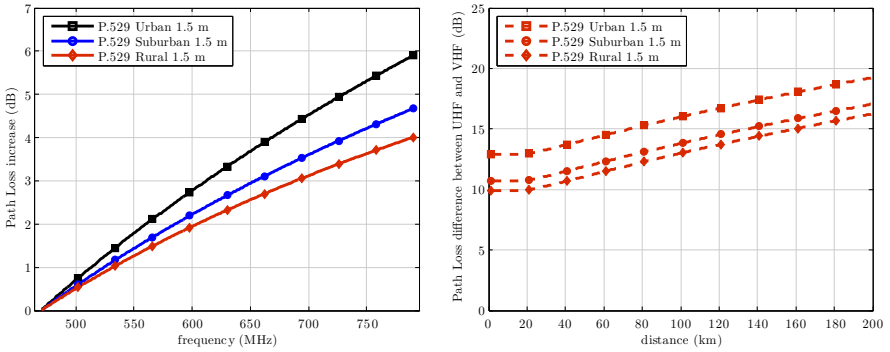

(a) UHF

(b) UHF compared to VHF

Figure 3.10: Path loss increase with respect to the lower bound of UHF frequency band (470 MHz) for portable outdoor (1.5 m) reception at $d = 20$ km and as a function of the distance.

Portable outdoor reception is also affected by absorption produced by the materials surrounding the receiver such as building materials, vegetation or vehicles. As an example, ITU-R P.833 Recommendation [68] provides values for attenuation due to vegetation in woodland reception conditions. According to this, a path loss attenuation difference of 0.08 dB/m is found between 466.475 MHz and 105.9 MHz and a difference of 0.05 dB/m is found between 949.0 MHz and 466.475 MHz, based on measurements. These additional attenuations may also be considered in network planning of the services.

Portable indoor reception

Portable indoor reception is another particular scenario which involves accounting for the building penetration, from outdoor-to-indoor and also propagation inside the building where the signal finds different obstacles as well as walls and floors.

The building penetration loss is defined as the difference, in dB, between the mean field strength registered inside and outside a given building at the same height above ground level. Different measurement campaigns report the height loss for different environments in VHF and UHF bands. The VHF measurements are linked to the deployment of Digital Audio Broadcasting (DAB) services in Band III in the UK [69, 70]. The UHF measurements are linked to the deployment of DVB – Handheld (DVB-H) services [71]. The results indicate that the mean value of building penetration loss is 9 dB and 3 dB in VHF and UHF bands, respectively. However, due to the disparity of values found in

Table 3.5: Building penetration loss in VHF and UHF bands

Band	Mean Value (dB)	Std. Dev (dB)	90% confidence interval
Band III	9	3	13.9
Band IV/V	3	6	11.8

the measurement campaigns associated values of standard deviation are given in Table 3.5. The values for a confidence interval of 90% are also given.

Regarding indoor propagation, a common approach in many existing planning tools is to predict the path loss outside in the proximity of the buildings and then add a loss (mean value and standard deviation) in order to estimate the loss inside the building. In this case, the penetration loss can be divided in multiple factors such as wall loss, room loss, floor loss and building loss. These factors are frequency-dependent. However, it is commonly assumed that the same values apply for the frequencies in the same band. The frequency behaviour of the signal is taken as the free space loss term, given in equation (C.1).

Portable (handheld) reception is also characterized by body loss. Radiated energy is absorbed by human tissue what leads to additional loss. ITU-R P.1406 [72] provides loss factors of typical body loss for both waist- and head-height reception. The attenuation is higher when the antenna is at waist height. A median body loss of 10 dB and 20 dB is found for the lower end of VHF band for waist and head height levels, respectively. For the upper end, loss is reduced to 7 dB and 16 dB, respectively. For UHF, the loss at 470 MHz is around 5 dB and 13 dB whereas for 790 MHz it is around 9 and 15 dB, respectively.

3.3.2 Link Budget and Coverage Definition Implications

In order to illustrate the advantage in terms of a link budget gain, it is possible to translate the gains into an extension of the area extension where all services can be received in a traditional deployment. The area extension is calculated using the different propagation models presented here. The relative increase in distance is performed assuming an initial distance of 20 km. Assuming a cell of circular shape, the area gain is equal to the square of the cell radius gain. Table 3.6 presents the corresponding coverage extension for the different environments and models considered in the analysis[4]. The highest advantage is found when it is possible to spread the RF channels of the RF-Mux evenly

[4]The models in Table 3.6 are coded as A: P.525, B: P.529 Urban Large, C: P.529 U. Medium, D: P.529 Suburban, E: P.529 Rural, F: P.1546 Land, G: P.1546 Sea

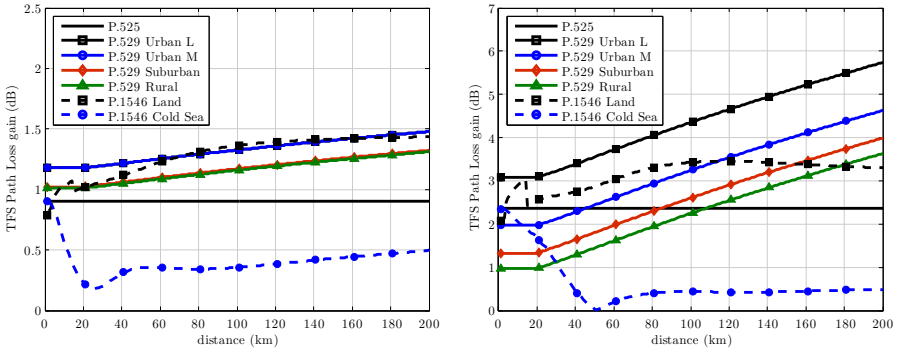

(a) VHF (b) UHF

Figure 3.11: Path loss gain for VHF (117.5 - 191.5 - 205.5 - 219.5) and UHF (474 - 578 - 682 - 786) frequency arrangements with inter-RF FI.

Table 3.6: Area increase for all services in the RF-Mux with respect to a traditional DTT network

RF-Mux frequencies (MHz)	A	B	C	D	E	F	G
117.5 - 191.5 - 205.5 - 219.5	23%	15%	15%	15%	13%	11%	3%
191.5 - 198.5 - 205.5 - 212.5	11%	7%	7%	6%	6%	5%	1%
474 - 578 - 682 - 786	72%	42%	25%	16%	12%	27%	29%
618 - 626 - 634 - 642	4%	2%	2%	1%	1%	2%	2%

across the broadcast bands. Conversely, when the allocation is made by means of adjacent RF channels, it is not possible to exploit large path loss gains.

Note that the area extension by inter-RF FI can be translated into a coverage gain when also other parameters involved in the coverage calculation are taken into account. In order to illustrate the practical coverage gain, an study in [25] presents the reception of 4 RF channels transmitting a DVB-T2 signal. Whereas the individual reception of at least 1 RF channel is possible in a wide area (around 3000 km^2), reception of the complete service offer is, however, restricted to locations closer to the transmitter station (1350 km^2). Service area can be increased by 60% (2150 km^2) when implementing inter-RF FI.

For planning issues coverage is calculated according to the equivalent field strength needed to ensure that the minimum values of signal level (given by

Table 3.7: Frequency dependent parameters at receiver side

	VHF Rec	UHF Rec	Variation
F	6 dB	6 dB	-
L_f	2 dB	4 dB	-
G_d	7 dB_d	11 dB_d	$10\log_{10}(f/f_R)$
A_a	1.7 dBm^2	-4.6 dBm^2	$10\log_{10}(\frac{1.64{\lambda_f}^2}{4\pi})$
P_{mmn}	2 dB	0 dB	-

the C/N system threshold and the noise power) can be achieved at the required percentage of locations. For this purpose the following formulas are used:

$$\begin{aligned} P_{s_{min}} &= P_n + C/N_{th} \\ \phi_{min} &= P_{s_{min}} - A_a + L_f \\ \phi_{med} &= \phi_{min} + P_{mmn} + C_l \\ E_{med} &= \phi_{med} + 120 + 10\log_{10}(120\pi) = \phi_{med} + 145.8 \end{aligned}$$

where $P_{s_{min}}$ is the minimum receiver input power (dBW), ϕ_{min} is the minimum power flux density at receiving place (dBW/m^2), ϕ_{med} is the minimum median power flux density (dBW/m^2), E_{med} is the minimum median equivalent field strength ($\text{dB}\mu\text{V/m}$). P_n is the noise power (dBW), C/N_{th} is the system required C/N (dB), A_a is the effective antenna aperture (dBm^2), L_f is the feeder loss (dB), P_{mmn} is the allowance for man-made noise. C_l is the location correction factor to be applied according to the percentage of locations to be covered. Note that for portable reception, building penetration loss as well as heigh loss should be also considered.

According to the previous equations, even when the C/N_{th} is the same for each RF channel, the required received signal level differs from RF channel to RF channel. In general, values are provided for a reference frequency (i.e. f_R = 200 MHz for VHF and f_R = 650 MHz for UHF, according to [46]). Table 3.7 summarizes the values given for network planning and their differences with frequency for fixed rooftop reception.

Reference [46] also establishes a practical equation for frequency interpolation of the minimum median field strength the UHF band with a variation of $K\log_{10}(f/f_R)$. K takes a value of 20 for fixed reception and 30 for portable reception.

Table 3.8: Standard deviation of the time variability for VHF and UHF bands

Band	$d = 50$	$d = 100$	$d = 150$	$d = 175$
VHF Land and Sea	3	7	9	11
UHF Land	2	5	7	-
UHF Sea	9	14	20	-

Time and Location Variability

DTT reception is characterized by a rapid transition between perfect (or quasi-perfect) reception and no reception at all. It is critical to determine those areas which are going to be covered and those which are not. Taking into account the worst case in the area would imply a high cost. Thus, coverage needs to be guaranteed for a given percentage of locations. In general, small areas (typically 100 m x 100 m) with 'good' coverage are those in which 95% of locations are covered.

Received signal strength present variation in time and location domains around the mean signal strength derived from the propagation models. ITU-R P.1406 Recommendation [72] indicates how median signal strength received from a transmitter varies over time and distance. This effect is linked to the refraction index of the atmosphere, which changes over time.

Table 3.8 shows the standard deviation of the time variability for VHF and UHF.

It shows that the highest variability is found for UHF frequencies in the maritime environment, whereas VHF presents the largest differences for terrain paths. The variability is also higher for large distances rather than short ones.

Regarding location variability, it is mainly caused by shadow fading, reflection and scattering. These effects cause variations of the signal strength between different areas (generally of hundreds of squared meters). These variations are also taken into account by means of a standard deviation. ITU-R P.1406 presents expressions of the standard deviation according to different environments. ITU-R P.1546 derives a simple expression for the location variability standard deviation in dB, σ_L, based on measurement campaigns:

$$\sigma_L = K + 1.3 \cdot \log_{10}(f) \tag{3.14}$$

Where K is set to 1.2 for mobile receivers below clutter height in urban and suburban areas; 1.0 for roof-top reception near clutter height; and 0.5 for receivers in rural areas.

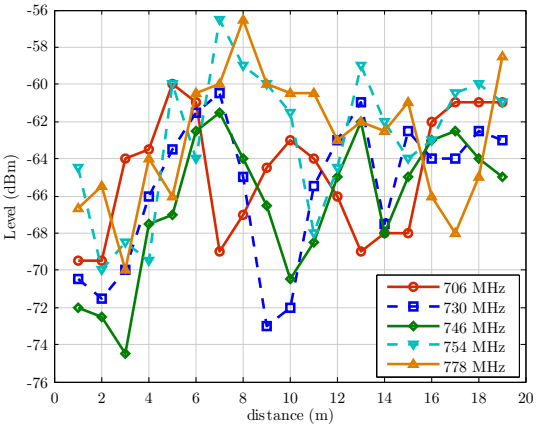

Figure 3.12: Local variation of the signal level at 10 m height.

Regardless of the environment, there exist a maximum difference in the standard deviation of 0.16 dB between RF channels in the VHF band and 0.3 dB in UHF.

For planning purposes a larger location variability standard deviation value is used to account for multipath fading and for variations over larger areas. Typically a value of 5.5 dB is used for DTT in VHF and UHF bands. In [73], authors indicate that the value of 5.5 dB is pessimistic for UHF band.

3.3.3 Analysis and Modelling of the Coverage Gain based on Outdoor Field Measurements

A set of measurements provided by the Swedish operator Teracom is processed and analysed in order to evaluate the potential coverage gain by inter-RF FI from a real network deployment. Figure 3.12 shows an example of the signal level variations at 10 m measured over 5 RF channels (706, 730, 746, 754, and 778 MHz) in a 20 m path. It can be seen that whereas the frequency difference between RF channels is not high (below 100 MHz), some points present a difference of various dB. The mean signal level is 1 to 5 dB stronger than the worst RF channel, depending on the position. The RF channel limiting the reception of all RF channels is not always the same (e.g 778 MHz values are not always the lowest). The largest differences within these frequencies are around 10 dB.

Measurement data at 3 m height (see Appendix A) is used to evaluate the imbalances existing between RF channels and the derived coverage gains when

Table 3.9: RF channel allocation in the measured areas and maximum frequency separation

	Frequencies (MHz)				
Area	f_1	f_2	f_3	f_4	$f_4 - f_1$
A	498	546	578	626	128
B	514	722	754	786	272
C	578	602	626	698	120
D	474	530	674	730	256
E	562	618	682	754	192
F	594	674	786	802	208

using inter-RF FI. The data is obtained by measuring the signal strength of a series of different RF channels in a cyclic manner. Measurements are taken in 6 different areas (A to F) for the RF channels collected in Table 3.9 in Appendix A. The fifth column of the table also depict the frequency separation between the maximum and minimum frequencies of the 4 RF channels (f4 - f1). As it can be observed, the distribution of the channels inside the UHF band differs in each area since both the maximum separation between them and their location within the band are not the same.

Modelling the signal level imbalances between RF channels

In a first stage, the measurements are processed in order to study the frequency dependency of the imbalances between the level of the RF channels for each given location and area. From this, a model is developed to estimate the signal imbalances between pairs of RF channels in the UHF band[5] .

The level difference (imbalance) between each pair of frequencies (f_j and f_i) is computed for each measurement location. The resultant series of values are separated into an average value and a standard deviation as depicted in Figure 3.13 (left) and Figure 3.13 (right), respectively. According to this analysis, the differences between the signal level of two RF channels increase with frequency both in average and standard deviation. The highest values reach up to 10 dB average difference with standard deviations ranging 2 to 5 dB.

[5]The content of this section is partially published in: J. J. Giménez, D. Gozálvez, D. Gómez-Barquero, and N. Cardona, "Statistical model of the imbalance between RF channels in DTT network," *Electronics Letters*, vol. 48, no. 12 pp. 731-732, June 2012. Reproduced by permission of the Institution of Engineering & Technology.

With these calculations, it is possible to establish a model (Equation 3.15) that fit the measurements by means of two different factors:

- A mean value (ΔP_{PL}). The mean value of the difference between the signal strength of two channels is modelled by means of an offset component which depends on the ratio between frequencies f_j/f_i.
- A statistical component (ΔP_{FS}). The variability of the imbalances within each measured area is modelled by means of a random distribution $\Delta P_{FS} \sim \mathcal{N}(0, \sigma^2_{FS})$ which depends on the frequency separation between the channels $\Delta f = f_j - f_i$ as an exponential-based function with three parameters (K_1, K_2 and K_3) given by Equation 3.17.

$$\Delta P(dB) = \Delta P_{PL}\left(\frac{f_2}{f_1}\right) + \Delta P_{FS}(\Delta f) \tag{3.15}$$

$$\Delta P_{PL} = K_{PL} \cdot \log_{10}\left(\frac{f_2}{f_1}\right) \tag{3.16}$$

$$\sigma_{FS} = K_1 + K_2 \cdot \exp^{-\frac{\Delta f}{K_3}}, \Delta f \in [1, 384] MHz \tag{3.17}$$

In order to parametrize the model to the measurement data, the non-linear function minimization method described in [74] is used. With this, the model is fit to the measurement data by estimating the K_{PL}, K_1, K_2 and K_3 parameters that apply to the 6 areas.

The dash-dotted curve in Figure 3.13 (left) corresponds to the mean value of the imbalance ΔP_{PL} computed with the model in equation (3.16) and the obtained K_{PL}=44.

Figure 3.13 (right) depicts the standard deviation of the received signal strength imbalance for each pair of RF channels according to the frequency separation between the channels in each pair. According to the figure, we can see that the standard deviation varies between 2.5 dB and 5 dB depending on the frequency separation. The dash-dotted line represents the standard deviation obtained by the model in equation (3.17) with $K_1 = 6.4$, $K_2 = -4$, and $K_3 = 327$.

Figure 3.14 compares the PDFs of the received signal strength imbalance computed with the model in (3.15) and the real imbalance obtained in the measurement data for 3 data sequences. The model closely approximates the measurement data.

Modelling of the coverage gain with inter-RF FI

In order to characterize the coverage gain when different RF channels are bundled, the difference between the equivalent SNR of the RF-Mux and the mini-

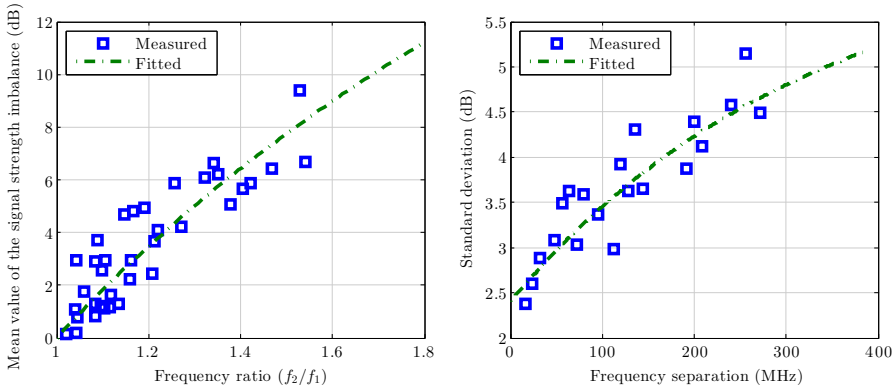

(a) Mean value (b) Standard deviation

Figure 3.13: Mean value and standard deviation of the received signal strength imbalance between two RF channels as a function of f_2 and f_1. Reproduced by permission of the Institution of Engineering & Technology.

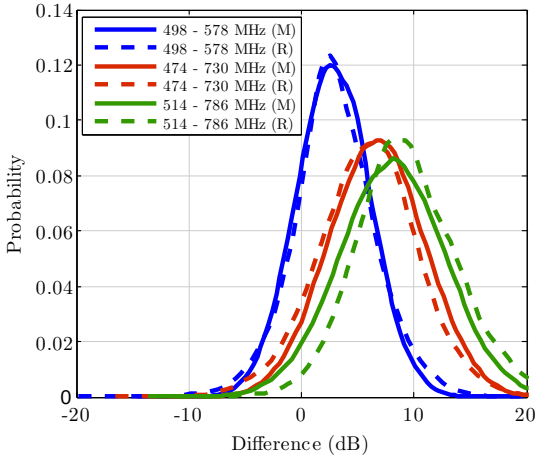

Figure 3.14: PDFs of the received signal strength imbalance between two RF channels with different frequency separations according to the proposed model (M) and the measurement data (R). Reproduced by permission of the Institution of Engineering & Technology.

mum SNR is calculated. Since the level of the measurements is normalized, the

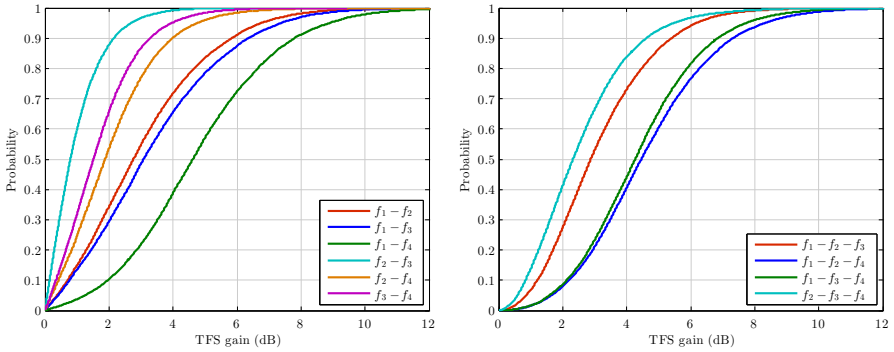

(a) 2 RF channels

(b) 3 RF channels

Figure 3.15: CDF of the coverage gain per transmitter area. $\delta = 20dB$.

signal level of each RF channel is set to any other SNR by adding an offset δ (e.g. 0 dB, 10 dB, 20 dB,...) to each of the RF channels as:

$$SNR_{i\delta_{dB}} = S_{i_{dB}} + \delta_{dB} \tag{3.18}$$

As an illustrative example, computing the coverage gain for area B for 4 RF channels (f_1, f_2, f_3 and f_4) shows that increasing the SNR provides the most conservative gain values. The coverage gain is found to be a Rayleigh-like distribution with an average of around 4.5 dB but with significantly higher values for a portion of locations. It is also significant that the number of locations without gain is minimum. Figures 3.15 depicts the CDFs of the gains for different frequency combinations with 2 and 3 RF channels.

Table 3.10 summarizes the average gain for all the possible combinations between 4 RF channels for the 6 transmitter areas assuming a value of $\delta = 20$ dB.

In general, gains are higher for the RF-Muxes with 4 RF channels. However, there exist cases in which 2 RF or 3 RF channels already achieve similar gains. Such cases in which the gains are quite similar to those reached with 4 RF channels are indicated in **bold** in the same table.

Results show that the gain increases with the frequency separation between the highest and lowest RF channels (f_{max} and f_{min}, respectively). The gain reaches the highest value for the maximum frequency separation between the RF channels in the RF-Mux. The reason is that the higher the frequency separation between f_{max} and f_{min} is, the higher the signal strength imbalance between them is (and also is the difference between SNR_{eq} and SNR_{min}, which

Table 3.10: Coverage gain for RF-Mux combinations

TFS-Mux	A (dB)	B (dB)	C (dB)	D (dB)	E (dB)	F (dB)
$f_1 - f_2$	1.2	3.1	1	1.5	1.7	1.2
$f_1 - f_3$	1.9	3.4	1.3	3.2	2.6	**3.2**
$f_1 - f_4$	**3.2**	**4.8**	1.8	3.6	**3.7**	**3.3**
$f_2 - f_3$	1.3	1.0	1.1	2.4	1.6	2.5
$f_2 - f_4$	2.5	2.1	1.6	2.8	2.5	2.6
$f_3 - f_4$	1.7	1.7	1.2	1.4	1.8	0.9
$f_1 - f_2 - f_3$	2.2	3.1	1.7	3.8	2.8	**3.8**
$f_1 - f_2 - f_4$	**3.9**	**4.7**	2.3	**4.4**	**4.1**	**3.9**
$f_1 - f_3 - f_4$	3.3	**4.4**	2.2	3.6	3.7	3.0
$f_2 - f_3 - f_4$	2.9	2.6	2.0	3.0	2.9	2.6
$f_1 - f_2 - f_3 - f_4$	**3.8**	**4.4**	**2.5**	**4.3**	**4.1**	**3.8**

is directly involved in the gain calculation). Hence, the number of RF channels in the RF-Mux is not a critical parameter for the gain. Instead, the TFS gain also depends on the internal distribution of the RF channels within the UHF band. In particular, it tends to increase with the average separation between f_{max} and each RF channel f_i.

A more precise analysis of the effect of the distribution of the RF channels within the UHF band can be derived from Figure 3.16, where the gains are compared for different RF channel aggregations with the same maximum frequency separation. Gains are similar for each area.

In general, the SNR of the received RF channels is larger for the RF channels in the lower side of the UHF band than for those allocated in the upper side. Hence, the equivalent SNR, defined in equation (3.7), will be lower when increasing the number of RF channels located in the upper side of the band (low values for the mean f_{max} - f_i). Therefore, the gain for these RF-Muxes will be also lower.

According to the behaviour observed and after a deep analysis of the measurement data, the coverage gain can be predicted by using the proposed parametric equation [75]:

$$G_{RFMux}^{model} = K_0 + K_1 \cdot \log_{10}(\frac{f_{max}}{f_{min}}) + \frac{K_2}{N_{RF} - 1} \sum_{i=1}^{N_{RF}-1} \frac{f_{max} - f_i}{f_{max}} \qquad (3.19)$$

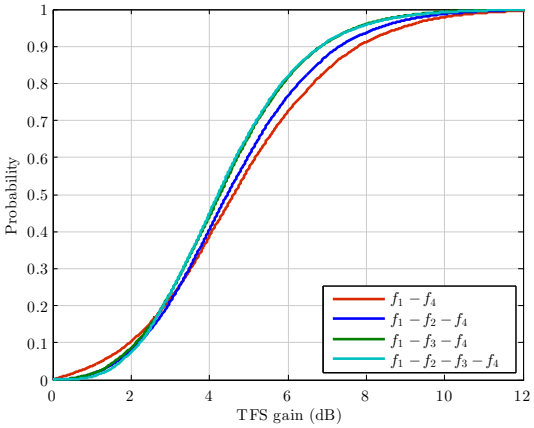

Figure 3.16: CDF of the coverage gain per transmitter area considering 4 RF channels. $\delta = 20dB$.

where K_0, K_1 and K_2 are the parameters to be adjusted to measurements and N_{RF} is the number of RF channels that conform the RF-Mux. The term that depends on $\frac{f_{max}}{f_{min}}$ represents the averaged contribution to the coverage gain due to the imbalance between the most distant RF channels within the RF-Mux (f_{max} and f_{min}), which is consistent with the average RF channel imbalance for 2 RF channels described in equation (3.16). Since the gain not only has a strong dependence on the maximum frequency separation but also on the distribution of the channels within the band, the model also accounts for the relative position of the RF channels (f_i) to the maximum RF channel (f_{max}), as indicated in the last term of the equation. Note that the frequencies are introduced in MHz in the model.

According to the average gain calculated for each area data set, the three K-parameters are estimated by minimizing the mean square error between the real value and the model. For the model characterization, 4 areas (A, B, C, and D) are taken into account whereas areas E and F are left aside and will be used for the validation of the model. The estimation of the K-parameters results: $K_0 = 1.2$, $K_1 = 28.7$, and $K_2 = -3$. Therefore, the coverage gain is characterized by:

$$G^{model} = 1.2 + 28.7 \cdot \log_{10}(\frac{f_{max}}{f_{min}}) - \frac{3}{N_{RF} - 1} \sum_{i=1}^{N_{RF}-1} \frac{f_{max} - f_i}{f_{max}} \qquad (3.20)$$

The comparison between the measurements and the values from the model for areas A to D results in errors of -0.3, -0.1, 0.4 and 0.5 dB, respectively. In order to verify the performance of the model, coverage gain values from measurements in areas E and F are compared to the application of the model to the frequencies of the multiplexes in each area and for the 11 possible combinations among them. The estimation errors obtained are in general below 0.5 dB. There are some exceptions where error reaches 1 dB. In general, the model approaches the gain values obtained from measurements. With this model a gain of 4.0 dB is reached considering an ideal deployment of the RF-Mux in which 4 RF channels are evenly distributed in the mid part of the UHF band (e.g RF channels 546, 602, 658 and 706 MHz).

Illustrative example of the coverage advantage with inter-RF FI

The actual impact of the inter-RF coverage gain is evaluated next. The study consist in computing the percentage of locations that are able to receive each RF channel as a function of a SNR offset which is added to relative SNR value of each RF channel. This leads to a different SNR per RF channel for a given location. With this, the equivalent SNR of the RF-Mux is computed. In order to define a coverage target, SNR threshold has been set to 15 dB. Thus those RF channels at a given location with an SNR greater than 15 dB are covered. The same applies for the equivalent RF-Mux SNR.

Figure 3.17 depicts the result of the study. Straight curves represent the percentage of locations which are covered at least by 1, 2, 3 or 4 of the RF channels for each given SNR Offset. Note that being covered by at least 4 RF channels means that the location is able to receive the complete service offering. The dashed curve represents the percentage of locations covered when an RF-Mux is used instead. It can be seen that the RF-Mux reaches coverage for a high percentage of locations with a lower SNR offset than the required for full reception without multi-RF aggregation. On the contrary, whereas there is a high percentage of locations that are able to receive at least 1 RF channel, they are not covered by the RF-Mux. The required SNR offset increase to achieve full coverage with the RF-Mux is lower than the required to receive all RF channels independently.

3.3.4 Analysis of the Coverage Gain based on Indoor Field Measurements

Indoor field measurements over six operational multiplexes were obtained at 4 residential flats in the Stockholm area (see Appendix A). The measurements,

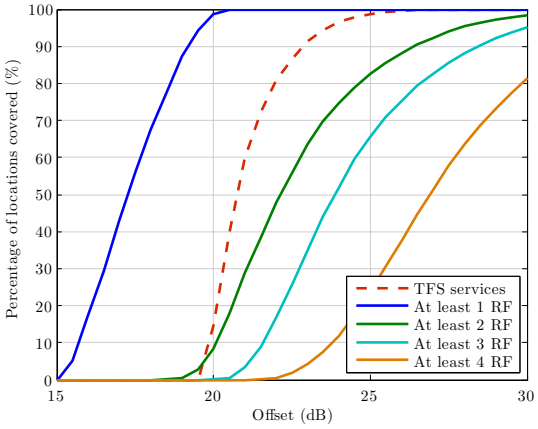

Figure 3.17: CDF of the coverage gain per transmitter area considering 4 different mean SNR parameters (δ).

which were conducted over paths of some meters inwards the buildings, show the field strength differences as a function of the frequency and distance.

The average signal level is in most cases higher for the lower frequencies. However, the level of these imbalances is different at each measured flat. In some of them it reaches up to 10 dB. These differences could be caused by the antenna diagrams, the higher path loss for high frequencies, the differences in each environment and the frequency dependency of the receiving antenna. In addition, small scale variations are also observed. From the measurements it can be seen that the signal variation is approximately cyclic with the location inside the room. These variations are typically in the order of ± 3 dB from the average level over an observed distance of 2 meters. Variations up to ± 6 dB are also observed. The signal level can differ over 10 dB by moving only 1 decimetre. The signal level variation for different frequencies seems not to be correlated. In fact, the signal variations are higher for higher frequencies, and thus, shorter wavelength. The total signal level difference between two RF channels can be up to 20 dB. Figure 3.18 shows an illustrative example of the imbalances between 2 RF channels in 4 of the measured rooms.

The coverage gain is evaluated for 4 RF channels assuming different frequency allocations. For each of the ten measured paths, the average TFS gain is calculated at $\delta = 20$ dB. The selection of the RF channels is done to provide maximum frequency differences of 6, 14, 30 and 33 8 MHz RF channels (48, 112, 240 and 264 MHz).

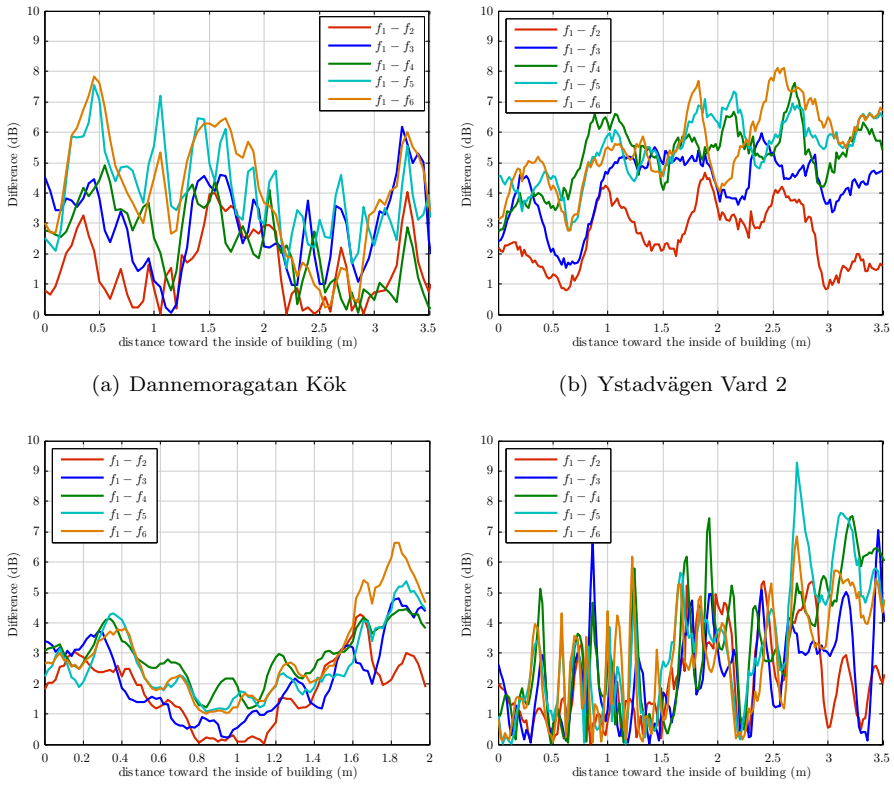

(a) Dannemoragatan Kök

(b) Ystadvägen Vard 2

(c) Edvin Adolphssons väg Vard 2

(d) Näsbydalsvägen Vard 1

Figure 3.18: Difference between 2 RF channels in indoor areas.

According to the results, gains increase with the maximum frequency separation between RF channels. Compared to the gains achieved in outdoor reception, those obtained in indoor environments are higher.

3.4 Interference Robustness Gain

The same mechanism of SNR averaging by inter-RF FI with RF channel imbalances can provide a robustness gain against interferences. This potential advantage is evaluated by means of a simple model based on Shannon capacity. A RF-Mux of 4 RF channels is considered. The C/I of 3 RF channels is set to

Table 3.11: Average coverage gains for indoor scenarios

Figure	48 MHz	112 MHz	240 MHz	264 MHz
A	3.0	4.6	**7.5**	7.1
B	2.6	3.9	8.2	**8.9**
C	2.9	4.0	4.7	**6.9**
D	3.3	4.0	4.2	**5.7**
E	3.1	5.0	5.7	**7.9**
F	1.9	2.6	2.6	**3.2**
G	1.3	1.9	3.3	**3.4**
H	2.2	3.3	5.5	**6.3**
I	2.1	3.8	6.6	**7.0**
J	3.0	3.6	**4.8**	4.5

Table 3.12: Increased robustness against interferences

Imbalance (dB)	C/I RF-Mux (dB)	Gain (dB)	Penalty (dB)
0	15.0	0	0
3	14.3	2.3	0.7
6	13.5	4.5	1.5
9	12.9	6.9	2.1

a fixed value C/I_{base}, the C/I of the other channel is set 3, 6 or 9 dB below C/I_{base}. The equivalent C/I of the RF-Mux is calculated according to Equation 3.7. The difference between the equivalent C/I and C/I_{base} provides the performance loss of the RF-Mux with respect to the C/I of the RF channels which are not affected by interferences when inter-RF FI is not implemented. On the contrary, the difference between the equivalent C/I and the C/I of the interfered RF channel provides the corresponding gain for the reception of all services.

Table 3.12 shows the results of the analysis. The first column corresponds to the imbalance selected for one of the RF channels. The second column is the C/I calculated for the RF-Mux. The gain column corresponds to the that obtained with respect to the interfered channel. The penalty refers to the loss with respect to the good channels.

In the worst case in which one of the 4 RF channels is completely lost, the reception of all services would still be possible with a C/N degradation of 4 dB. In this case, with a classical DTT system the 25% of the services will be completely lost even when the other RF channels are not interfered. Inter-RF FI allows receiving 100% of the services but at the expense of a C/N penalty compared to the non-interfered RF channels in a classical transmission.

Note that when comparing these two situations, the correct demodulation of the RF-Mux allows the reception of the complete set of RF channels while without inter-RF FI, the reception of the whole set of services is not guaranteed. Note also that this situation applies when a proper robust MODCOD is configured. For example in this case a code rate 3/4 should be selected since 1 of the 4 RF channels is degraded.

An illustrative example of the actual gain of inter-RF FI in such interference situation is provided next. The example consist of the following assumptions:

- An operator disposes of 4 RF channels each one configured with a DVB-T2 mode: 6 MHz, 32k extended, 1/128, PP7, 64QAM 3/4. This mode offers a capacity of 25.6 Mbps with a C/N threshold of 15.1 dB in AWGN.

- 1 of the 4 RF channel is interfered (completely erased) and the operator knows a priori which channel it is.

- The operator decides to re-allocate the services being interfered into the other 3 RF channels by changing the MODCOD of the 3 RF channels to increase capacity.

The total capacity in the classical network with one interfered RF channel is reduced to 76.8 Mbps (25.6 Mbps x 3) instead of the 102.4 Mbps with 4 RF channel. Allocating 25.6 Mbps in the 3 remaining 'good' channels implies modifying MODCOD to e.g. 256QAM 3/4. The new capacity per multiplex would be 34.1 Mbps (a total of 102.3 Mbps with 3 channels) but with a C/N threshold of 20 dB. Therefore, whereas changing MODCOD would introduce a loss of 5 dB, TFS would allow the reception of all services with a penalty of 4 dB (1 dB effective gain).

Note that the potential interference over one of the RF channels is not deterministic, thus the advantage of inter-RF FI is higher in terms of network planning.

3.5 Capacity gain by Multi-RF Channel Aggregation

Capacity gains are enabled by the wider space to allocate services when multiple RF channels are aggregated. CB permits to increase service data rate since data is compound by that received from more than one RF channel, thus exceeding the maximum data rate provided by a single RF channel. TFS cannot exploit this feature since data is distributed across multiple RF channels in a slot-by-slot manner which do not permit to combine the capacity of multiple RF channels. Furthermore, the required tuning gaps to allow single-tuner operation may limit the maximum data rate of the services below that of a single RF channel transmission (see Chapter V).

TFS and CB can both exploit a capacity gain from a more efficient statistical multiplexing of the delivered services since the process is done considering the complete number of services planned to be allocated in the RF-Mux. StatMux gain is achieved by the ability of dynamically assigning a corresponding bit rate according to the quality requirements of the encoded video streams. The randomness of the encoded data allows extra space (bit rate) to allocate more services.

Note also that the bundling of multiple RF channels allows for a more efficient use of capacity. With single RF channels it is not always possible to use the complete capacity of the multiplex to allocate services. Most of the remaining free space is used to allocate low data rate services such as interactive services or radios. The aggregation of RF channels allows for accumulating the free spaces to potentially allocate a new service.

3.5.1 Statistical Multiplexing

The required bit-rate for encoding a TV service strongly depends on the type of video coding used. SDTV has been traditionally encoded using MPEG-2 in many European countries. HDTV is encoded using H.264/AVC which provides 50% increased efficiency with respect to MPEG-2. HEVC is expected to increase efficiency over H.264/AVC up to 60%.

In a CBR system, each video service in a multiplex is allocated a fixed bandwidth (bit-rate) regardless of the content properties. Thus, the capacity of the multiplex can be divided in a fixed way, what do not guarantee an optimum bandwidth usage. With VBR, video codecs produce streams with a dynamic bit rate depending on the encoded content. Complex sequences (e.g. a sport program) require high bit rate in order not to limit picture quality. Low-complexity sequences (e.g. a news program) require lower bit-rates.

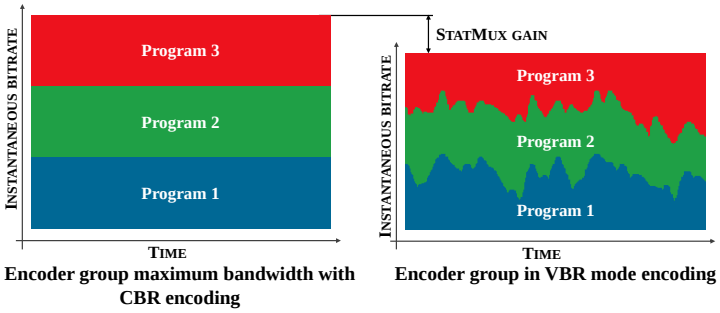

Figure 3.19: Constant bit rate (CBR) encoding vs. Variable bit rate (VBR) encoding with statistical multiplexing (StatMux).

StatMux takes advantage of the fact that, for a given video quality, the instantaneous overall peak bit rate of all video streams together is significantly lower than the sum of the peak bit rates of each individual video stream, assuming a central control unit that dynamically allocates capacity to each service while trying to keep the quality of all services constant and potentially the same [76]. The so-called StatMux gain is defined as the percentage reduction of the required bit rate compared to fixed bit rate encoding for a given quality. Performance of StatMux depends on the bandwidth of the transmission channel, the number of services that are multiplexed and the statistical properties of service traffics. Obviously, there is no gain for a single service, but the gain increases as a function of the number of services until there is a point where it saturates. In a traditional network, the number of StatMux encoded video streams is limited to the maximum capacity of a single RF channel. With TFS or CB, encoding is made considering the capacity of all the RF channels in the RF-Mux together. Thus, the number of video streams that can be jointly encoded is higher. Figure 3.19 illustrates the difference between CBR (Constant Bit Rate) encoding and VBR encoding with StatMux.

The gains are dependent on the nature of the video content, resolution and the multiplex capacity. The particular implementation of the system is also relevant. A buffering system allows to accommodate the bit-rate demands among services. The gain increases with the number of channels since the high and low bit-rates are averaged across a large number of services. The bit-rate savings are, according to the same study, independent on the content (SD or HD) and the compression (MPEG-2 or H.264).

The highest bit-rates savings are obtained when the multiplexed services are uncorrelated and they bit-rate targets are similar. Slight reduction of the gain is expected when one or some services are assigned a higher priority to

Table 3.13: Statistical multiplexing gain with MPEG-4 AVC. Source: Thomson

Number of HD programmes	StatMux gain
1	0%
3-4	15%
9-12	30%
18-24	32%

give a higher quality or when HDTV and SDTV are multiplexed together. In the latter case a bit-rate increase in one HDTV service will be compensated by a bit-rate reduction in some SDTV services. A particular case to avoid is the multiplexing of the SDTV and HDTV versions of the same program, which will be correlated, thus demanding bit-rates at the same time.

StatMux gain figures for H.264/AVC coding standard are collected in Table 3.13. The values are provided by Thomson in [46].

The maximum StatMux gain for HDTV is reached when multiplexing 18 to 24 programmes, in which case the StatMux gain is about 32%, corresponding to a (virtual) capacity gain of 47% (1/(1-0.32) = 1.47). However, the gain already reaches saturation with a fewer number of services.

StatMux with multiple RF channels

The effect of StatMux when multiple RF channels are aggregated is studied with the following assumptions regarding the bit-rate requirements of the services in the next-generation DTT.

- 720p/50 and 1080i/25 video services are encoded using H.264 and require 7 Mbps (CBR).
- 1080p/50 services are encoded using H.264 and require 10 Mbps (CBR).
- UHDTV 4K is encoded in HEVC[6], requiring 15 Mbps.
- Although video takes the majority of the available data rate, other data that need to be transmitted per service include:

[6]The performance of StatMux in HEVC is unknown and should be thoroughly studied. However, HEVC is expected to give similar performance regarding StatMux gain. Reduced bit-rate for HD video (in the range of 50% for equal perceptual video quality) will probably reduce StatMux gain with TFS or CB (large StatMux gain will already be exploited with 1 RF channel). However, 1080p HDTV and UHDTV video streams are expected to provide large StatMux gain with respect to allocation in a single channel.

Table 3.14: StatMux gain (in number of services) with the bundling of RF channels

RF-Mux	HD 720p/50 H.264	HD 1080p/50 H.264	UHD 4K HEVC
1 RF	1	1	0
2 RF	4	2	1
3 RF	6	4	3
4 RF	8	6	4

- Audio. The commonly used standards are Dolby Digital (448 kbps), AAC (320 kbps) and HE-AAC (160 kbps or 192 kbps) (0.3 Mbps is used in the calculations).
- Service Information and EPG: 0.1 to 0.3 Mbps (0.15 Mbps is used).
- Interactive services and Teletext: 0.1 to 1 Mbps (0.2 Mbps is used).
- Accessible content such as subtitles, audio description...(0.2 Mbps is used).

As an example, Table 3.14 summarizes the achievable gain in number of services considering a typical DVB-T2 multiplex configuration leading to 40.2 Mbps (8 MHz, 32k ext, 1/128, PP7, 256QAM, 2/3).

Gains around 2-4 HD services are already feasible for a bundling of 2 RF channels. Gain increases to 6-8 services for 4 RF channels. The benefits of the StatMux with UHDTV services are feasible when aggregating more than 2 RF channels.

3.5.2 Bit-Rate Increase with CB

CB allows for directly increasing the service data rate by the bonding of multiple RF channels compared to single PLP without CB. In fact, the bonding of 2 RF channels allows up to twice the service data rate. A high data rate service can be divided into two or more streams which feed the inputs of the CB system. The implementation of CB permits increasing the peak service data rate with the same C/N threshold requirement. For instance, whereas doubling data rate from DVB-T2 8 MHz 16k 1/16 PP2 QPSK 4/5 (10.34 Mbps) to 16QAM 4/5 (20.74 Mbps) would suppose a C/N threshold increase from 4.7 dB to 10.8 dB in AWGN, CB with 2 RF channels would enable the same total capacity without a coverage penalty.

Capacity could be slightly increased with the bundling of adjacent RF channels, what would allow for eliminating the need of guard bands between RF

Table 3.15: Capacity gain by the bonding of consecutive RF channels

Mode	RF BW (MHz)	CB BW (MHz)	Guard (MHz)	% gain
8 MHz ext	7.77	16	0.23	1.44
6 MHz ext	5.83	12	0.17	1.42

channels. Table 3.15 shows the potential capacity gain with the bonding of two consecutive RF channels. The results show a capacity increase around 1.4% considering a 6 MHz and a 8 MHz DVB-T2 signals.

A potentially larger capacity gain could be obtained by the use of scalable video coding (SVC). In general, the use of SVC allows for extracting different video streams (layers) with different quality from a single video stream. The base layer provides the lowest level of quality and ensures backwards compatibility with the coding standard (e.g. H264/AVC, HEVC...). Additional enhancement layers improve the video quality of the base layer in the temporal, spatial or quality dimensions. The main idea behind SVC is to transmit the base and enhancement layers of the same video service as separated components that can be transmitted with an specific robustness to serve different types of users. The base layer is transmitted to ensure reception in the entire coverage area and for all receivers. Those users which are also able to receiving the enhancement layer can enjoy better video quality.

With CB, one RF channel can contain the base layer and the other the enhancement layer. The base layer could be used to provide mobile coverage using the UHF band and the enhancement layer could provide the complementary data to allow for fixed roof-top reception using e.g. UHF or VHF.

The SVC extension of HEVC, known as SHVC, could allow the transmission of an HD and an Ultra HD versions of the same video service without the need of simulcast (transmission of the same content with different quality in two separated services), thus, allowing for a potentially reduced total required capacity. Figure 3.20 depicts the principle of SHVC and the corresponding capacity gain when compared to simulcast.

3.6 Conclusions

This chapter has focussed on the characterization and quantification of the potential network gains by the aggregation of multiple RF channels. The analysis has covered the improved RF performance with inter-RF FI, dealing with its impact on coverage and interference robustness, and the capacity gains when using TFS and CB.

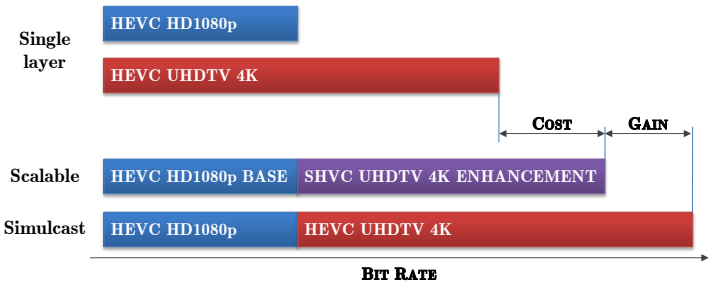

Figure 3.20: Gain by scalable video coding with respect to simulcast.

An information-theoretic approach to inter-RF FI and the performance evaluation of state-of-the-art OFDM-based DTT systems reveals that inter-RF FI could provide an advantage on averaging the SNR of the RF channels in a RF-Mux. In short, a weak channel in an RF-Mux can be compensated by means of a strong channel. However, performance is dependent of the MODCOD and and the level of the attenuation. Code rate should be adjusted according to the number of weak RF channels in the RF-Mux. With 2 RF channels and a completely erased channel, services can be recovered by means of a code rate below 1/2. Lower imbalances allow selecting higher code rates. The implementation of rotated constellations can improve performance for low code rates and low-order constellations. Inter-RF FI can also cope with the lack of enough time interleaving in slow time-varying channels providing high gains.

The nature of the imbalances among RF channels have been investigated taking into account propagation models available in the literature as well as field measurements in outdoor and indoor environments. The imbalances obtained by the study of the sources of imbalances in the UHF and VHF bands are collected in Table 3.16 for fixed roof-top reception.

In general, the imbalances come from the transmitter antenna diagram dependence with frequency, the noise figure of the receiver which increases with frequency, and the receiver antennas which compensate imbalances to some extent due to the increasing gain with frequency. Propagation is another important factor generating high imbalances between RF channels. The analysis of state-of-the-art propagation models reveal that, in average UHF band suffers around 10 dB more path loss than the VHF band. Sea path leads to the most homogeneous behaviour of the path loss among frequencies whereas paths with obstructions due to terrain or the presence of building create the highest imbalances.

Table 3.16: Overview of the imbalances between RF channels

	VHF (dB)	UHF (dB)
TX antenna	-	3-6
RX antenna	-	3-5
Noise figure	-	1-2
P.525	2.4	4.5
P.529	3	1.9-5.9
P.1546 Land	2.5	5
Longley-Rice	1.6-9.2	5.4

The analysis of measurements reveal that signal level differences increase with frequency separation up to around 10 dB for outdoor locations. An average gain with respect to the worst RF channel in the UHF band is found around 4 to 5 dB (for an RF-Mux with 4 channels). Portable indoor reception is especially affected by imbalances due to factors such as height loss, building penetration loss or body loss, which are more important at UHF than at VHF. Gains above 7 dB are found for a RF-Mux with 4 RF channels spread across the UHF band. The study reveals that the gain is mainly fixed by the most extreme RF channels. The number of channels in the RF-Mux has a limited impact on the achievable gains.

The processing of field measurements has led to the development of models for the estimation of the signal imbalances between pairs of frequencies in the UHF band as well as for the quantification of the TFS coverage gain as a function of the RF channels allocated per RF-Mux.

From the point of view of potential interferences on particular RF channels, inter-RF FI provides a gain for the reception of all services even when an RF channel is completely lost. However, the degradation in one RF channel affects the whole RF-Mux with a C/N penalty compared to the C/N of the non-interfered RF channels in a classical transmission.

The additional RF performance achieved by TFS and CB can be directly translated into a capacity gain by the selection of a less robust MODCOD. The use of CB enables increasing service data rate with the same robustness. Furthermore, both techniques can offer additional capacity gains linked to a more efficiency StatMux of VBR services. Gains around 2 to 4 UHDTV services using HEVC could be possible with the aggregation of 2 RF channel. Higher gains can be obtained with 4 RF channels (6 to 8 UHDTV services). CB is an interesting potential new use case with HSVC. In that sense, it is recommended

that the base layer is transmitted over the strongest RF channel so that a large number of users will be able to receive the service. A combination of a UHF and VHF channel can also provide advantages when the base layer is carried in the UHF band, enabling mobile reception of HD services, which are enhanced by additional data in the VHF for fixed reception.

Chapter 4

Advanced Network Planning (ANP) with Inter-RF Frequency Interleaving

4.1 Introduction

DTT networks are traditionally deployed by means of High-Power High-Tower (HPHT) transmitter stations which require frequency coordination between them. Frequencies are reused in distant stations to achieve an acceptable level of co-channel interference (CCI), what prevents adjacent areas from using the same frequencies to deliver services. Thus, only a limited amount of RF channels can be used per station. International frequency plans for terrestrial broadcasting services are agreed in order to allow for an efficient spectrum usage. In ITU Region 1, the GE06 [16] endows, on average, 7 RF channels per station in the UHF band out of the total 49 RF channels. Therefore, a group of 7 transmitters can use different frequencies. However, the reduced number of RF channels after the 700 MHz digital dividend, may require a tighter frequency reuse and an associated increased spectral efficiency to maintain the number of RF channels available per station.

Inter-RF FI (also referred to as TFS in this chapter for simplification) can increase the network spectral efficiency (in terms of bps/Hz) by potentially tolerating a higher C/I in the network deployments, as covered in Chapter 3.

This increased interference tolerance may be further exploited as a combination of a tighter frequency reuse together with a modified capacity per RF channel. The overall effect is a higher total capacity within a given spectrum taking into account also the frequency reuse.

The effect can be enhanced by the implementation of ANP strategies together with inter-RF FI. This concept involves the reduction of interferences coming from co-channel stations by means of Multiple Frequency Reuse Patterns (MFRP) and/or Mixed Polarization Network (MPN). With MFRP, subsets of RF-Mux frequencies are assigned to different stations (different spatial positions). With MPN, stations are assigned Horizontal (H) or Vertical (V) polarizations. A combination of both techniques is also possible.

This chapter investigates the spectral efficiency implications of inter-RF FI and ANP for MFN and SFN networks. Results are obtained for ideal networks made of hexagonal transmitter areas. Their application to real deployments are also discussed. The chapter is organized according to the following sections[1]. Section 4.2 discusses spectral efficiency offered by the conventional network planning of the DTT networks. Section 4.3 introduces ANP configurations. Section 4.4 briefly describes the simulation environment and methodology. Section 4.5 discusses the results. Conclusions are presented in Section 4.7. Note that an extensive description of the methodology followed in the study is provided in Appendix B.

4.2 Conventional Network Planning

DTT services are packed into multiplexes which are each allocated in RF channels in the broadcast bands (mainly VHF and UHF). One given DTT station delivers the set of RF channels at a particular frequency. To extend the coverage to an arbitrarily large area, frequency reuse is implemented at different transmitter areas due to the limited amount of spectrum. Figure 4.1 is an scheme of such scenario. The way the reuse is performed is mainly linked to the system robustness against CCI (expressed in terms of protection ratios). The required reuse limits the number of available RF channels per transmitter station.

Frequency reuse factor (η)

The frequency reuse factor, η, defines the average number of transmitter areas that use a different nominal frequency to transmit the same multiplex. With this approach, η different RF channels are necessary to build a network of one

[1]The main sections and results of this chapter are partially covered in [77].

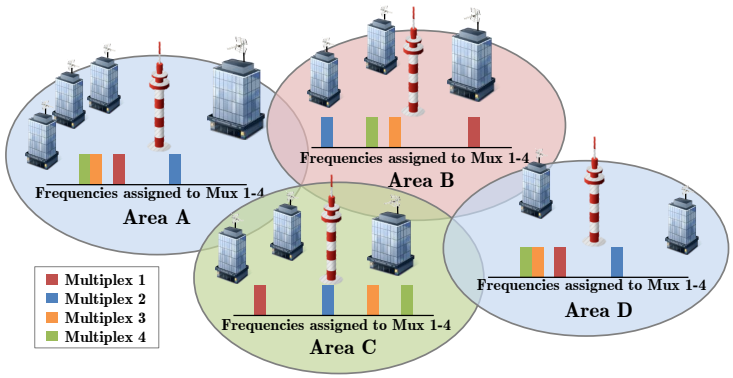

Figure 4.1: Frequency reuse scenario where 4 multiplexes are assigned different frequencies in each transmitter area.

Table 4.1: Number of available UHF 8 MHz channels per station as a function of η

Band (MHz)	M	$\eta = 3$	$\eta = 4$	$\eta = 7$
470-862	49	16	12	**7**
470-790	40	13	10	5
470-698	28	9	**7**	4

multiplex that uses a single RF channel per multiplex and transmitter area. With N_{RF} multiplexes per transmitter area a total of $\eta * N_{RF}$ frequencies are required to build the complete network [78]. Equation 4.1 defines the frequency reuse factor as:

$$\eta = \frac{M}{N_{RF}} \tag{4.1}$$

where M denotes the number of available RF channels.

Table 4.1 presents the number of RF channels available per station according to the frequency reuse factor and the number of RF channels in the UHF (before and after the release of the 800 MHz band and after the hypothetical release of the 700 MHz band). It can be seen that a frequency reuse of 4 will make possible to transmit 7 RF channels per station as in the current situation with the frequency reuse factor of 7 (see the entries in bold).

Network Spectral Efficiency (NSE)

Spectral efficiency is traditionally referred to the capacity per RF channel, without considering the influence of network planning. Assuming a simplified model for the capacity of the DTT system based on Shannon [4], the maximum theoretical rate in bits per second (bps) that can be transmitted to the reception point is given by:

$$R = B \cdot \log_2(1 + \gamma) \tag{4.2}$$

where γ is the carrier-to-interference plus noise ratio C/(N+I), in linear units, and B is the channel bandwidth (in Hz).

The available C/(N+I) and the frequency reuse factor limit the total capacity of the network for a given available spectrum. The Network Spectral Efficiency (NSE), in bps/Hz, accounts for the combined effect of capacity per multiplex (limited by C/(N+I)) and frequency reuse factor (η). The NSE is defined as:

$$NSE = \frac{1}{\eta} \cdot \frac{R}{B} = \frac{1}{\eta} \cdot \log_2(1 + \gamma) \tag{4.3}$$

The GE06 UHF plan defines typically 7 network layers each using about 7 frequencies (multiplexes) in the UHF band. The resultant plan was based on different requirements, generally aiming for nationwide coverage in each country, with different conditions in terms of size and shape of envisaged coverage areas as well as the wave propagation conditions [16].

Figure 4.2 shows a real example of the frequency reuse for the multiplex which carries the public state TV services (operated by Corporación RTVE) in different areas in Spain. 7 RF channels in the UHF band are reused along the country.

Inter-RF FI implications in the NSE

When inter-RF FI is implemented, the reception of a particular service is affected by the C/(N+I) of different RF channels, due to interleaving. Equivalent RF-Mux capacity can be estimated as the average capacity over N_{RF} RF channels which depends on the C/(N+I) of each RF channel and the employed QAM mapping, as explained in 3. Whereas, BICM capacity should be used, Shannon capacity is used instead in order to evaluate the potential of inter-RF FI regardless of a particular terrestrial broadcasting standard. Thus, NSE calculation with inter-RF FI can be simplified as:

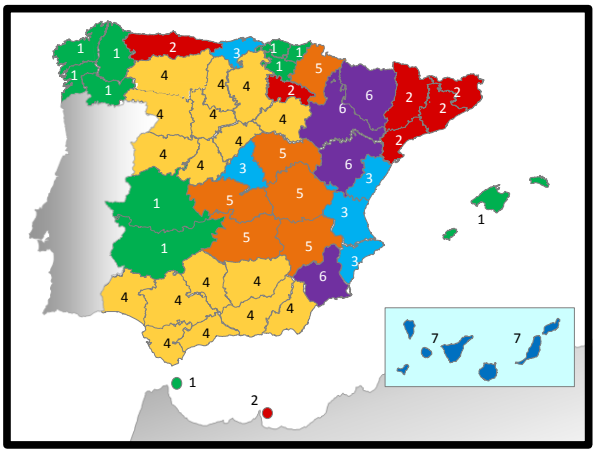

Figure 4.2: Frequency reuse in Spain for the public state TV multiplex. Frequencies are reused between different regional areas. About 7 RF channels in the UHF band are used at different transmitter stations. IEEE © 2015.

$$NSE_{inter-RF} = \frac{1}{\eta} \cdot \frac{1}{N_{RF}} \sum_{i=1}^{N_{RF}} \log_2(1+\gamma_i), \quad bps/Hz \tag{4.4}$$

where γ_i per RF channel directly depends on the network topology and frequency reuse pattern.

4.2.1 Pure Multiple Frequency Network (MFN) planning

Analog television broadcasting networks were usually based on HPHT transmitters, located at high prominent sites to cover extensive areas. These stations were configured with ERP ranging from 1 W ERP (small stations) to about 1 MW ERP (major stations). Due to the poor characteristics of the signals in terms of protection ratios, the same RF channels could not be reused in adjacent transmitters.

With a similar approach, DTT networks are traditionally deployed assigning different frequencies to multiplexes in each neighbour station in the target service area. The same RF channel is re-used only in regions separated by large distances, to avoid harmful CCI. Figure 4.3 depicts a basic scheme of a MFN where each transmitter area uses a different frequency to deliver DTT services. Note that f_1 is re-used in distant stations.

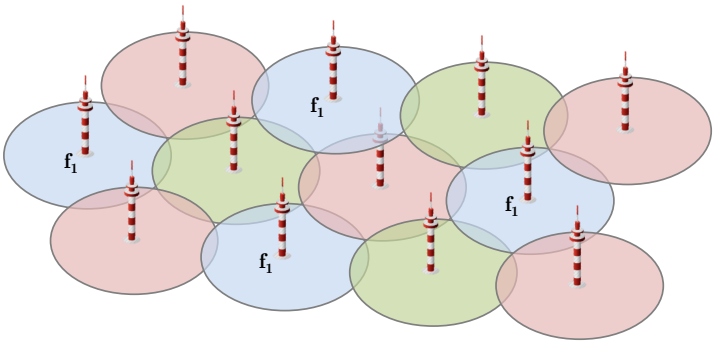

Figure 4.3: MFN basic scheme with frequency reuse.

At a given reception point, the wanted transmitter provides a certain field strength. Other transmitter stations from outside the service area using the same frequencies provide an interference contribution. Interferences are added so that the total interference power yields a C/(N+I) at the reception point. It is necessary to maintain a sufficiently high C/(N+I), γ_0, to meet the interference protection requirements of the system. Thus, the RF channels from a transmitter station cannot be reused in a transmitter that is too close to the first one. This minimum separation between co-channel transmitters (i.e. minimum reuse distance $D(\gamma_0)$) limits the amount of spectrum that can be used per transmitter station. Figure 4.4 shows an scheme of a standard MFN made of regular adjacent hexagonal cells of radius R. Each cell is assumed to have a single omni-directional antenna transmitter positioned in the cell centre.

Assuming that the RF channels are used in all the co-channel cells, the C/(N+I) in the centre cell at a given location j, γ_{MFN}, is defined by:

$$\gamma_{MFN} = \frac{P_0 \cdot G_{0,j} \cdot Q(\varphi_{0,j})}{\sum_{i=1}^{N_I} P_i \cdot G_{i,j} \cdot Q(\varphi_{i,j}) + P_{noise}} \tag{4.5}$$

where N_I is the number of interfering stations, Pi is the power of each transmitter station i, $G_{i,j}$ is a propagation related constant from transmitter i to receiver j, $Q(\varphi_{i,j})$ is the receiver antenna pattern attenuation relative to the pointing direction between a transmitter and the receiver, and P_{noise} is the noise power at the receiver.

The receiver antenna diagram weighs the interference contributions according to the angular (azimuth φ) direction between the main station and the co-channel stations. ITU-R BT.419 [59] recommends the value $Q(\forall\varphi) = $ -16 dB for

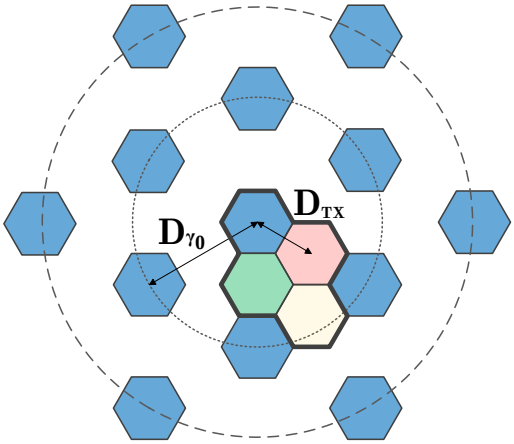

Figure 4.4: MFN scheme with frequency reuse factor $\eta = 4$. D_{TX} denotes the separation between transmitters (transmitter distance) and D_{γ_0} is the minimum reuse distance. The two first co-channel tiers are depicted. IEEE © 2015.

Cross Polarization Discrimination (XPD) for fixed reception frequency planning. Directional and polarization discrimination performance will be worse when using omni-directional antennas for portable indoor or mobile reception as identified in [79] where XPD is found to be in the range between -7 dB and -12 dB.

4.2.2 Single Frequency Network (SFN) planning

SFNs make use of the same frequencies in a group of adjacent transmitters (SFN cluster) to cover a complete or part of a target service area, as depicted in Figure 4.5. The service area could be a country, region or city. Thanks to the OFDM capability to overcome multipath by the Guard Interval (GI), signals arriving from those co-channel transmitters within the service area contribute constructively to the total wanted signal if allowed propagation delays are not exceeded [9].

The main advantages of SFN planning compared to MFN planning can be summarized as a potential higher spectrum efficiency and a diversity gain due to the superposition of signals from different transmitters. This also leads to an homogeneous field strength distribution within the service area and increased robustness against transmitter failures in dense SFNs. Furthermore, coverage

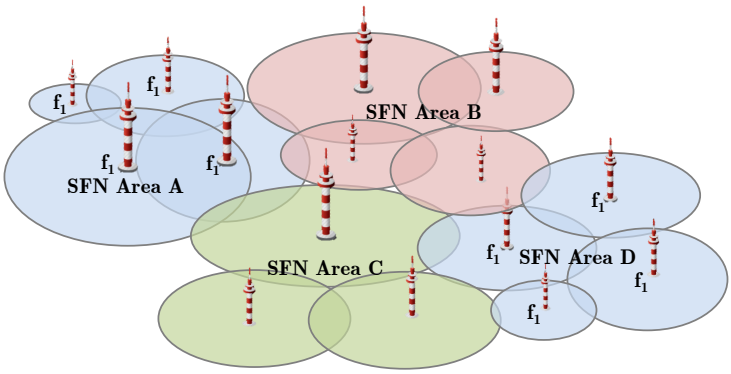

Figure 4.5: SFN basic scheme with frequency reuse.

extension is possible by the set-up of on-channel repeaters (gap-fillers) using the same frequency [80].

On the other hand, SFNs limit the practical granularity for the delivery of regional or local services to the size of the SFNs themselves. Time synchronization among transmitters is required in order to control delays. Frequency synchronization is also required at the transmitter and receiver to prevent carrier mismatches [80].

In a SFN, all the transmitters within the service area deliver the same signal synchronously. Thus, multiple replies of the same signal reach the receiver with different delays according to transmitter distances. From the receiver position, a similar effect as that from multipath is found. However, delays are expected to be much larger due to the large separation between transmitters (in the order of dozens of km).

OFDM systems can overcome signal delays by using longer transmitted symbols than the actual interval observed by the receiver. The signal with time interval T_s consists of a useful symbol part with time interval T_u and a Guard Interval (GI) T_g, as seen in Figure 4.6.

When the delay spread of the signal is shorter than the GI, no Inter-Symbol Interference (ISI) occurs and the signals contribute constructively. Signals received with excessive delay cause ISI. Signals in between contribute partially to the wanted and interfering signals. This effect is known as SFN self-interference. The minimum length of the GI should be established to overcome the maximum harmful delays. Given a transmitter distance, self-interference is reduced or eliminated by selecting a larger GI. The maximum transmitter distances, without causing self-interference, allowed by DVB-T and DVB-T2 systems are

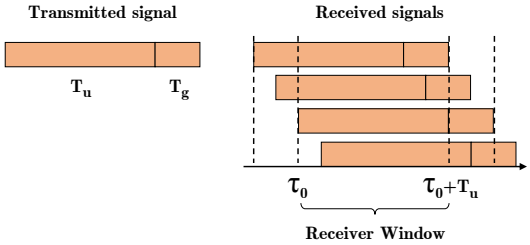

Figure 4.6: The transmitted symbol, T_s consists of the symbol T_u and the guard interval T_g (left). The received signal consists of multiple copies of the transmitted symbol. Delays are shown in comparison with the receiver window T_u used for detection.

Table 4.2: DVB-T parameters for 8 MHz and 8k FFT size

	1/4	1/8	1/16	1/32
T_g (μs)	224	112	56	28
d_{max} (km)	67.2	33.6	16.8	8.4

67.2 km (FFT 8k GI 1/4) and 159.6 km (FFT 32k GI 19/128), respectively, within an 8 MHz RF channel. Tables 4.2 and 4.3 collect the distances allowed according to the selected GI. Corresponding maximum transmitter distances for a 6 MHz channel are 8/6 larger.

The C/(N+I) at a given receiver location within the SFN is given by:

$$\gamma_{SFN} = \frac{\sum_{i=1}^{N_c} P_{j,i} w_i(t)}{\sum_{i=1}^{N_c} P_{j,i}[1 - w_i(t)] + \sum_{i=N_c+1}^{N_I - N_c} P_{j,i} + P_n} \tag{4.6}$$

where $P_{j,i} = P_i G_{i,j} Q(\varphi_{i,j})$ is the received power that depends both on propagation and the antenna diagram, N_c is the total number of transmitters in the SFN area and $N_I - N_c$ is the number of co-channel interferers from outside the SFN area. $w_i(t)$ is a weighting function which depends on the signal arrival time relative to the beginning of the FFT window; the equalization interval (T_{EI}); the useful symbol length (T_u) and the guard interval length (T_g) [46]:

$$w_i(t) = \begin{cases} 0 & t \notin T_{EI} \\ \left(\frac{T_u + t}{T_u}\right)^2 & t \in T_{EI} \ \& \ t < 0 \\ 1 & t \in T_{EI} \ \& \ 0 \le t \le T_g \\ \left(\frac{(T_u + T_g) - t}{T_u}\right)^2 & t \in T_{EI} \ \& \ t > T_g \end{cases} \tag{4.7}$$

Table 4.3: DVB-T2 parameters for 8 MHz and 32k FFT size

	1/128	1/32	1/16	19/256	1/8	19/128	1/4
T_g (μs)	28	112	224	266	448	532	NA
d_{max} (km)	8.4	33.6	67.2	79.8	134.4	159.6	NA

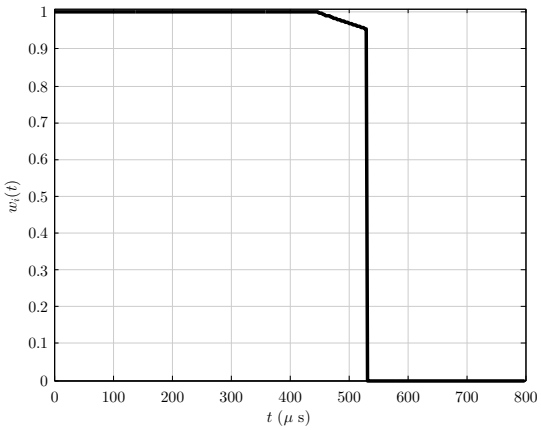

Figure 4.7: Weighting function $w_i(t)$ for $T_u = 3584$ μs, $T_g = 448$ μs and $T_{EI} = 532$ μs.

The potential length of T_{EI} depends on the RF bandwidth, FFT size and Pilot Pattern (PP) sequence of the signal, as well as on implementation constraints.

Figure 4.7 shows the weighting function $w_i(t)$ for $T_u = 3584$ μs, $T_g = 448$ μs and $T_{EI} = 532$ μs as a function of the contribution arrival time.

Different strategies of FFT window synchronization can be implemented at receivers as explained in [81]. Basically, the strategy employed defines the peak of the received signal impulse response the receiver uses for synchronization and where the position of the FFT window is set relative to the peak.

Whereas a natural strategy would be to synchronize to the strongest signal, more sophisticated ones are based on the definition of thresholds, the calculation of the centre of gravity or the finding of the position which leads to the maximum C/I.

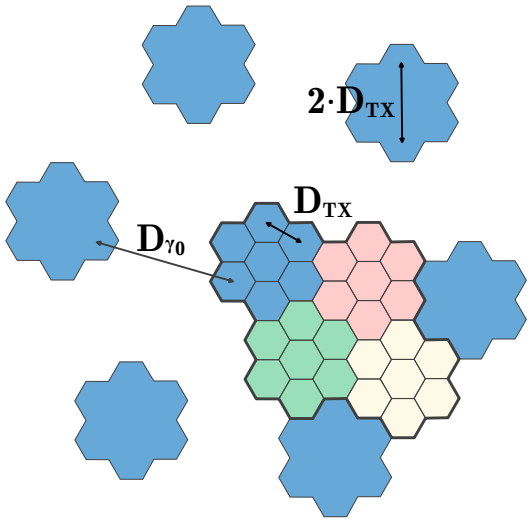

Figure 4.8: SFN scheme with a transmitter cluster of 7 stations and frequency reuse factor $\eta = 4$. Again, D_{TX} denotes the separation between transmitters and D_{γ_0} is the minimum reuse distance. IEEE © 2015.

MFN planning using SFN clusters

MFN planning using SFN clusters is more spectral efficient than pure MFNs (i.e. cluster size = 1) within a single network (e.g. a country) since they allow large reuse distances. However, the need of frequency reuse when there exist other adjacent networks (e.g. neighbour countries) limits the NSE. Ideally, it is desirable that the SFN cluster size is limited in such a way that there is no self-interference within each cluster. In such situation, the only interference comes from the frequency reuse of the SFN clusters.

The frequencies used in such medium-small SFNs may be reused across the network in a similar way as with an MFN. Figure 4.8 shows a medium-small regional SFN made up of a cluster of 7 transmitter stations and $\eta = 4$.

Most of the European countries planning for SFN foresee regional SFN with areas of up to 200 km diameter. However, the size of the regions is very different from one country to another, even for countries of comparable size [82].

Network planning using Large area SFNs

Large area SFNs, or national SFN, can be seen as SFN clusters with a large number of transmitters so that interference from frequency reuse (unless reuse

equal to 1 or 2 is used) is negligible. These networks suffer, instead, from self-interference (not enough GI), which may require a more dense transmitter infrastructure or larger overhead. A complete implementation of such SFN is linked to the frequency coordination between countries, in particular at country borders, which may be difficult.

4.3 Advanced Network Planning (ANP) Strategies for Increased NSE

Receiving antenna directivity and polarization discrimination characteristics can be exploited to achieve effective reduction of the received interference and to maximize the C/(N+I). The implementation of inter-RF FI also allows for selecting a different frequency reuse pattern for each or some of the frequencies in the RF-Mux. Two different network deployment strategies are investigated: Mixed Polarization Network (MPN) and Multiple Frequency Reuse Patterns (MFRP).

4.3.1 Mixed Polarization Network (MPN)

MPN consists of a systematic use of different polarizations, horizontal (H) or vertical (V), for transmitters using the same frequency. Users within the coverage area of a given transmitter receive all frequencies with the same polarization. Co-channel interferences coming with the opposite polarization from distant stations are reduced to some extent by the antenna diagram $Q(\varphi)$. In general, it would be desirable to have as many as possible of the strongest interferers using the opposite polarization. Thus, the MPN scheme should be selected taking the frequency reuse pattern into account to minimize the number of neighbouring co-polar interferers which should ideally be the same for each station in the network. Although many possibilities exist, the MPN scheme depicted in Figure 4.9 has been found to provide a good performance for the frequency reuse pattern $\eta = 4$ and $\eta = 7$ reported about in this dissertation. For frequency reuse $\eta = 3$ it is possible to design a pattern with a column-by-column cross-polarization configuration (instead of using 2 adjacent rows as shown in the figure).

Thanks to the antenna polarization discrimination a given receiver in the centre cell benefits from an interference reduction, which increases C/(N+I). Both a traditional and a network implementing inter-RF FI can benefit from the reduction of the interference level at receiving points.

A similar MPN scheme can be synthesized for a network using SFN clusters to minimize the number of co-channel interferer clusters.

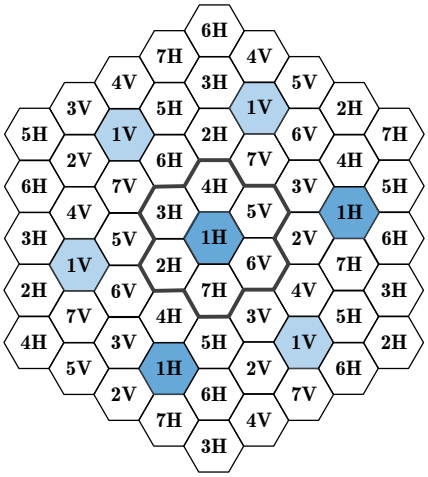

Figure 4.9: MPN configuration using systematic polarization variation in the stations in the network. 'H' denotes horizontal and 'V' vertical polarization. With the proposed MPN scheme for $\eta = 7$, only 2 over 6 co-channel stations produce co-polar interference (dark cells). IEEE © 2015.

Multiple Frequency Reuse Patterns (MFRP)

The use of MFRP exploits the C/(N+I) differences among RF channels due to interferences coming from different directions. MFRP consists in the application of a different reuse pattern (with the same η) to the different frequencies (or groups of frequencies) of a RF-Mux at a particular site. Each transmitter broadcasts the same number N_{RF} of RF channels, but for a given area the different frequencies have different frequency reuse patterns. The received interference level of the different RF-Mux frequencies typically varies significantly as a result of differences in the location of the corresponding co-channel stations and due to differences in antenna diagram weighting.

Depending on η the number of reuse patterns that can be applied to each ensemble of frequencies is different. With $\eta = 7$, two patterns are found whereas with $\eta = 3$ there is only one pattern. For $\eta = 4$, three different patterns can be found as shown in Figure 4.10. Note that these patterns are just mirrors ($\eta = 7$) or rotations ($\eta = 4$) of each other[2].

[2]There exists a fourth symmetric pattern, which is ideal for Non-TFS and may also be used for TFS (inter-RF FI), but with less gain than the three described non-symmetrical patterns. Any rotation of a symmetric pattern with $\eta = 3$ and $\eta = 4$ results in the same pattern.

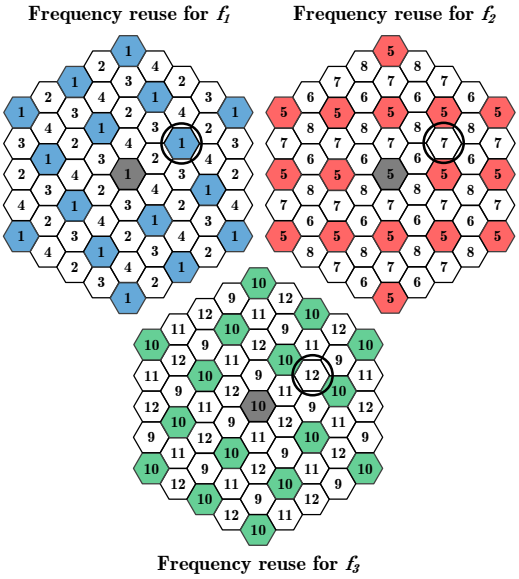

Figure 4.10: MFRP network configuration for 3 frequency reuse patterns with $\eta = 4$. Note that the wanted transmitter is located in the centre hexagon. Each frequency (f_1, f_2 and f_3) in the centre hexagon receives interferences from a different cell. IEEE © 2015.

For $N_{RF} = 3$ this means that each RF-Mux frequency gets a unique frequency reuse pattern. For $N_{RF} = 6$, each pattern is used by two frequencies ($N_{RF} = 9$: three frequencies, etc). Thanks to the varying frequency reuse patterns, interference contributions from a particular neighbouring transmitter only affects (for $\eta = 4$) one third of the N_{RF} frequencies.

Multiple Frequency Reuse Patterns and Mixed Polarization Networks

Both of the described methods (MFRP and MPN) may be combined in the same network. The combination is straightforward: the polarizations in Figure 4.9 are overlaid on top of the frequency reuse patterns of Figure 4.10. The three resulting frequency reuse patterns with different polarization for $\eta = 4$ are shown in Figure 4.11. It should be noted that on average only one third of the eight closest interfering transmitters use the same polarization as the wanted transmitter. Figure 4.12 (top) shows the resulting distribution of co-polar and cross-polar co-channel transmitters with respect to the central cell with $\eta = 4$.

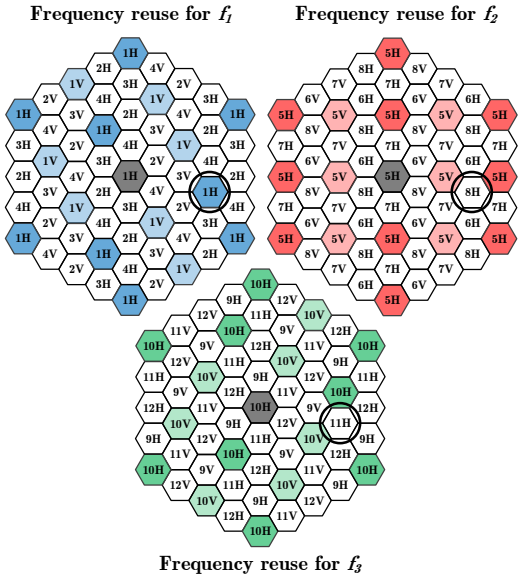

Figure 4.11: Network scheme with a combinations of the MPN and MFRP. Each frequency (f_1, f_2 and f_3) in the centre hexagon receives interferences from a different cell and in some cases with orthogonal polarization. IEEE © 2015.

With MFRP, interferers are not co-located for the used frequencies, i.e. a given co-channel transmitter station only interferes on one third of the RF-Mux frequencies, and with MFRP+MPN the effect of polarization discrimination is added, thus, leading to a less number of high signal strength interferers.

The same principles, discussed here for pure MFNs, are also applicable to networks using SFN clusters. This allows further NSE increase for this type of networks, where each cluster takes a similar role as an individual transmitter in the pure MFN case, i.e. polarizations and frequency reuse patterns are alternating on the basis of SFN clusters instead of individual transmitters. Figure 4.12 (bottom) depicts the SFN clusters scheme of the MFRP+MPN strategy.

4.4 Methodology Considerations

NSE evaluation for the different network configurations is conducted by computer simulations over an ideal hexagonal network. Although Appendix B provides a detailed explanation of the most important aspect of the methodo-

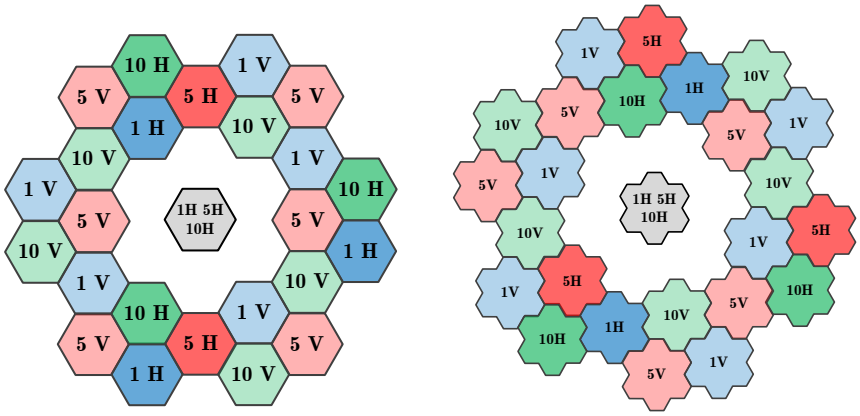

(a) MFN (b) SFN

Figure 4.12: Schemes of the stations interfering the wanted transmitter area for different frequencies with MPN and MFRP. The number of co-polar co-channel stations is reduced with this configuration. The number and position of the cross-polar interfering stations depends on the selected frequency reuse pattern. IEEE © 2015.

logy, this section focuses on the most important topics previous to the analysis of the results.

4.4.1 Network Configuration and NSE Calculation

The regular hexagonal network is assumed to be implemented by means of transmitter station with omnidirectional antenna diagrams. Stations are separated 60 km and 80 km with effective antenna heights of 250 m and 400 m, respectively. This configuration resemble typical Western and North European scenarios [83]. Received C/(N+I) is calculated for 6 evenly distributed RF channels in the UHF band 470 to 694 MHz. The use cases with 2 and 3 RF channels are also evaluated.

Fixed roof-top reception is assumed at 10 m above ground level with a directional antenna which characteristics are described in ITU-R BT.419 [59]. Table 4.4 collect the most relevant simulation parameters regarding propagation, transmitter and receiver sides.

The following system and network combinations are studied and compared:

- Reference case:

Table 4.4: Simulation configuration and network parameters

Propagation and coverage features	
Frequencies	474 514 554 594 634 674 MHz
Reception Type	Fixed rooftop at 10 m
Propagation Model	ITU-R P.1546-4 (Land)
Propagation Standard Deviation	5.5 dB
Location Probability	95%
Time availability	99%
Transmitter characteristics	
Tx antenna	Omni-directional
Effective Tx antenna height	250/400 m
Tx distance	60/80 km
Receiver characteristics	
Rx antenna direction in MFN	Strongest transmitter
Rx antenna direction in SFN cluster	Highest C/I
FFT time window synch. strategy [81]	Maximum C/I
Rx antenna model	ITU-R BT.419-3
Rx antenna gain	11 dB_d
Eff. antenna aperture	$\frac{\lambda^2 G}{4\pi}$
Feeder loss	4 dB
Equivalent noise BW	7.61 MHz
Rx Noise Figure	6 dB

  - Non-TFS: traditional network in which the RF channel with the worst RF level limits coverage.

- Combinations of ANP strategies which are compared to the reference case:
  - Non-TFS+MPN: Non-TFS case with systematic polarization (H/V) repetition.
  - TFS: spectral efficiency is given by the average spectral efficiency of the RF-Mux channels.
  - TFS+MFRP: MFRP configuration with the application of inter-RF FI.

– TFS+MPN: MPN configuration with the application of inter-RF FI.

– TFS+MFRP+MPN: Mixed MFRP and MPN with inter-RF FI.

Performance is evaluated over interference-limited networks, with a fixed high ERP so that noise power is negligible. Performance is also discussed considering a range of ERP values.

Each configuration is compared for pure MFN, a network of SFN clusters and a large area SFN, in all cases with different frequency reuse factor. Pure MFN networks are studied for frequency reuse $\eta = 3$, 4 and 7. Clusters of 7 transmitter stations are considered in MFNs made of SFN clusters for $\eta = 4$ and 7. Large area SFN networks are analysed for $\eta = 3$ and 4. Results are also presented for frequency reuse factor 1 for comparison. Special attention is paid to $\eta = 4$ and $\eta = 7$ since they allow the implementation of MFRP.

The field strength at the receiver location is computed by means of the ITU Recommendation ITU-R P.1546 [65]. The local received power from each transmitter is also affected by random frequency-independent but directional-dependent shadow fading and frequency-dependent fading (independent of transmitter).

The ITU model provides the received field strength exceeded for 50%, 10% and 1% of time. In order to account for different correlation situations between stations a random statistical distribution of field strength values is calculated. From this distribution, three different cases of signal time correlation are established:

- Case C. The received field strength for all stations and frequencies is assumed to reach their 1% time value at the same time.

- Case U1. Field strength values from different stations do not reach their peak values at the same time. However, the frequencies originated in the same station are considered to be fully-correlated.

- Case U2. All signals are assumed to be uncorrelated regardless their frequency and location.

A log-normal fading distribution at the top of the wanted and interfering signals allows to calculate a given coverage percentage for C/(N+I). The NSE considered to be available at the reception point is the one available with 95% coverage probability for 99% of time. The location with the worst value within the cell is taken as the worst point.

4.4.2 Limitations of the Methodology

The use of the described simulation environment has implications on the accuracy of the obtained results and their applicability to real network deployments.

In particular, the hexagonal model does not directly reflect a real deployment. On one hand, the results are focused on a HPHT deployment of transmitters. For these, the typical configuration is to assume equal ERP per station, what leads to equal transmitter distances. However, the geographical distribution of transmitters in a real network does not follow a regular pattern due to the irregularity of the terrain. Moreover, coverage areas usually include different types of stations (e.g. repeaters, low-power stations, gap-fillers...) what also leads to unequal transmitter distance.

Regarding SFNs, they are usually built-up by means of different types of transmitters, where low power transmitters (e.g. gap-fillers) are used to extend the coverage provided by the high power stations. Although SFN gain has been accounted for as constructive, according to [84] there are situations in which SFN signals can contribute destructively. This mainly occurs when contributions are received with equal strength and similar delays, what causes a C/N loss. However, an SFN cluster with 7 transmitters and the use of directional antennas generate a channel in which a strong transmitter dominates and the other transmitters contribute in a limited way to the C/(N+I). This could not be the case in a real network, thus it should be taken into account in further studies.

The received signal level from interferers depends on propagation characteristics. The ITU-R P.1546 model is found to deviate for rural area calculations at large distances [85]. According to the model, the field strength values predicted are not specific for a given polarization. Thus, vertical polarization wave propagation is configured to be the same as horizontal polarization wave propagation. The existence of differences between both polarizations are not taken into account in this study.

As well, receiving antennas could have a stronger or lighter effect on cross-polar discrimination what would result in a different performance of the MPNs. Regarding the MFRP, current networks do not necessary apply the same frequency reuse pattern to all frequencies transmitted per station. Thus, the starting point of the analysis where the frequency reuse pattern apply to each station could be reconsidered for a more realistic approach.

In addition, multipath propagation has not been taken into account since its effect with fixed roof-top reception is limited. Additional degradation due to frequency selectivity and de-polarization should be taken into account for a more accurate analysis. However, similar effects are expected for Non-TFS and TFS so that net effects on gains are likely to be small.

Table 4.5: NSE (bps/Hz) with pure MFNs for $\eta = 3$, $\eta = 4$ and $\eta = 7$. Case $D_{TX} = 60$ km, $h_{eff} = 250$ m. Fully correlation (C) and uncorrelated variants U1 and U2.

	$\eta = 3$			$\eta = 4$			$\eta = 7$		
Network Configuration	C	U1	U2	C	U1	U2	C	U1	U2
Non-TFS	1.27	1.35	1.31	1.11	1.20	1.13	0.97	0.99	0.95
Non-TFS+MPN	1.31	1.39	1.30	1.24	1.30	1.21	0.98	1.01	0.96
TFS	1.62	1.77	2.31	1.40	1.49	2.01	1.12	1.18	1.50
TFS+MPN	1.68	1.79	2.37	1.49	1.59	2.09	1.15	1.19	1.52
TFS+MFRP	-	-	-	1.48	1.95	2.06	1.17	1.39	1.53
TFS+MPN+MFRP	-	-	-	1.58	2.04	2.15	1.20	1.43	1.56

4.5 NSE Evaluation for Traditional and ANP

4.5.1 Pure Multiple Frequency Networks

Table 4.5 shows the NSE (bps/Hz) reached with different planning strategies within pure interference-limited MFNs. Results are presented for frequency reuse factors 3, 4 and 7 within the $D_{TX} = 60$ km and $h_{eff} = 250$ m scenario. Fully-correlated (C) and uncorrelated (U1 and U2) approaches for the co-channel interference time correlation at the receiver point are considered. Note that with frequency reuse factor $\eta = 3$ it is not possible to implement more than one frequency reuse pattern. Thus, the entries of the table involving this situation are kept blank.

The results show that, for all cases, the networks present higher NSE when decreasing the reuse factor from 7 to 4 and 3. Although the C/(N+I) increases with the reuse factor, less spectrum can be used per station. These two effects roughly balance each other for each use case, but with a clear advantage for lower reuse factors. In particular for $\eta = 7$, although achieving a high CCI performance, only 1/7 of the spectrum can be used per station. Regarding CCI time correlation, the uncorrelated approaches provide the highest NSE values. The values for Non-TFS configuration, which presents the lowest performance, are taken as reference. Figure 4.13 depicts the NSE increase for the different network configurations with respect to the reference case for each frequency reuse factor (i.e. each value corresponds to the increase with respect to the classical Non-TFS case).

The NSE gain achieved by MPN is larger for $\eta = 4$ (around 8%-11%), since the effect of the orthogonal polarization discrimination at the receiver provides a high C/(N+I) increase. The number of co-polar transmitter stations in the

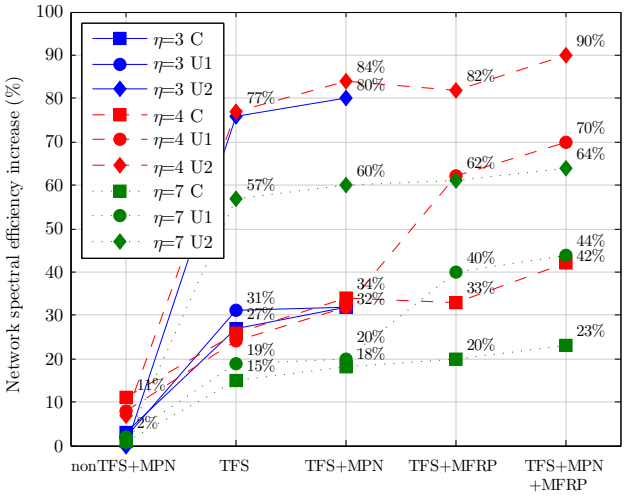

Figure 4.13: NSE increase (% bps/Hz) for different MFNs with reuse factor 3, 4 and 7. For each reuse factor, the Non-TFS case is taken as reference. Transmitter distance $D_{TX} = 60$ km and effective antenna height $h_{eff} = 250$ m. Fully correlation (C) and uncorrelated variants U1 and U2. IEEE © 2015.

first ring with $\eta = 4$ and $\eta = 3$ is 2 out of 6. However, with $\eta = 3$ these transmitters are closer. Similar gains are achieved with the three correlation approaches.

The use of TFS (inter-RF FI) achieves higher values than the cases without TFS. The best performance is reached for the fully uncorrelated case with $\eta = 3$ and $\eta = 4$ (77% increase). For the correlated case (C), the highest increase is reached for $\eta = 4$ (31%). The main advantage of using inter-RF FI without ANP is that the increased NSE comes without network planning/implementation modifications.

Regarding the combination TFS-MPN, reduced gains are found in comparison with the Non-TFS+MPN case.

The additional gain obtained with TFS and MFRP depends on the number of frequency reuse patterns that can be configured for a given reuse factor. For $\eta = 4$ and $\eta = 7$, 3 and 2 different patterns can be found, respectively, whereas for $\eta = 3$ there is only one. The most important gains come from the MFRP+MPN case when considering the time uncorrelated approach since there exist large differences in the received signal level from different stations at each given point in the time domain. As said before, the network with $\eta = 3$ cannot benefit from the gains provided by MFRP. With $\eta = 7$ the reduced

number of multiple patterns reduces the achievable gain for this frequency reuse, in contrast to $\eta = 4$.

The most relevant gains are achieved with the combination of TFS, MPN and MFRP (up to 90% gain with $\eta = 4$ uncorrelated U2 and 42% with the fully-correlated approach). The use of TFS+MFRP and TFS+MPN+MFRP provides higher NSE for $\eta = 4$ than the maximum achievable with $\eta = 3$ (with TFS+MPN) for the uncorrelated approach U1. Therefore, the random variability of the signals coming from different stations in a real network may lead to high gains. Note that when considering the GE06 plan MFN reference network with $\eta = 7$, TFS and ANP already provide gains, reaching a minimum gain of 23% NSE increase when combining all the techniques. In general, the most important gains with the fully uncorrelated (U2) approach are found for TFS whereas the effects of including MFRP or MPN are limited.

Although in this section only results for the $D_{TX} = 60$ km, $h_{eff} = 250$ m configuration are displayed by means of figures, it is worth to comment that the NSE increases for the $D_{TX} = 80$ km, $h_{eff} = 400$ m. In general, for the same transmitter distance, NSE increases with effective transmitter antenna height. NSE increase is, however, reduced (around 10% gain for the TFS+MPN+MFRP uncorrelated case).

For comparison purposes, MFN with $\eta = 1$ has also been calculated. It provides the lowest NSE (around 0.5 bps/Hz for the Non-TFS case and around 1 bps/Hz with TFS+MPN. In this case the wanted hexagon always present an adjacent CCI cell.

4.5.2 MFNs of SFN Clusters and Large area SFNs

Table 4.6 compiles the NSE reached within MFNs made of SFN clusters. The cluster size is 7 transmitters, all of them using the same polarization. Results are presented for frequency reuse factors 3 and 4 within the $D_{TX} = 60$ km and $h_{eff} = 250$ m scenario. Since it is not possible to implement more than one frequency reuse pattern with $\eta = 3$, the entries of the table involving this situation are not filled.

Results show that the network with frequency reuse $\eta = 3$ is more spectral efficient than when $\eta = 4$ is implemented. In the first case the main differences arise when using inter-RF FI with respect to the reference Non-TFS case due to its impact on averaging imbalances between RF channels. Figure 4.14 also presents the NSE increase achieved by each configuration.

With $\eta = 3$ and 4 the performance of MPN is low since it is not possible to mitigate the interferences coming from the 7 transmitters in the most interfering clusters. The limited effect of MPN and the non-existence of more than a single

Table 4.6: NSE (bps/Hz) with MFNs of SFN clusters for $\eta = 3$ and $\eta = 4$. Case $D_{TX} = 60$ km, $h_{eff} = 250$ m. Fully correlation (C) and uncorrelated variants U1 and U2.

	$\eta = 3$			$\eta = 4$		
Network Configuration	C	U1	U2	C	U1	U2
Non-TFS	2.33	2.23	2.23	1.79	1.76	1.69
Non-TFS+MPN	2.34	2.24	2.24	1.84	1.82	1.72
TFS	2.69	2.51	3.28	2.07	1.98	2.57
TFS+MPN	2.69	2.52	3.30	2.06	2.04	2.57
TFS+MFRP	-	-	-	2.61	2.14	2.72
TFS+MPN+MFRP	-	-	-	2.65	2.23	2.77

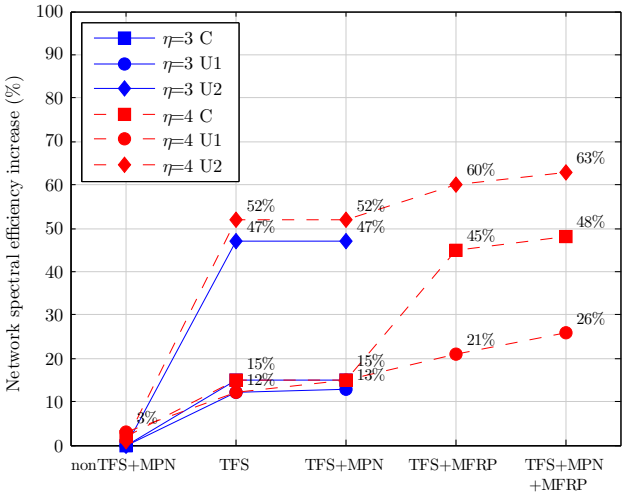

Figure 4.14: NSE increase (% bps/Hz) for MFNs of SFN clusters with reuse factor 3 and 4. For each reuse factor and network type, the Non-TFS case is taken as reference. Transmitter distance $D_{TX} = 60$ km and effective antenna height $h_{eff} = 250$ m. Fully correlation (C) and uncorrelated variants U1 and U2. IEEE © 2015.

frequency reuse pattern for $\eta = 3$ do not provide important additional gains to those achieved with inter-RF FI.

High NSE is achieved with $\eta = 4$ for MFRP and the combination of MFRP and MPN configurations. The most relevant gains are found for TFS in combination with ANP. In particular, the gain for TFS+MPN+MFRP reaches 26%,

Table 4.7: NSE (bps/Hz) with Large area SFNs for $\eta = 3$ and $\eta = 4$. Case $D_{TX} = 60$ km, $h_{eff} = 250$ m. Fully correlation (C) and uncorrelated variants U1 and U2.

	$\eta = 3$			$\eta = 4$		
Network Configuration	C	U1	U2	C	U1	U2
Non-TFS	1.99	1.89	1.90	1.46	1.42	1.38
Non-TFS+MPN	2.21	2.13	2.11	1.64	1.60	1.57
TFS	2.33	2.18	2.92	1.73	1.64	2.19
TFS+MPN	2.54	2.42	3.17	1.89	1.81	2.38
TFS+MFRP	-	-	-	-	-	-
TFS+MPN+MFRP	-	-	-	-	-	-

48% and 63% with $\eta = 4$, for the fully-correlated and uncorrelated approaches U1 and U2, respectively.

Regarding the configuration 80 km transmitter distance and 400 m effective antenna height, which results are not graphically presented, although the NSE is larger, its increase with respect to the Non-TFS case is reduced (around 60% to 50% for the TFS+MPN+MFRP case).

Again, $\eta = 1$ provides the lowest NSE for the different cases under analysis. The results are similar as in a MFN due to the existence of adjacent co-channel stations to the edge of the SFN.

NSE has been calculated for the large area SFN case as shown in Table 4.7. It may be possible to implement MFRPs in a large area SFN network with the frequency reuse factors $\eta = 3$ and $\eta = 4$ used in this study. However, this case is not taken into account since the most important interference contributions come from the same SFN due to self-interference when the delay between the signals coming from two transmitters in the SFN exceed the permitted delay to be considered as constructive interferences.

Large area SFN networks can benefit from the effects of using MPN to mitigate the self-interferences. Likewise, the use of TFS alone or in combination with MPN provides a C/(N+I) increase. Figure 4.15 shows the gains achieved for large area SFNs and ANP.

If compared to the network of SFN clusters the use of TFS and TFS with MPN provides higher advantage in the large area SFN network. This is mainly due to the fact that potential CCI stations are located closer to the receiver location than those CCI from a co-channel cluster. Conversely, the decreased C/(I+N) in a large area SFN provides lower NSE.

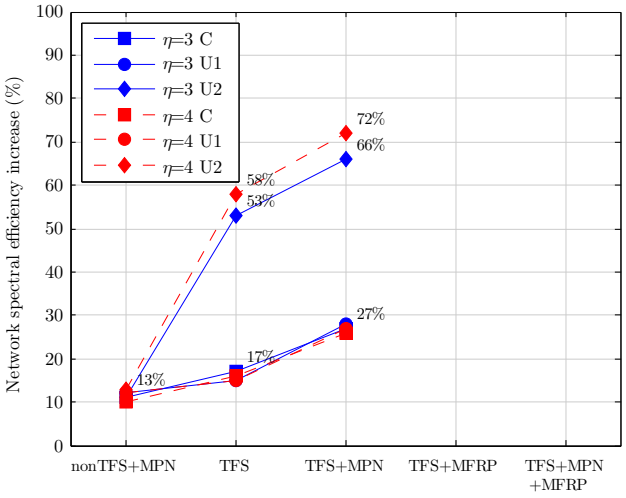

Figure 4.15: NSE increase (% bps/Hz) for Large SFNs with reuse factor 3 and 4. For each reuse factor and network type, the Non-TFS case is taken as reference. Transmitter distance D_{TX} = 60 km and effective antenna height h_{eff} = 250 m. Fully correlation (C) and uncorrelated variants U1 and U2. IEEE © 2015.

4.6 Application of the Results to Current and Next-Generation DTT Networks

To approach the implication of ANP, the three different network topologies (MFN, MFNs of SFN Clusters and Large area SFNs) are compared with respect to the GE06 reference network with $\eta = 7$ and without inter-RF FI. Thus, it is possible to quantify the potential NSE gains of each case with respect to the current $\eta = 7$ schemes.

The analysis is made considering frequency reuse factors $\eta = 4$ which can exploit all the proposed ANP strategies. The achievable gains are computed considering the results derived from the 3 correlation approaches. Table 4.8 collects the maximum and minimum NSE increase derived from simulations.

It can be seen that all of the topologies analysed provide higher NSE than the reference $\eta = 7$ network, even without inter-RF FI. MFNs provide the lowest increase. However, the maximum increase for the MFN with $\eta = 4$ reach more than 100% when using TFS (inter-RF FI) and TFS with ANP. An interesting result is that large area SFNs do not provide as much NSE increase as the MFNs made of SFN clusters due to the presence of self-interferences. The use of MFNs of SFN clusters outperform any other network topology.

Table 4.8: Minimum and maximum NSE increase (%) for $\eta = 4$ compared to Non-TFS MFN $\eta = 7$ (GE06 plan) from cases C, U1 and U2

	MFN		SFN Clusters		Large-SFN	
Network Configuration	Min	Max	Min	Max	Min	Max
Non-TFS	14	21	77	84	43	53
Non-TFS+MPN	27	31	81	89	61	69
TFS	44	111	100	170	65	130
TFS+MPN	53	120	106	170	82	150
TFS+MFRP	52	116	116	186	-	-
TFS+MPN+MFRP	62	126	125	191	-	-

The MFN with SFN clusters and $\eta = 4$ can obtain a high performance when combining TFS and ANP.

In general, the NSE within the network of SFN clusters is higher than for a pure MFN since the co-channel stations inside each cluster do not create interferences, and the cluster size allows for increased reuse distances for a given reuse factor. Furthermore, with SFN clusters, the 7 stations in each interfering cluster reach the reception point in the SFN with similar field strength (similar distances) what makes C/(N+I) decrease.

NSE gains with ANP are also evaluated considering limited transmitter power (ERP). In general terms, NSE values decrease whereas NSE gain is increased when ERP decreases. Similar values as those presented in this paper apply for a large range of ERP values from 10 to 100 kW, which are typical ERP used by transmitter DTT stations. It should be noted that the gains reached by the use of TFS or TFS with MFRP collapse to the gains reached by only TFS with low ERP and MFNs. The combination of TFS with MPN achieves higher gain that the only TFS case also with low ERP and MFNs. For SFN clusters, the combination of TFS with MPN or MFRP collapses to the gain of only TFS for low ERP. Thus, in a real network where ERP is limited to a certain (high) value, TFS and ANP could provide higher NSE gains when using tighter frequency reuse than those achieved in the pure interference-limited cases. The reduction of interference levels in the MFN has a more important effect than the achievable reduction in SFNs.

4.6.1 Applicability to Portable and Mobile Reception

DTT networks designed for wide area coverage using fixed roof-top reception also allows for portable/mobile reception within a limited area, in which co-

verage is typically noise limited. The portable/mobile reception therefore normally has some interference margin. When TFS/ANP is applied, and introduced together with a reduction in frequency reuse factor, the general C/(N+I) level will increase, but the fixed roof-top coverage would be maintained thanks to TFS/ANP, as shown in this study, but with a larger total capacity (more multiplexes will fit the available spectrum thanks to the lower frequency reuse factor). The portable/mobile reception would also experience an increase in general interference level, for which TFS/ANP would provide some protection, although probably less than for fixed reception, due to lack of antenna azimuth discrimination and lower XPD performance. If the net effect is negative the original interference margin would be reduced or even be negative, depending on the use case. Indoor reception, having a higher path loss would have a higher interference margin and is therefore less likely to experience a negative effect on coverage.

4.6.2 Dependency with the Number of RF Channels

From the point of view of TFS/CB and ANP, the number of RF channels has an impact on the achievable performance. It is important to note that in order to exploit the benefits of the MFRP approach there should be at least as many RF channels as pattern versions for a given reuse factor. With frequency reuse 4, 3 different MFRPs are found. Thus, optimum performance is found when each frequency of the RF-Mux can experience a different reuse pattern, what is achievable when there exist 3 or more RF channels in the RF-Mux. Frequency distribution within the band is also an important consideration since frequencies with a large frequency separation suffer from a higher field strength imbalance. For a case with the same ERP being used on all RF frequencies (traditional DTT situation due to regulation constraints) the reception of the Non-TFS cases is limited by the RF channel with the lowest field strength (in average, the RF channel with the highest frequency). Higher gains are expected when there is a high RF channel within the RF-Mux. Results are also obtained for 3 and 2 RF channels within the RF-Mux. The selected frequencies are 514 MHz - 554 MHz - 594 MHz and 514 MHz - 594 MHz, respectively. The reuse patterns that provide the highest performance are selected. For frequency reuse factor $\eta = 4$ and for the fully correlation case (C) the NSE increase with 3 and 2 RF channels is 17% and 30% for MFNs; 19% and 14% for MFNs of SFN clusters; and, 22% and 19% for Large area SFNs.

Note also that the advantages of TFS and TFS with ANP will not be exploited by those RF channels that cannot be aggregated into a RF-Mux. Conversely, those RF channels could still benefit from the use of MPNs.

4.7 Conclusions

The results presented in this study reflect the potential benefits of implementing inter-RF FI and ANP strategies over DTT networks based on a regular hexagonal lattice.

The increased interference immunity offered by inter-RF FI may be exploited in a tighter frequency reuse together with an appropriately chosen capacity/robustness combination, which maximizes the overall capacity per transmitter station of the total available spectrum. Furthermore, network planning could be optimized taking the characteristics of inter-RF FI within a RF-Mux into account. Different ANP strategies allow for higher network spectral efficiency per RF channel by means of different reuse patterns for the frequencies in use (MFRP) and the use of systematic H/V polarization at different sites (MPN). The increased robustness against interferences by inter-RF FI and ANP can lead to the same capacity per multiplex being achieved with $\eta = 3$ or $\eta = 4$ instead of $\eta = 7$. This would directly imply a network spectral efficiency gain of 75% without increasing the bit rate per multiplex (retaining the same coverage). In the possible situation of a 700 MHz band release a total of 28 UHF channels will remain for terrestrial broadcasting. $\eta = 7$ will only made 4 RF channels per station available. A new plan with $\eta = 4$ will increase the number of multiplexes per station from 4 to 7, thus achieving the same total capacity as the current DTT network.

The introduction of ANP techniques can increase network spectral efficiency not only for pure MFNs but also for SFN, especially for networks using SFN clusters which size is dimensioned according to GI and transmission mode. The achievable gains provided by TFS/CB in combination with ANP for $\eta = 4$ are found to range 42%-90%, 26%-63% and 27%-72% for MFN, MFN of SFN clusters and large SFN deployments, respectively. Although the reality may not be 100% de-correlation or 100% correlation, these results suggest that inter-RF FI with ANP may offer very high network spectral efficiency gains.

Note that the obtained gain figures apply within the context of simulations using a theoretical regular network deployment and standard terrain characteristics. The achievable gains in a real network deployments can be higher or lower according to the particularities of the network and the level of interferences reaching the receiver. High interference levels on particular RF channels will cause a severe impact on the performance of the classical network case since it will limit the reception of the complete service offering. Conversely, high gains are expected with inter-RF FI alone or with inter-RF FI. Achievable gains are also sensitive to the number of RF channels in the RF-Mux and the interference levels suffered in each frequency.

Chapter 5

Implementation Aspects of TFS and CB

5.1 Introduction

TFS and CB enable the combination of multiple RF channels to transmit services. As explained in Chapter 2, the implementation of both techniques differ substantially. Whereas with TFS service data is split and sequentially transmitted over a different RF channel, with CB data is simultaneously received from the RF-Mux. This Chapter investigates the implementation requirements of each technique from the point of view of the transmitter, the receiver and the network infrastructure.

The key point in implementing TFS and CB is the necessity of more than one tuner for CB and the need of the fulfilment of timing requirements with TFS when the number of tuners is less than the number of RF channels in the RF-Mux. Such case imposes the allocation of guard times for frequency hopping operation. Single tuner is seen as a feasible option though it requires the redesign of current chip-sets to allow fast tuning and synchronization operations. Furthermore, the necessity of guard times between during the hopping time to a different RF channel increases the capacity overheads, what makes the service peak data rate decrease, and requires proper framing and data scheduling. The possibility to implement TFS with two tuners relaxes the implementation requirements, reducing or even eliminating tuning gaps. The investigation is focused on the use of a single-tuner approach for TFS and the use of two tuners for TFS and CB. Although set-top-boxes have traditionally included a single tuner for DTT reception, there exist more advanced terminals

also including two tuners for Personal Video Recorder (PVR) opertion where one program is recorded while another is viewed. Thus, it is reasonable to consider the possibility that these implementations are extended to support TFS or CB implementation.

The present study covers the main characteristics of the system from a generic and standard-independent point of view. Examples are provides based on the state-of-the-art standards that already consider the use of TFS: DVB-T2, where TFS is part of an informative annex, and DVB-NGH, where TFS is adopted. CB is also approached considering the basic operational blocks of the ATSC 3.0 standard, which shares similarities with the aforementioned standards.

The chapter is organized as follows: Section 5.2 investigates the requirements for a proper distribution of data for optimum TFS performance as well as the necessary scheduling for a proper data allocation following the single and dual-tuner approaches. Section 5.3 evaluates the main operations involved in the tuning process as well as the restrictions that limit peak service data rate with TFS. Section 5.4 looks into the implementations aspect of standalone CB and when inter-RF FI is implemented. Section 5.5 analyses the signalling requirements of both techniques. Section 5.6 deals with the main network topology issues focusing on the distribution and broadcasting of the content as well as the implementation of ANP strategies. Section 5.7 provides the conclusions of the analysis as well as some recommendations for TFS and CB implementation.

5.2 Transmitter Implementation with TFS

TFS is implemented so that each RF channel transmit the same type of frames as in a classical transmission but with a different content. Frames do not contain information of a restricted set of service but of all the services in the RF-Mux. To this purpose, data of each service must be encoded separately but distributed in multiple frames (according to the number of RF channels) previous to transmission. This involves changes in the classical single RF channel modulators though most of the blocks in the chain are still valid or can be adapted to TFS operation. At the BICM output, a framer block is in charge of the sequential allocation of data into the frames. One frame per RF channel needs to be generated. However, the disposal of the data of a service in each frame is different since data belonging to a given service is not received simultaneously from more than one RF channel. Figure 5.1 depicts basic modulator and demodulator schemes for TFS with M services within a RF-Mux of N RF channels.

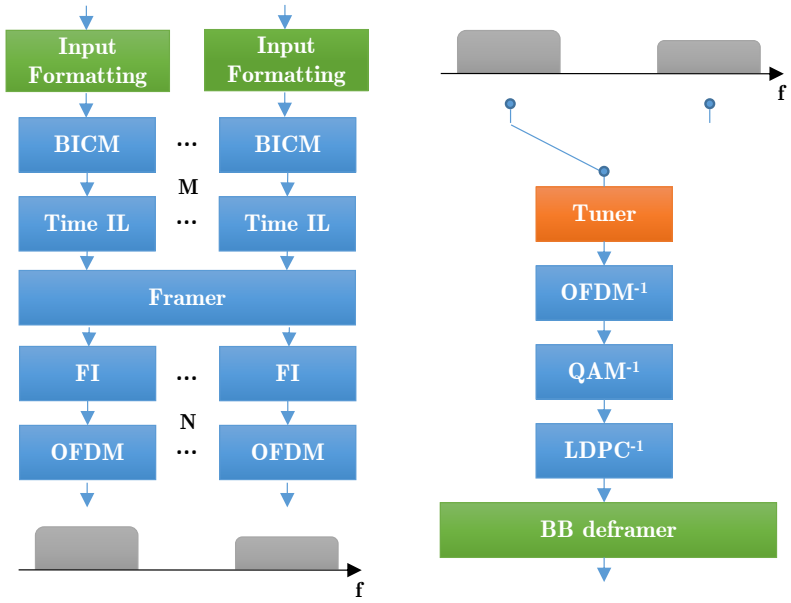

(a) Transmitter (b) Receiver

Figure 5.1: Transmitter and receiver chains for TFS operation.

The following subsections delve into the processes taking place at the modulator to ensure TFS operation.

5.2.1 FEC and Interleaving

A proper FEC and interleaving are part of the core elements of the system operating TFS to exploit frequency diversity. This operation should ensure that each FEC word is evenly spread across all of the RF channels in the RF-Mux to maximize performance. This way, the FEC code can exploit the diversity of the system by averaging the signal imbalances in each codeword.

With TFS, the spread of the FEC words across the RF-Mux is conduct by means of time interleaving. In broadcasting systems, TI is generally used to combat impulsive noise and fast fading that mainly occurs in fixed and mobile reception, respectively. A number of FEC words belonging to the same service are jointly interleaved by the TI. The resultant interleaved frame is partitioned in fragments (data slices) that are transmitted in a sequential manner in the

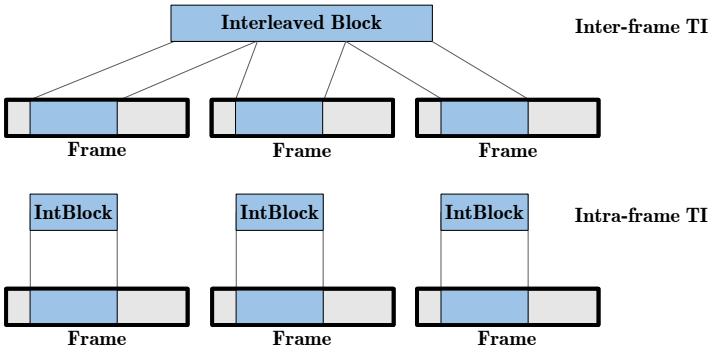

Figure 5.2: Inter-frame TI and Intra-frame TI.

time domain. Ideally, interleaving duration should be as large as possible so that data is transmitted more than once per RF channel (i.e. RF_1, RF_2, RF_3, RF_1, RF_2, ...) to guarantee an even distribution of the slices across the RF-Mux and enhance time diversity. In practice, one complete TFS cycle (one round per RF-Mux) should be at least guaranteed in order to compensate the signal variations within the RF-Mux.

How interleaved cells are mapped to frames consists mainly in two strategies: intra-frame TI and inter-frame TI. With intra-frame TI, the interleaved frame is transmitted within frame duration. With inter-frame TI, one interleaved frame is split and transmitted over multiple frames, extending interleaving duration beyond frame duration. It is also possible to accomplish a more uniform distribution of the data within a frame by sub-slicing which divides the interleaved frame into smaller units that are spaced across a frame.

Time Interleavers are mainly divided into two categories. Block Interlaver (BI) is the solution adopted in DVB-T2. BI and Convolutional Interleaver (CI) are also adopted in DVB-NGH and ATSC 3.0. Figure 5.3 depicts the resultant time-interleaved data to be transmitted in 4 RF channels by means of a BI. According to this example, FEC words are written column-by-column, partitioned into smaller units (one per RF channel) and read row-by-row. On the other hard, Figure 5.4 shows an example of the operation using a CI which ensures that each frame carries a quarter of the data of each FEC word.

Time Interleaving Trade-Offs

The use of TI impacts on the hardware complexity of receivers as well as imposes limitations in performance in terms of time diversity and latency.

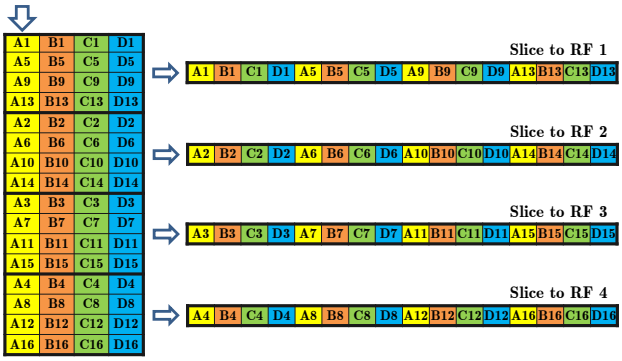

Figure 5.3: Block interleaver operation to evenly spread data across 4 RF channels using intra-frame TFS.

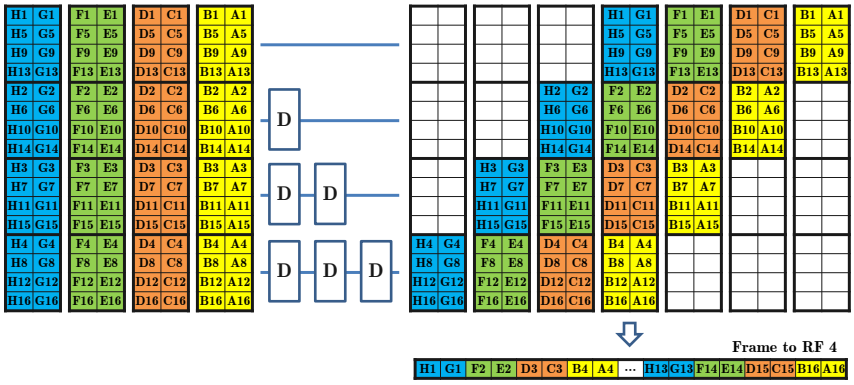

Figure 5.4: Convolutional interleaver operation to evenly spread data across 4 RF channels using inter-frame TFS.

The required operations for interleaving and de-interleaving increase the end-to-end delay of the system. However, while this consequence may not be critical for the majority of services, the increased zapping time [86][1] impacts the user experience. Zapping delay is produced when using TI since it is necessary to finalize the deinterleaving process before being able to change the service.

The main requirement at the receivers when implementing TI is that they must incorporate enough memory in order to perform time deinterleaving

[1]The zapping time involves the time interval required to display a new service once the user has decided to change the service he/she was watching.

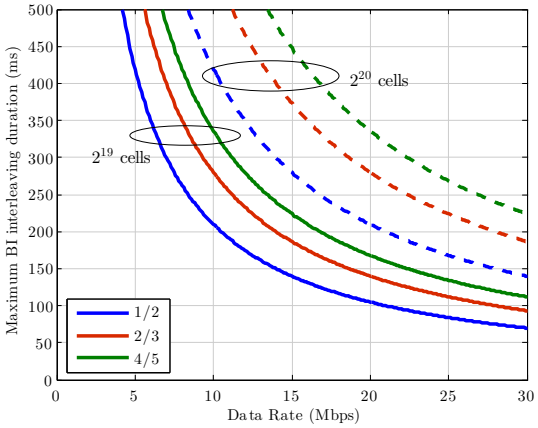

Figure 5.5: Service peak data rate as a function of the TDI memory and code rate. Modulation is 256QAM.

(TDI). The available TDI memory limits the peak service data rate and the interleaving duration. For instance, DVB-T2 establishes a TDI memory of $2^{19}+2^{15}$ cells as a compromise between hardware complexity and performance. DVB-NGH sets the memory to 2^{18} since CI doubles BI duration and the use of Adaptive Cell Quatization (ACQ)[2] for the robust modes (QPSK and 16QAM) allows further reduction of the memory requirements. Note that the number of cells that fit in the TDI memory is the same regardless of MODCOD. The maximum interleaving duration and maximum service data rate increases with higher spectral efficiencies. The maximum interleaving duration in a BI can be computed as:

$$T_{max} = \frac{M_{TDI} \cdot \mu_{MOD} \cdot \eta_{COD}}{R_{PLP}}, \tag{5.1}$$

where M_{TDI} is the available TDI memory (in cells), μ_{MOD} is the number of bits per constellation symbol (e.g., 8 bits for 256QAM), eta_{COD} is code rate defined as the ratio between the number of source bits and the number of encoded bits per FEC word, and R_{PLP} is the data rate of any PLP (service), in bps. Figure 5.5 depicts the maximum interleaving duration that is supported as a function of the TDI memory, data rate, and MODCOD.

[2]Adaptive Cell Quantization permits reducing the memory consumed to store a cell by reducing the quantization order. This is possible with robust modes that accept an increased quantization noise.

It can be seen that no more that 11 Mbps can be provided per service considering the 256QAM 2/3 mode with 2^{19} cells and an interleaving duration of 250 ms, which is the maximum frame duration in DVB-T2. Doubling TDI memory allows doubling maximum data rate for this case.

However, service data rate is not only restricted by the TDI memory since the necessary frequency hopping time (tuning gap to be ready to receive data from a new RF channel when using a single tuner imposes severe limitation which are investigated in the following sections.

Optimal cell distribution with rotated constellations

As introduced in previous chapters, inter-RF FI performance can be extended by using rotated constellations (RC). Aside from the application of proper rotating angles according to each regular QAM constellation, the use of RC is rigged with a component interleaver to separate the I and Q components of each rotated symbol. In DVB-T2 this is achieved by a time shifting of the Q component (Q-delay) so that the Q component of symbol n is transmitted with the I component of the symbol n+1. This ensures each component of the same symbol experiences a different fading realization. When using TFS, it is desirable that each component is transmitted in a different RF channel. A component interleaver is introduced in DVB-NGH just before the TI and after rotation. The component interleaver achieves that the I and Q components of the 2DRC symbol are transmitted in two different RF channels. The interleaver is sub-optimum for 4DRC, specially with 2 RF channels. Figure 5.6 shows two examples of the component interleaver operation with 2 and 4 RF channels and one TFS cycle per RF-Mux. The N_c cells of an incoming FEC word are written in a matrix of dimension $N_{RF} \cdot N_k$ rows per $\lceil N_c/(N_{RF} \cdot N_k) \rceil$ columns[3]. The output is generated by reading the matrix row-by-row. The Q-shifting operation can be summarized according to the requested performance features:

- Non-TFS operation. All shifts are equal to $D/2$, where D is the number of dimensions.
- TFS operation with 1 TFS cycle per TI period ($N_k = 1$). This can be achieved by a cyclic shift calculated as $c \mod N_{RF}$.
- TFS operation with N_k cycles per TI period. Shifts that are multiple of N_{RF} must be skipped. Only $N_{RF} - 1$ shifts are kept to maximize the temporal separation between components.

[3]Note that if the number of cells is not an integer number, the matrix must be padded.

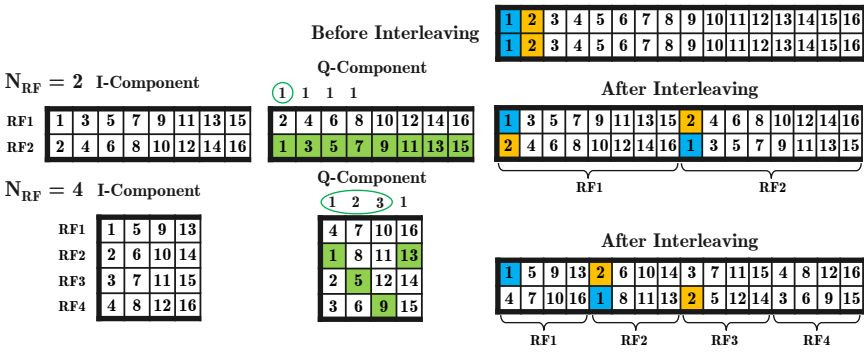

Figure 5.6: Component interleaving operation with 2 and 4 RF channels.

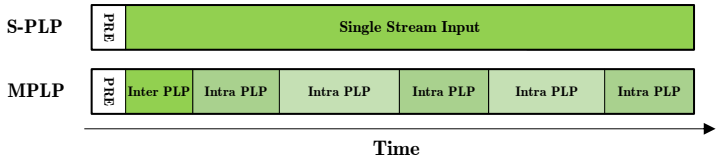

Figure 5.7: Single PLP mode (up) and Multiple PLP mode (down).

5.2.2 Frame Composition and Transmission Modes

The frame builder arranges service data into frames. With TFS, the frames to be transmitted in each RF channels are jointly generated so that the modulator feeds the RF system with as many signals as RF channels in the RF-Mux.

The services are introduced in each frame by means of TDM slots carrying service data. The concept of PLP introduced in DVB-T2 enables to provide service specific transmission parameters such as modulation, code rate and TI, which permit setting specific robustness and capacity. Figure 5.7 depicts the frame structure when using a single PLP or multiple PLPs. With MPLPs, services with different robustness can be transmitted within the same frame. Inter-frame PLPs are used once per frame whereas Intra-frame PLPs can be transmitted with sub-slicing so that more than one slot of the same service is transmitted per frame. The frame is completed with preamble symbols carrying reference and signalling information for the reception of the data.

TFS is defined to be operated using MPLPs where each PLP carries the data of one service. The frame structure per RF channel is similar as that with a single channel except that each frame carries data of all PLPs (services) in

the system instead of only that from the PLPs sent in one RF channel in a classical transmission.

The preamble consumes transmission time, as well as the necessary signalling to identify the elements in the frame. DVB-T2 introduces the concept of a common PLP (inter-PLP) carrying data that is shared between different PLPs such as the EPG what reduces overhead. With TFS, the common information carried in an inter-PLP shall be sent on all RF channels with identical scheduling in each frame, increasing overhead.

With inter-frame TFS the slices of a PLP are transmitted frame by frame in a different RF channel. Inter-frame TFS is the only TFS operation mode possible for short frames using a single tuner. In DVB-NGH, inter-frame TFS is envisaged to be operated between FEFs[4]. Inter-frame PLPs can also use TFS in this operation mode but they require inter-frame time interleaving in order to exploit frequency diversity within the RF-Mux.

Intra-frame TFS operates between the intra-frame PLPs which are transmitted across different RF channels. Hence, a frame containing slots of all services is transmitted in each RF channel. Intra-frame TFS allows for intra-frame TI and also inter-frame TI when interleaved data extends to more than one frame.

5.2.3 Scheduling Operations

Scheduling operations are necessary when the number of RF channels is greater than the actual number of tuners at the receiver since it is necessary to accommodate data into the frame in a regular manner so that the receiver is able to recover it sequentially. When the number of tuners equals the number of RF channels the slots where services are allocated could be time-overlapped. However, this scheme is not considered in TFS though it would reduce TFS to a CB-like system.

The scheduler is in charge of taking decisions on the construction of the frames which involves the frame builder and BICM modules, as well as generating the in-band signalling information that is inserted in each interleaving frame (see 5.5). Data allocation is determined for each frame and depends on the instantaneous number of cells to be transmitted. It should be noted that the size of the frame in OFDM symbols is constant during transmission.

Scheduling for inter-frame TFS is done on a frame or super-frame basis with different alternatives to ensure that frequency hopping can be performed frame-by-frame, as depicted in Figure 5.8. Co-timed frames require synchronization so that all of them start at the same time. Since frequency hopping is performed

[4]DVB-T2 defined FEFs which allow the transmission of future systems conveyed in frames within existing DVB-T2 frames in a TDM manner.

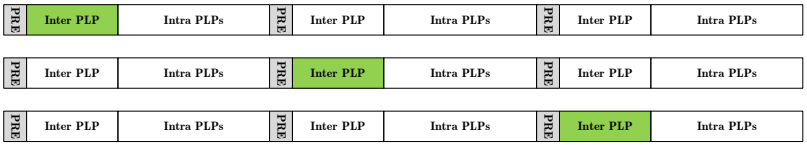

(a) Co-timed frames

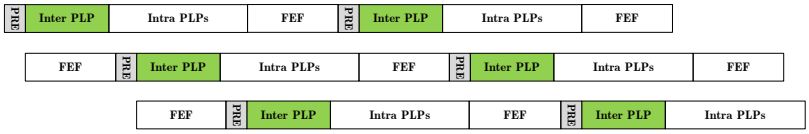

(b) Co-timed super-frames

Figure 5.8: Scheduling for inter-frame TFS.

between Inter-PLPs, Intra-PLPs of other frames (e.g. FEFs) should be used to achieve the required tuning gaps between slots. This is easily achieved since each frame may carry other services (PLPs) unless short frame duration is configured. Shyncronization between super-frames may allow a more efficient scheduling since each super-frame can be delayed by the necessary tuning gap, thus allowing for more frequent frequency hopping. As an example, DVB-T2 super-frames include an integer number of DVB-T2 frames and FEFs which could be arranged to accommodate the TFS slots. In such case it is possible to find an integer number of frames and FEFs per RF channel so that super-frames can be synchronized. For example, a super-frame in RF 1 can start with a frame containing an inter-PLP. Then, the super-frame in RF 2 should start with a FEF of duration equal to the inter-PLP in RF 1 plus one tuning gap, and so on.

The selected alternative mainly influences zapping time and flexibility. Zapping time depends on the synchronization between frames and the number of TFS cycles. Case A present the largest zapping time but frames start at the same point in time. Case C achieves the shortest zapping time but extra frames need to be used (FEFs in the figure), what involves capacity overheads. On the other hand, inter-frame TFS provides flexibility for configuring the required time gaps for frequency hopping.

The scheduling with intra-frame TFS is defined for the Intra-PLP sub-slices in each frame. The process bases on the number of FEC words to be allocated per frame for each PLP, which can dynamically change from frame to frame, the number of RF channels in the RF-Mux (N_{RF}) and the number of sub-slices

per frame (N_{subs}). This determines the total number of sub-slices to be filled in a frame duration for all RF channels in the RF-Mux as:

$$N_{subs_{total}} = N_{RF} \cdot N_{subs} \tag{5.2}$$

Figure 5.9 depicts the process graphically. In step 1, the current data per PLP to be transmitted in the frame must be divided by the total number of sub-slices within the RF-Mux. This produces N_{subs} equally sized slices. The sub-slices can be evenly distributed in each frame and RF channel. The sub-slice interval, $D_{subslice}$, is the maximum separation between sub-slices corresponding to the same PLP in one frame. The necessary tuning gap between consecutive slices is achieved by time-shifting the sub-slices frame by frame, as described in step 3. The RF shift is produced according to the sub-slice interval and the number of RF channels as:

$$D_{RFshift} = \frac{D_{subslice}}{N_{RF}} \tag{5.3}$$

RF shift must result in an equal or larger duration than the required time for frequency hopping. After RF shifting, those sub-slices exceeding the frame duration are cyclically shifted to the beginning of the frame, what conforms the final parts of each frame to be transmitted. After scheduling process, the frame builder fills the frames with signalling information (preamble), an inter-PLP with commmon information, if any, and other PLPs.

It should be noted that the divisions described in the scheduling method are supposed to produce an integer value result. Thus, padding cells should be added when this is not possible.

Note also that one sub-slice may be divided into two parts which are located at the beginning and end of the same frame, as it happens with PLP4 and PLP2 in the second and third RF channel in Figure 5.9. Since scheduling is done frame by frame it is possible that two consecutive slots end and start in the same RF channel, what will not cause a tuning operation. However, when frequency hopping is done at frame edge it is necessary to employ a guard period between frames to prevent a similar situation. With intra-frame TFS this guard period may be enabled by the use of and inter-frame PLP or other kind of frames (e.g. FEFs, as described in DVB-T2/NGH).

The scheduling process for intra-frame TFS enables the use of co-timed frames so that all RF channels are synchronized at the transmitter side (i.e. preamble symbols are located in the same positions in time for all the RF channels in the RF-Mux).

The intra-frame TFS scheduling provides a regular frequency hopping within each frame. When using VBR services, it is not possible to ensure a regular frequency hopping for all frames. Furthermore, it is not possible to allocate

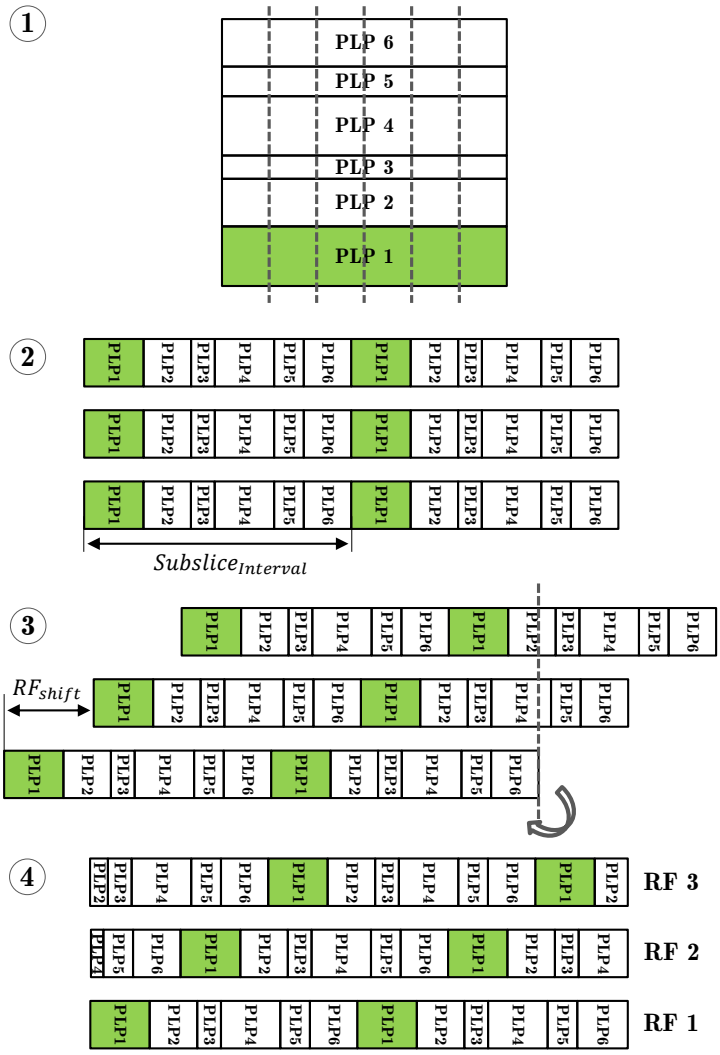

Figure 5.9: Scheduling for intra-frame TFS.

VBR slots unless peak data rate is limited. If not, it would not be possible to achieve and optimim TFS diversity. With CBR regular scheduling can be achieved within a frame and also across frame boundaries.

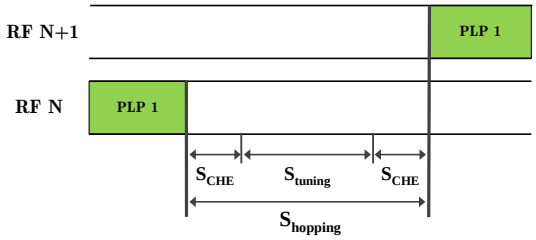

Figure 5.10: Frequency hopping timing restrictions with a single tuner.

5.3 Receiver Operation for TFS Reception

The reception of a desired service in a traditional transmission without TFS is performed by tuning the RF channel carrying the data of the desired service. No tuning operations are required until the user deliberately selects a service transmitted over a different RF channel. With TFS, however, the reception of a service is performed by means of frequency hopping over the different RF channels within the TFS-Mux where each RF channel carries portions of data that belong to the intended service.

Ensuring the TFS reception with a number of tuners smaller than the number of RF channel, and in particular when using a single tuner, involves operative limitations. Irrespective of the TFS mode, it is necessary to establish a time gap ($t_{hopping}$) between consecutive data slices in two different RF channel.

The minimum time gap is constrained by the time employed by the tuner to perform a switching between frequencies, and the necessary time for channel estimation.

DTT systems make use of pilot-aided channel estimation. When channel is estimated in the time-domain, time interpolation between pilots sequences is implemented. A particular number of symbols is needed for such process according to the configured PP. Thus, it is necessary to finalize the channel estimation in the time domain for the current RF channel and start the channel estimation of the following RF channel previous to the correct reception of the data. Figure 5.10 depicts these intervals which values are, in turn, function of the symbol period T_S (which depends on the FFT size and GI) and the selected PP. According to this, $t_{hopping}$ can be expressed as:

$$t_{hopping} \geq T_S \cdot S_{tuning} + 2 \cdot T_S \cdot S_{CHE} \tag{5.4}$$

where S_{tuning} is the entire number of symbols used during tuning operation and S_{CHE} is the number of required symbols for channel estimation.

5.3.1 PLL+AGC and Synchronization Operation

The required number of symbols depends on the processes that take place at the receiver for tuning operation which involve the following:

- PLL (Phase Locked Loop) tuning. The PLL consist of a variable frequency oscillator (VFO) and a phase detector and is aimed at generating an output signal which frequency coincides with the frequency of the input signal. This is achieved by reducing the phase differences between the input and the output signal.

- AGC (Automatic Gain Control) stabilization. The AGC is aimed at producing an output signal with stable amplitude to feed the A/D converter.

- Frequency and Timing synchronization for a proper symbol tracking.

PLL and AGC implementation should minimize tuning times in order not to introduce excessive delays that are translated into data rate overheads. State-of-the-art techniques such as Direct Digital Synthesizer (DDS) could allow fast frequency change and AGC operation. Reference [87] explains the design of an AGC for WLAN application that reaches stabilization with a gain error less than 1 dB in 5.6 μs. In [88] a TFS-like system for Ultra Wide Band (UWB) applications is presented which allows frequency hopping between different channels in about 9.5 ns. The tuning time could be further decreased if it could be possible to store the current AGC level to be used as a coarse estimation of the initial AGC level of a following switching to the same RF channel. Furthermore, if it is not possible to store the values for all RF channels in the RF-Mux, prediction of the AGC value of the following RF channel may use the value of the current RF channel in order not to start from scratch.

Synchronization error estimation is paramount to identify the beginning of the OFDM symbols and to ensure inter-carrier orthogonality in order to prevent ISI and Inter-Carrier Interference (ICI),respectively. Several studies have focused on these issues and have proposed different approaches to estimate timing and frequency offsets. Symbol timing offset is estimated blindly in [89, 90] or with the aid of pilot symbols [91]. Frequency offset estimators for OFDM systems are developed in [92, 93]. Joint frequency and timing synchronization are investigated in [94–97] based on pilot sequences or blindly [98–101].

Regarding frequency, time and symbol synchronization, there are two main operations involved in the reception of the TFS signal (and also in a classical transmission) where synchronization is achieved: initial scan, tracking and channel zapping [54].

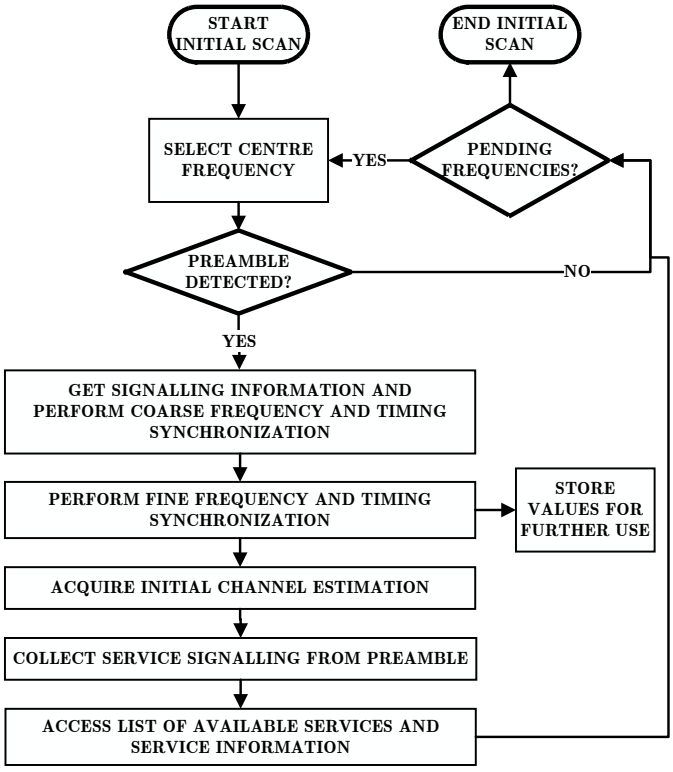

Figure 5.11: Flow chart of the possible Initial Scan process for TFS.

Initial Scan

The initial scan is executed when the receiver has no knowledge of any available DTT service and will have to perform a frequency scan of the broadcast band in order to determine the existence of any RF channel carrying a DTT signal. This process involve to determine the format of the existing DTT signal and its quality. Thus, it is necessary to recover signalling information regarding modulation and coding parameters as well as perform a coarse time and frequency synchronization. Figure 5.11 is a flow chart describing the operations conducted during the initial scan.

Besides the discovery of the basic transmission parameters of the signal, the preamble symbol(s) enables a first estimate of frequency and time synchronization in order to compensate the tolerances at the receiver frequency reference or a deliberated offset introduced at the network side in the planning process (e.g. to control interference between networks), and adjust the FFT window position, respectively.

The frequency offset correction is performed thanks to the preamble. In DVB-T2, preamble symbol P1 allows correction when the transmitted signal is inside +/- 500 kHz range from the centre of the bandwidth (in 8 MHz channels). A peak of correlation between a reference signal and the received signal reports the number of carriers that the symbol is shifted, thus, providing a coarse frequency offset.

To perform fine synchronization, the receiver should use a synchronization algorithm that typically makes use of the continual pilots for frequency-error measurement together with the impulse response estimate derived from the scattered pilots for fine adjustment of the FFT window position. Once RF and sampling frequency offset have been corrected and time synchronization achieved it is possible to receive the preamble symbols, recover the signalling information and disclose the service information.

Tracking and Channel Zapping

At this stage it is assumed that the receiver has visited all the frequencies, so that the initial scan and set-up processes have been achieved, and that it is perfectly synchronized to the last tuned frequency. All control loops and tracking are stable. A similar strategy as that explained for the AGC could be used in the synchronization process when RF switching occurs. Since the other frequency has been visited in a previous instant, synchronization will not have been fully lost. Thus, synchronization measurements and corrections (i.e. time and frequency offsets) stored in a previous visit could be used to speed up the process. Figure 5.12 depicts the process during TFS reception. Note that in this case zapping process can also be speed-up since the synchronization correction of the RF channels could be already known.

5.3.2 Channel Estimation

Broadcast systems use pilot patterns to compensate for the variations of the channel in the time and frequency domains. The pilots are positioned in different sub-carriers in OFDM symbols. D_X is referred to as the separation of the pilot carriers in each OFDM symbol whereas D_Y defines the number of OFDM symbols that conform a pilot sequence.

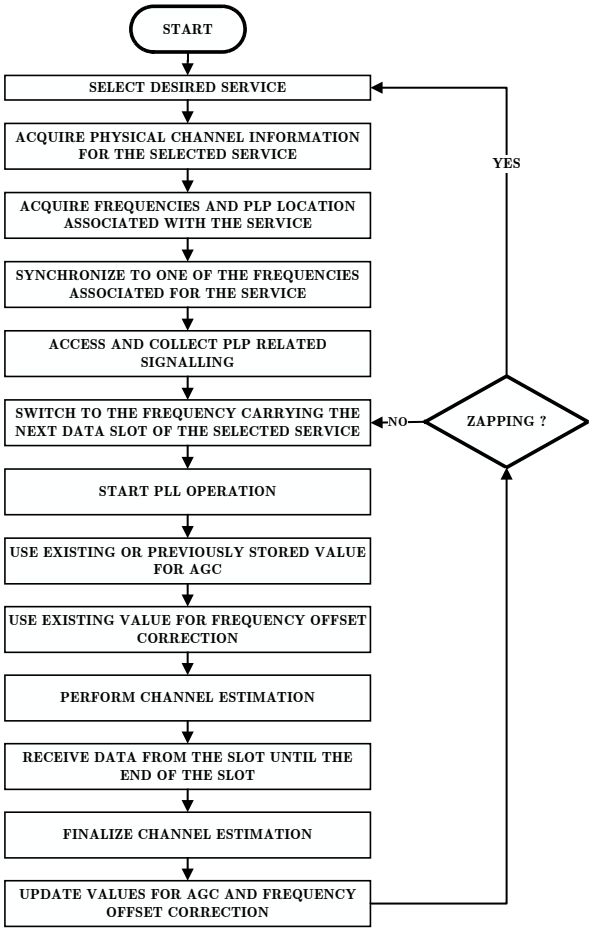

Figure 5.12: Flow chart of the possible Tracking and Channel Zapping processes for TFS.

The PP should be selected according to the expected channel between transmitter and receiver. High dense PPs reduce transmission capacity since less data carriers are available whereas increase performance due to a more reliable channel estimation.

The necessary time for channel estimation before and after a slot, t_{CHE}, is dependent on:

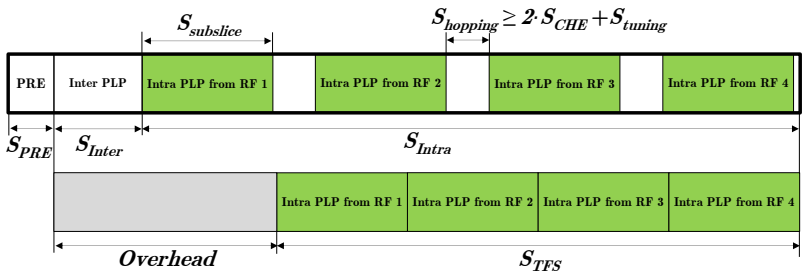

Figure 5.13: Capacity overheads by tuning gaps with intra-frame TFS.

- Bandwidth and FFT size, which define the duration T_U, measured in cycles of the elementary period T, dependent of the system bandwidth.
- OFDM guard interval T_{GI}, which define the symbol period as $T_S = T_U + T_{GI}$.
- Scattered PP time density.

Channel is estimated in the time domain by means of interpolation. In general, the number of symbols involved in time interpolation is given by D_Y-1. Receiver must wait until the complete reception of the pilot sequence to perform interpolation. Extra-dense pilot patterns may be used to allow for frequency-only interpolation (similar to $D_Y = 1$) so that it is not necessary to perform time interpolation, thus reducing the required time for channel estimation with TFS t_{CHE}.

5.3.3 Operation Limitations with Single-Tuner TFS

The most restricting operation mode with a single tuner approach is intra-frame TFS since all tuning operations need to be done within frame duration. During frequency hopping there is no data reception. This causes a capacity overhead that limits peak data rate per PLP if compared to the maximum data rate available in a frame without tuning gaps. Figure 5.13 depicts a scheme of the received data within a frame duration considering that the service fills the complete frame except the tuning gaps (either for intra-frame frequency hopping or at frame boundaries). Some variables, in terms of symbols, are also depicted to calculate the actual payload capacity with TFS.

The following equations and assumptions are used in calculation, mainly based on DVB-T2 parameters.

The tuning time, in symbols, is defined as:

$$S_{tuning} = \lceil \frac{T_{tuning}}{T_S} \rceil \tag{5.5}$$

where T_S is the symbol period.

The total amount of symbols required for channel estimation is given by:

$$S_{CHE_T} = 2 + N_{RF} \cdot N_{subs} \cdot S_{CHE} \tag{5.6}$$

Where $S_{CHE} = 2(D_Y - 1)$. Note that it is assumed the existence of two symbols at frame edges (i.e. the first and last Intra PLPs symbols).

In order to allocate the necessary time gap for tuning between frames, one Inter PLP of size $S_{Inter} = S_{tuning}$ is used.

The number of available symbols of the Intra-PLP part of a frame is reduced to:

$$S_{Intra} = S_{frame} - S_{PRE} - S_{Inter} \tag{5.7}$$

Where S_{frame} is the frame duration expressed in symbols, S_{PRE} is the number of preamble symbols in a frame, which depends on the FFT size, and S_{Inter} is the number of Inter PLP symbols.

The actual number of symbols available for the Intra-PLPs with TFS is:

$$S_{TFS} = S_{Intra} - S_{CHE_T} - (N_{RF} \cdot N_{subs} + 1) - N_{RF} \cdot N_{subs} \cdot S_{tuning} \tag{5.8}$$

Note that the required number of data symbols is one more than actual data since one sub-slice of N symbols is normally split over $N + 1$ symbols.

Finally, the capacity overhead introduced by TFS can be calculated as:

$$\%_{overhead} = \frac{S_{TFS}}{S_{Inter} + S_{Intra}} \tag{5.9}$$

It can be observed that the available number of Intra PLP symbols per frame is reduced when increasing the number of RF channels within the TFS cycle since, in overall, the total time for frequency hopping increases. The same occurs when increasing the number of TFS cycles per frame.

Table 5.1 provides the capacity overhead considering DVB-T2 parameters. The worst case for symbol period (32k 19/128) is selected. The number of RF channels is 2 and 4. Required symbols for tuning, S_{tuning}, and the value for D_Y are 1 or 2. The overhead is calculated according to the ratio expressed in Equation 5.9. Note also that DVB-T2 defines two type of preamble symbols (P1 and P2). The length of the P1 is fixed to $2048 \cdot T$, being T the elementary period. Note that one symbol for carrying the common information of the PLPs

Table 5.1: Peak service data rate overhead. 8 MHz 32k 19/128 256QAM 2/3.

RF-Mux	S_{tuning}	D_Y	%Overhead	Mbps
4	1	2	51.3%	16.07
4	1	1	38.7%	20.23
2	1	1	29.6%	23.22
4	2	2	56.8%	14.25
4	2	1	47.2%	17.42
2	2	1	36.7%	20.90

is also added. The total frame length cannot exceed 250 ms and a maximum TDI memory of 2^{19} is considered.

Increasing the number of RF channels in the RF-Mux or the tuning gap and decreasing the pilot pattern density in the time domain makes peak service data rate drop. One of the most critical parameters is the value D_Y. If tuning gap could be only 1 symbol (which means less than 4 ms for tuning in the 8 MHz 32 19/128 case), transmission could benefit from service data rates around 20 Mbps with up to 4 RF channels.

However, the service data rate limitation does not only comes from the scheduling of TFS. The available memory at the receiver causes severe limitations in many cases. Doubling TDI memory to 2^{20} cells will lead to the following situations:

- Overhead will be reduced to 38.5% and 27.8% with $D_Y = 2$ and $S_{tuning} =$ 2 and 4 and 2 RF channels, respectively.
- Overhead will be reduced to 22.0% with 2 RF channels and $D_Y = 1$, $S_{tuning} = 2$.
- With $S_{tuning} = 1$ and $D_Y = 1$, overhead is 17.0% and 23.5% with 2 and 4 RF channels.

Note that in some cases a maximum frame length of around 300 ms would also be beneficial.

5.3.4 Dual-Tuner Approach for TFS Operation

The scheduling for intra-frame TFS with a dual tuner approach should not be constrained by the necessary frequency hopping time. In the worst case, a PLP requiring a high peak capacity would be transmitted during the complete intra-frame PLP part duration of a frame, as depicted in Figure 5.14.

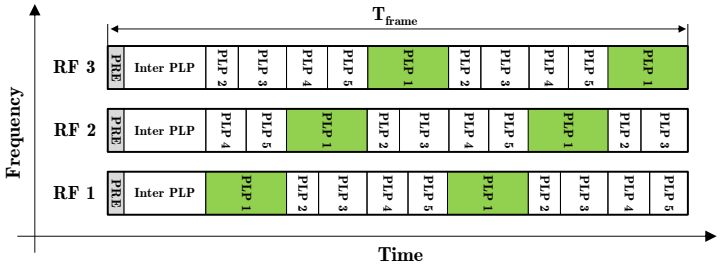

Figure 5.14: Scheduling for intra-frame TFS with a dual tuner.

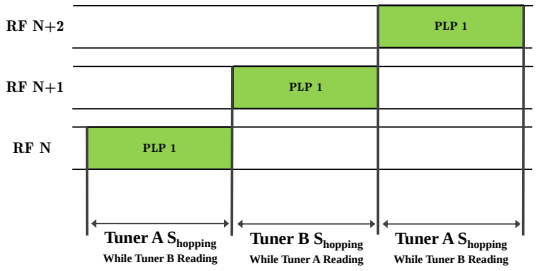

Figure 5.15: Alternative tuning process for dual-tuner TFS.

Moreover, in this case it would not be necessary to dedicate a extra symbols for tuning between frames.

The operation of TFS with two tuners should be done alternatively, i.e. while one tuner is tuned to the frequency where the desired data slot is located, the other tuner will be performing the required operations to start receiving data once the other tuner is free. This situation provides relaxed timing and PLP peak capacity constraints as soon as one tuner have enough time for frequency hopping while the other tuner is receiving data, what is directly linked to the number of RF channels. The more the number of RF channel, the less the time for frequency hopping between two RF channels since the slot duration decreases, considering the maximum possible data rate. Figure 5.15 depicts the aforementioned situation.

5.4 Transmitter and Receiver Implementation with CB

The implementation of CB is less demanding than that of TFS though it requires the use of multiple tuners at the receiver. In fact, an additional tuner is required per bonded RF channel and single-tuner operation is not possible. The high cost of an implementation with a large number of tuners and the possibility to achieve high service data rate gains already with a low number of RF channels (e.g. 2 RF channels) makes it reasonable to consider CB with 2 tuners.

CB can be implemented with the reuse of all existing blocks in a standard Single-Input Single-Output (SISO) receiver extended with additional specific blocks or with a newly designed chain that allows the processing of a high capacity stream, what would increase complexity. When reusing the architecture of the existing modulators, the basic CB operation (*plain Channel Bonding*) do not introduce important modifications on the transmitter side since data is sent over single RF channels as in a classical transmission. Figure 5.16 (left) depicts the transmitter and receiver chains for plain CB. The data packets of a PLP pass through an input formatting block, where the baseband headers (BB header) are inserted. The BB header contains a timestamp that allows for correct reordering of the packets at receiver side.

A stream partitioner is required to split the high-capacity data stream into two sub-streams that feed corresponding standard single-RF channel modulator inputs. The inverse mechanism must be implemented at the receiver to allow the data combination by means of a combination circuit. The independent transmission of the data using two chains enables the transmission of the services over two RF channels regardless of their allocation in the frequency band. Thus, CB operation can be performed over adjacent or non-adjacent RF channels.

One of the key elements of the system is the block involving inter-RF frequency interleaving (*SNR averaging*) when it is implemented. Whereas the common modulation of the streams could directly allow for frequency interleaving across all RF channels, the use of independent BICM modules per stream requires of a specific block that allows a common coding of data or a cell exchange so that one half of data is sent over each RF channel (see Figure 5.16-right). The cell exchanger is placed after the TI process. Thus, at a cell level, odd cells of the incoming streams could be straight transmitted wheareas even cells could be exchanged. At the receiver, it is necessary to implement a high-speed bus so that data can be re-exchanged and decoded.

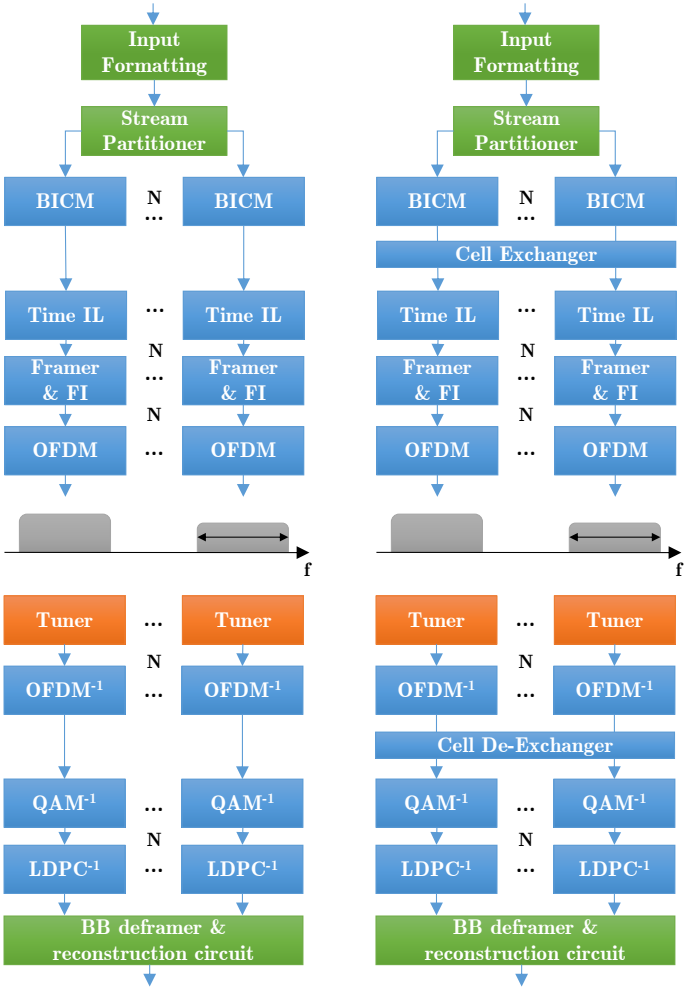

(a) Plain CB (b) CB with SNR averaging

Figure 5.16: Basic transmitter and receiver chain for CB with and without inter-RF FI.

5.5 Signalling Requirements for TFS and CB

Signalling information is carried in the preambles of the signals to allow the detection of the signal and the decoding of each service or PLP. Part of the

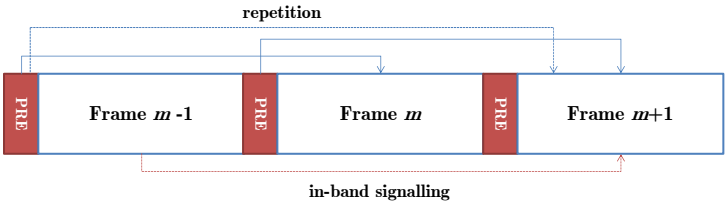

Figure 5.17: Signalling with TFS. Signalling information of the preamble refers to the next frame and the next-but-one frame (when it is repeated). The in-band signalling of the current PLP refers to the next-but-one interleaving frame.

preamble information shall remain static (e.g. signal bandwidth and OFDM parameters) within a super-frame whereas other information can change from frame to frame (PLP-specific parameters such as MODCOD).

The recovery of the signalling information in a classical system is performed by the decoding of the preamble symbols, which are generally transmitted with a robust mode. The use of a PLP containing common information of multiple services also requires its decoding frame by frame. When operating TFS, preamble and common PLP signalling must be transmitted in all frames so that it is possible to recover information whatever the tuned RF channel is. Furthermore, the data conveyed in a common PLP should be transmitted with improved robustness since inter-frame TFS is not permitted for this PLP since signalling information must be accessible at any time once one an arbitrary RF channel is received. When performing sequential frequency hopping it is not possible to recover this signalling unless it is contained in the same data slot that is being received.

In-band signalling allows the transmission of the signalling together with the data so that there is no need to access the preamble symbols or other PLPs, so that continuous data reception is possible. In-band signalling is introduced in the first time interleaving frame. The use of in-band signalling requires that the receiver is already synchronized.

With TFS, in-band signalling is a useful means to allow continuous reception of the slices of a PLP. The in-band signalling carries information of the next-but-one frame. Note, however, that the in-band signalling shares the same MODCOD as that of the slot data which is generally less robust. The repetition of part of the signalling information contained in the preamble allows the transmission of the dynamic signalling for the next-but-one frame with TFS, as depicted in Figure 5.17.

The main parameters that need to be signalled for TFS and CB operation involve those indicating the indexing of RF channels. With TFS, the mapping of the PLPs is also important.

Indexing of the RF Channels with TFS and CB

The number of RF channels (NUM_RF) that belong to the RF-Mux needs to be signalled. A 3-bit field could be enough for such purpose with TFS allowing the signalling of up to 7 RF channels. For CB it could be enough with 2 bits if no more than 3 RF channels are going to be bonded. Note that NUM_RF = 0 is used for the regular single-RF operation.

For each RF channel, it is necessary to discover its frequency and its position in the RF-Mux. A loop may allow for listing the index of each RF channel (RF_IDX, 3 bits) and its center frequency (FREQUENCY).

The number of bits assigned to the frequency field could vary according to different approaches. If frequency is indicated in MHz or with the number of RF channel depending on the band (e.g. channel 21 in UHF corresponds to 474 MHz in Europe) instead of being signalled in Hz, the signalling overhead could be reduced (from 32 bits to 7 or 10 bits, respectively). If a larger unit of granularity is used, e.g. 1 kHz, 12 bits shall be enough. Indicating the frequencies as offsets, in number of RF channels, with respect to the RF channel with index 0 would only require 6 to 7 bits, depending on the frequency band. However, the initial frequency should still be indicated.

With TFS, each frame should carry the index of the RF channel in which it is transmitted so that the following RF channel to be tuned is the one with one index greater than the current one. When the index reaches the value NUM_RF-1, the next index will be RF_IDX = 0.

Mapping of PLP Data with TFS

The mapping of the data into frames must be indicated, specially for single-tuner TFS.

With TFS, a PLP carrying common information should appear in the same position in all frames.

The use of inter-frame TFS should be indicated for the PLPs transmitted once per frame. To this purpose a flag could be used to identify if the PLP appears on the same RF channel frame after frame or in a different RF channel using TFS.

For the PLPs using intra-frame TFS, the starting RF channel on which the first sub-slice for each PLP is allocated needs to be signalled as well as the starting position of the first intra-frame PLP. The starting position and the sub-slice interval (indicating the number of OFDM cells from the start of one sub-slice of one PLP to the start of the next sub-slice of the same PLP on the same RF channel) allows to calculate the position of the 'folded' PLPs. As well, the total number of sub-slices across all RF channels in a frame duration should also be indicated, as derived in Equation (5.2).

Other Signalling Considerations with CB

For CB, the current PLP should indicate the number of additional bonded RF channels (NUM_CHAN_BONDED, again 2 bits), with a maximum value of NUM_RF. The parameter set to '0' indicates that CB is not used for the current PLP.

When NUM_CHAN_BONDED is greater than 0, the CB mode (plain CB or CB with SNR averaging) needs to be signalled (CB_MODE, 1 bit).

An RF_IDX field with 2 bits needs to be included to indicate the indices of the bonded RF channels for the current PLP as well as the order of the channels.

5.6 Impacts of TFS and CB on Network Topology and Deployment

5.6.1 Network Topology

DTT networks are traditionally deployed using a wide set of stations including high and low power transmitters, repeaters with frequency transposing, on-channel repeaters, etc. to enable an efficient coverage extension. Behind the broadcast network there are several processes that include the distribution of the contents from the broadcasters to intermediate stages (contribution network) that multiplex the signals and generate the necessary data for modulation. Data is transported to the broadcast stations where the modulation and transmission processes take place. Figure 5.18 depicts an scheme of the distribution of the RF-Mux data to broadcasting stations.

Distribution Network. Distribution network is in charge of providing the data that is modulated at the transmitter sites. A core element (i.e. an encapsulator or a T2 gateway, in DVB-T2 terminology) receives one or more MPEG Transport Streams (MPEG-TS) containing service data and signalling information and generates a series of frames containing the information required for a modulator to construct the frames and also synchronization data to be used e.g. for SFN transmission. These frames are distributed to all transmitters by a dedicated network (fiber, IP, satellite...). With TFS or CB, the gateway ensembles all the service data to be transmitted and generates a single frame that will be sufficient to feed a modulator input that creates the signals that are transmitted in each RF channel in the RF-Mux.

The frames generated by the gateway generally consist of MPEG-TS data with a small additional proportion of control information data. Thus, no significant increase in distribution capacity is required. However, the big data

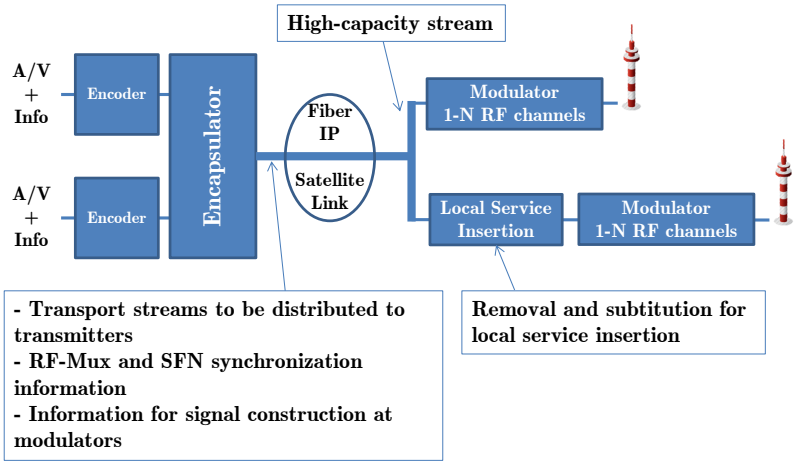

Figure 5.18: RF-Mux services data distribution to stations. Encoding and encapsulation processes take place at the broadcaster or operator head-end facilities. Afterwards a stream containing service data as well as synchronization and modulation information are transported to each station by means of wired or wireless systems. Modulation takes place at the transmitter stations.

rate of the unique signal generated in the gateway requires of big capacity. A possible solution is to split this signal into smaller sub-streams that could be transmitted using different networks and re-constructed and error-repaired at the transmitter site. The amount of capacity required to distribute the signal to the modulator interface is practically the same as that required in a classical network with the same number of RF channels.

One of the key issues with the use of encapsulators is how to signal the frequencies to be used in each transmitter. In SFN operation, the frequencies of the RF-Mux can be indicated in the encapsulated signal so that all stations will generate the modulated signals with the correct frequency. However, in case of MFN transmitters, the frequencies indicated in the encapsulated signal should be replaced or translated to the actual frequencies to be used in each station.

Local service insertion. Several broadcasters deliver regional-specific programs (news programs, special events,...) at certain hours at different areas carried using the same TV service which provides the global (national) service. This is currently done by the replacement of the national service by a regional produced service consisting of the re-multiplexing of the complete multiplex (RF channel) carrying the service. With TFS and CB, this operation is diffe-

rent since the signals of all RF channels are generated at the same time. Two possible solutions could be implemented to solve the issue:

- Distributed encapsulators/gateways (one per region/local area). MPEG-TS distribution to each gateway where regioal services are inserted as national services. The output of the gateway could be distributed to all the transmitter stations (MFN or SFN) in the same regional area.
- Central encapsulator/gateway. The RF-Mux frames are created but including some PLPs which are filled with dummy packets. The dummy packets are replaced at each region area with the corresponding program by means of a re-multiplexer.

RF-Mux synchronization. The signals in the RF-Mux should be synchronized to fulfil with the frame scheduling. Synchronization is already a requirement for SFN transmitters to compensate time delays between signals from different transmitters. Synchronization information is generated by the gateway so that each modulator can compensate delays and transmit the signals with the proper timing. With TFS and CB, a similar mechanism should be implemented not only for SFN transmitters but also for MFN ones, though the frequencies used will be different. Although it is not common, MFNs can also be built up of distributed transmitters each one radiating a particular sub-set of frequencies. In this case, the full set of signals of the RF-Mux needs to be transmitted to each station, though only some RF channels will be radiated, what it is not an efficient solution.

Synchronization requirements have also impact on other kind of transmitters commonly used such as repeaters:

- On-Channel Repeaters (gap-fillers). This kind of repeaters receive one or some RF channels and directly amplify and transmit them using the same frequency. This generates and artificial SFN-like echo (gap-filler and propagation delays) at the receiver. When TFS is used and only a sub-set of RF channels is repeated there exist an extra delay (of a few micro-seconds) that may be negligible in comparison with the tuning gaps when using TFS with a single tuner but could be critical when gaps are eliminated when using more than one tuner. With CB, the same consideration needs to be taken into account since all RF channels should be generated at the same time.
- MFN Regenerators. Contrary to gap-fillers, regenerators process the signal so that the signal is error-corrected and transmitted instead of merely amplified. This process generate delays that require of a frequency transposing of those RF channels which are regenerated. These delays make

impossible the operation of TFS and CB when only a sub-set of RF channels are regenerated. There is no problem is the complete RF-Mux is regenerated.

5.6.2 Coverage Issues

All RF channels in an area could be potentially used with TFS and CB. However, it is possible to aggregate groups of 2-3 RF channels together since gains are already relevant in these cases. Any combination could be used depending on business cases. Note also that both techniques could be used by a single broadcaster operating more than one RF channel per site (intra-broadcaster RF-Mux) or by multiple broadcasters co-operating (each broadcaster having 1 or more RF channels).

As well, any set of VHF and UHF channels can be used with TFS as soon as the signals have the same bandwidth. There is no channel bandwidth restriction for CB since the tuners are locked each one to a different channel and the frames can be configured with different bandwidth. This is it possible to bundle two channels in different bands.

Coverage will automatically be harmonized for all RF channel when using inter-RF FI. Thus, both techniques can average the potential imbalances between RF channels in the same band. However, special attention should be paid when bonding channels from different bands and/or different levels. Without inter-RF FI and when using CB, the RF channel with the lowest C/N restricts the coverage of the whole RF-Mux.

TFS and CB with inter-RF FI could still be used in case of different coverages. For example, there exist rules in some countries where public service broadcasting and private broadcasting do not share the same coverage targets. The following example illustrates two alternatives to enable the use of inter-RF FI when one multiplex must cover a 99.8% population whereas the target for other multiplexes is 98%. One possible solution could be to dedicate 1 multiplex to 99.8 % coverage and 6 multiplexes with inter-RF FI to 98% coverage or use 7 multiplex with inter-RF FI for 98% population and 1 classical multiplex to cover the remaining 1.8%.

5.6.3 Network Deployment with ANP

The different ANP strategies developed in Chapter 4 are analysed here from the point of view of their implementation in current and future DTT networks. ANP topologies are fundamentally related to the use of MPN and MFRP.

MPNs basically consist on the use of a different polarization in co-channel station to achieve an interference signal level decrease. From the operator

perspective, the use of MPN requires that the stations are configured with the proper polarization. This has an impact also on the users since those located in a particular transmitter area may require the acquisition of a new aerial antenna or the reconfiguration of their existing antenna according to the configured polarization. Those users actually receiving horizontal polarization should apply a change in their antenna. In principle, the change could be practically done by a 90° rotation (change H to V polarization) of the existing aerial. In some cases reception could still be possible with the existing antenna for those locations close enough to the transmitter station (where field strength exceeds the polarization discrimination of the antenna). Note that MPNs can be implemented with and without TFS. It is evident that when TFS is used the DTT network should be adapted to benefit from the increased spectral efficiency.

The use of MFRP will require no changes from users since it only has implications in frequency planning (network operator).

A complete frequency replanning is necessary in order to implement a tighter frequency reuse (e.g. $\eta = 4$) with TFS and/or ANP. Replanning will be anyway necessary in order to accommodate the DTT service in the broadcasting band resulting after the release of the second digital dividend.

The implementation of frequency reuse $\eta = 4$ instead of $\eta = 7$ could allow for a potential power saving in the complete network. The capacity per multiplex could decrease to 4/7 the original capacity while the total capacity is kept constant. Assuming a fixed power per multiplex and a required C/N per multiplex of e.g. 20 dB, this new capacity per multiplex allows a theoretical C/N decrease from 20 dB to 11 dB (9 dB power reduction while keeping coverage per multiplex). The total power to serve 7 multiplexes with $\eta = 4$ supposes a power saving of 77% with respect to the power needed to serve 4 multiplexes with $\eta = 7$.

5.6.4 Legislation and Regulatory Aspects

The introduction of TFS and CB will require legislation modifications in some countries to implement the network in the optimum way, i.e, to pack all services together (to exploit capacity gains) and to spread them across different RF channels (to improve RF performance) or even between different bands (e.g. UHF/VHF). In analogue TV, a broadcasting licence holder was the holder of an RF channel, thus, one service was transmitted over one RF channel. The introduction of DTT has already required an adaptation of the legal framework governing broadcasting licensing in many countries so that one frequency (multiplex) is shared by several broadcasters [102].

TFS and CB can be run by a single operator as soon as it holds two or more RF channels. A complete separation between contents (broadcasters) and transmission (operators) or the co-operation between broadcasters allows that a larger amount of RF channels can be used for transmission. Optimally, the RF resource should be used as a block while capacity can be proportionally distributed among broadcasters. In the majority of countries, DTT spectrum capacity is allocated to one or more network or multiplex operators (e.g. Germany, UK, Italy, Spain...). In countries such as Sweden and Finland, capacity is assigned directly to individual channels.

In general, it is desirable that all operators deliver their services with the same coverage availability in their target service areas. Inter-RF FI enables that all services are received with the same SNR. To this purpose, a low level (high frequency) RF channel should be compensated by a high level (low frequency) one. All available RF channels could potentially be used. However, important gains are already achieved with 2 RF channels.

5.7 Conclusions

In this chapter, the main implementation aspects of TFS and CB have been investigated. The studies have been focused on the transmitter, receiver and network sides focusing on those aspects that limit the optimal operation of the techniques.

The main part of the investigation is focused on TFS since it is the most implementation-demanding technology specially for single-tuner operation. On the other hand, CB requires a tuner per RF channel and the partition of a high-capacity stream into low rate streams that are fed into single-RF modulators. Afterwards, receiver must re-join the data to decode the service. With TFS, frequency hopping operation involves the stabilization of AGC+PLL, channel estimation and synchronization processes what consume transmission time where service data cannot be sent. This leads to capacity overheads which have been studied according to different use cases taking DVB-T2 as a reference. The main conclusion is that a fast tuner (involving about 2 to 5 ms) and the use of time-dense pilot patterns are desirable to reduce the overheads at least to a 30% of the frame capacity, what would enable the transmission of UHDTV contents with HEVC.

Tuning gaps must be taken into account at the modulator when allocating service data. Intra-frame TFS is the most restrictive operation mode since frequency hopping is performed inside the frame duration. In addition, tuning gaps between frames must also be considered. In such case, low data rate services could be allocated at frame boundaries in order not to waste capacity.

Inter-frame TFS allows the implementation of the gaps by means of other kind of frames.

The operation of TFS with two tuners has been also studied. This approach would not require such an strict scheduling at least when there is enough time to alternate tuning operation so that one tuner can be re-tuned while the other is receiving data.

Nevertheless, tuning gaps are not the only features reducing service peak data rate. Whereas CB achieves inter-RF FI with an even distribution of data between the RF-Mux, TFS makes use of the time interleaver. The limited memory at the receiver for time de-interleaving also reduces peak data rate. The two main types of interleavers have been investigated together with TFS: block and convolutional TIs. A memory size of about 2^{20} cells is recommended when using a BI to increase the service peak data rates. Related to interleaving process, the use of a component interleaver when implementing rotated constellations has been assessed and its requirements for an optimal operation have been considered.

From the network perspective, a proper network deployment allows exploiting the advantages of multi-RF channel aggregation. From the operator's perspective, inter-RF FI would allow an homogeneous coverage for those services sharing the same RF-Mux. Co-operation between operators and broadcasters is recommended in order to apply TFS or CB to a high number of RF channels. However, the aggregation of 2 to 4 RF channels should be enough to exploit gains and to fit with the scheduling requirements when TFS is used. However, the sharing of spectrum resources between operators may require legislation changes in some countries. TFS and CB could be applied to any existing type of transmitter station. However, special attention must be paid to repeaters since they should operate over the complete set of RF channels in the RF-Mux.

Chapter 6

Conclusions and Future Work

6.1 Concluding Remarks

This dissertation has investigated and evaluated the potential for an efficient spectrum use in the next-generation DTT networks by means of the aggregation of multiple RF channels into one high-capacity multiplex (RF-Mux). Two techniques constitute the core of the dissertation around which the investigations are carried out: Time Frequency Slicing (TFS) and Channel Bonding (CB). TFS transmits the data of a service across several RF channels by splitting data into several time slots which are sent sequentially over different RF channels. These slots can be transmitted internally within a frame duration (intra-frame) or frame-by-frame (inter-frame). Reception by frequency hopping among the RF channels enables the re-composition of the stream and the demodulation and decoding of the service. With CB service data is received by tuning two or more RF channels simultaneously. After demodulation of each data stream, data is aggregated to generate a unique service.

The aggregation of multiple RF channels allows for several network advantages. This dissertation has assessed the potential coverage gain due to the increased frequency diversity when data is sent and frequency interleaved across an RF-Mux instead of limiting interleaving to a single RF channel. Inter-RF FI enables an averaging of the imbalances among RF channels. The signal level differences are mainly caused by the frequency-dependent performance of antenna systems and propagation. When inter-RF FI is used it is possible to provide a common coverage foot-print for all services in the RF-Mux.

In a classical transmission only those services carried in a potentially degraded RF channel are lost. The rest of services are not affected. An interference in a given RF channel influences the reception capability of all the services within the RF-Mux. The potential for an enhanced robustness against interferences with TFS and CB has been evaluated according to the number of interfered RF channels within the RF-Mux and the impact on the reception of the complete service offering.

Capacity gains have been studied in connection with a more efficient statistical multiplexing using TFS and CB, and the feasibility to increased peak service bit rate beyond that offered by a single RF channel. A proportional service bit rate increase to the number of bonded channels is feasible with CB. On the other hand, TFS imposes limitations in the maximum service bit-rate with respect to single RF channel transmission due to the necessary guard times to allow re-tuning operation when using less tuners than the number of bonded RF channels.

These gains can also be exploited by means on an increased network spectral efficiency. Current DTT networks are fundamentally interference-limited due to the required frequency reuse between neighbour stations. Frequency reuse factor $\eta = 7$ is commonly used in Europe. The release of the digital dividend, with the allocation of the 800 MHz band already to IMT and the possible release of the 700 MHz band, will only make 4 RF channels per station available with $\eta = 7$. A new plan with $\eta = 4$ will increase the available number of channels per station from 4 to 7, thus retaining a similar number of RF channels as in the current DTT networks. The investigation on Advanced Network Planning (ANP) strategies reveals the possibility to obtain a total increased network spectral efficiency by tighter frequency reuse factors and the implementation of different network topologies deliberately selected to allow for an effective reduction of the co-channel interferences. Mixed polarization networks (MPNs) achieve reduced interferences with the alternate selection of H/V polarization in the co-channel stations. Multiple frequency reuse patterns (MFRPs) make use of a different frequency reuse pattern for each (or a set) of the frequencies in the RF-Mux. ANP can be partially applied to classical networks by means of MPN. Though TFS and CB with inter-RF FI already allows for reducing frequency reuse factors, their combination with ANP could take further advantage of the increased protection against interferences. The gains with MFRPs mainly depend on the number of RF channels in the RF-Mux and the number of patterns available for the given frequency reuse since it is desirable that each frequency implements a different pattern.

The study of the implementation aspects of TFS and CB has been focused on transmitter, receiver and network operations. An appropriate data scheduling for TFS guarantees the correct distribution of data across the RF channels.

TFS can be operated with one tuner or more than one tuner. Single-tuner TFS is the most challenging operational approach due to the required tuning and synchronization process between RF channels. The introduction of guard periods can solve the issue but it generates additional capacity overheads. From the cost-effectiveness perspective, the operation of TFS with two tuners could eliminate the timing restrictions. For CB, one tuner is required per RF channel but data can be processed in multiple BICM chains since service data is split into multiple streams, each one feeding one RF channel input. One tuner is required per RF channel to recover data which are recombined after decoding into a single stream.

The implementation of TFS and CB requires that an operator should dispose of more than one RF channel in the network. Adaptation of regulation in some countries, in the basis of licensing capacity instead of frequencies, could enable an optimum implementation of TFS and CB in the broadcast bands since the RF-Mux could span several RF channels.

6.1.1 Increased Frequency Diversity

DTT systems achieve frequency diversity by means of COFDM and interleaving whereby the FEC codewords are spread across the active carriers of the OFDM symbols covering the entire transmission bandwidth. When interleaving is limited to a few MHz, robustness against multipath fading is achieved. This is currently achieved by the common bandwidths used in the DTT systems (e.g. 6 or 8 MHz). If frequency interleaving extends across multiple RF channels (inter-RF FI) and potentially over hundreds of MHz , it is possible to average the signal variations between different RF channels.

Information theory has been used to asses the bounds of the potential gain of TFS and CB when inter-RF frequency diversity is applied. Physical layer simulations, validated according to state-of-the-art DVB standards, have been conducted to evaluate the performance in real systems. As a general rule, a weak channel can be compensated by means of a strong channel. Performance is dependent of the modulation order and code rate, which determine the spectral efficiency of the system. High attenuations in one RF channel cannot be compensated with high code rates. Rotated constellations can improve the performance beyond non-rotated constellations with a proper inter-RF FI and when I/Q components are transmitted over different RF channels. Gains are obtained for high code rates (i.e. $\geq 1/2$) and even for lower code rates when there is a high rate of lost data. Code rate should be adjusted according to the number of weak RF channels in the RF-Mux. The use of inter-RF FI in slow time varying channels can also suppose an advantage to cope with the insufficient time interleaving in such cases.

The nature of the imbalances among RF channels have been investigated. The main sources are the transmitter antenna diagram dependence with frequency (3-6 dB imbalances), the noise figure of the receiver which increases with frequency, and the receiver antennas which compensate imbalances to some extent due to the increasing gain with frequency. Propagation is another important factor generating high imbalances between RF channels. The analysis of state-of-the-art propagation models reveal that, in average UHF band suffers around 10 dB more path loss than the VHF band. Sea path leads to the most homogeneous behaviour of the path loss among frequencies whereas paths with obstructions due to terrain or the presence of building create the highest imbalances.

A set of field measurements taken in the Swedish DTT network at different frequencies and in different populated areas are used to characterize and model the coverage gain by TFS and CB. The measurements analysis shows that the signal level differences increases with frequency separation up to around 10 dB, in average, for outdoor locations. Portable indoor reception is especially affected by imbalances due to factors such as height loss, building penetration loss or body loss, which are more important at UHF than at VHF.

The introduction of TFS and CB with inter-RF FI make it possible to average the differences between the RF channels in the RF-Mux. This means that the reception of all services is not conditioned by the SNR of the weakest RF channel, as in a classical transmission. Instead, there is a global SNR for the RF-Mux and it is the same for all services (assuming all of them use the same MODCOD configuration). However, those locations which where able to receiver some of the strongest RF channels will be unable to receive anything with TFS or CB. Coverage gains around 4-5 dB are found in the UHF band for TFS with a RF-Mux of 4 channels, according to measurements. The results also reveal that the achievable coverage gain is mainly fixed by the two most separated RF channels and does not necessary increase when adding more RF channels. When CB does not implement SNR averaging, the bonding of two separated RF channels could limit the reception area to that of the strongest RF channel.

6.1.2 Capacity Gains

The additional RF performance achieved by TFS and CB can be directly translated into a capacity gain by the selection of a less robust MODCOD. Furthermore, these techniques can offer additional capacity gains linked to a more efficiency StatMux of VBR services and the possibility to increase service bit rate. HEVC is expected to be the reference video coding standard for the next-generation DTT, outperforming H.264/AVC by more than 50%. The allocation

of services into single RF channels limits the StatMux gain for high data rate services such as UHDTV due to the limited number of services in the StatMux process (e.g. 2-3 services of 15 Mpbs in a 40 Mbps DVB-T2 multiplex). The joint multiplexing over a large number of services allows obtaining a gain in number of services. Gains around 2 to 4 UHDTV services are possible with the aggregation of 2 RF channel. Higher gains can be obtained with 4 RF channels (6 to 8 UHDTV services).

CB is an interesting potential new use case with HSVC. In that sense, it is recommended that the base layer is transmitted over the strongest RF channel so that a large number of users will be able to received the service. A combination of a UHF and VHF channel can also provide advantages when the base layer is carried in the UHF band, enabling mobile reception of HD services, which are enhanced by additional data in the VHF for fixed reception. TFS can also exploit a data rate increase with HSVC when using two tuners each one receiving one layer. However, the maximum bit rate per layer is still limited by the required time gaps for tuning.

6.1.3 Robustness against Interferences and Advanced Network Planning (ANP)

Inter-RF FI allows for an increased protection against potentially interfered RF channels within the RF-Mux. Even when e.g. 1 of the 4 RF channels of the RF-Mux is completely lost, it could still be possible to receive the complete set of services with the proper MODCOD.

The increased interference immunity offered by inter-RF FI may be exploited in a tighter frequency reuse together with an appropriately chosen capacity or robustness combination, which maximizes the overall capacity per transmitter station of the total available spectrum. Two ANP strategies have been identified in this dissertation to provide higher network spectral efficiency by means of different reuse patterns for the frequencies in use (MFRP) and the use of systematic H/V polarization at different sites (MPN). The investigations have been focused on MFNs, an MFN of SFN clusters and a large SFN using a theoretical regular network deployment and standard terrain characteristics. MPNs can be used in the current networks without inter-RF FI but with limited gain (around 10%). The use of TFS without ANP already achieves important gains (up to 77 % in MFNs and around 60% in SFNs). The effect of MPN with TFS is more significant in SFNs than MFNs. The highest gain figures are achieved when introducing MFRPs with gains up to 90% in MFNs and up to 63% in SFNs. The results reveal network spectral efficiency gains with $\eta = 7$ compared to $\eta = 4$ beyond 100% when TFS and MFRP are used, in particular when SFN clusters are implemented. The achievable gains in real

network deployments can be higher or lower according to the particularities of the network, and the level of interferences reaching the receiver, which will require further study.

6.1.4 Implementation Aspects

One of the most important features conditioning the feasibility of TFS and CB is the required number of tuners at the receiver side. CB requires as many tuners as bonded RF channels. With TFS, the operation when the number of tuners is lower than the number of RF channels requires a proper scheduling to enable the evenly distribution of the services across the multiple RF channels and to allocate the data into slots so that no overlapping is generated at the receiver. The necessary gaps for tuning impose important performance limits that lead to a reduction of the maximum possible bit rate per service. Even when a short tuning time of a few microseconds is possible, the frequency hopping operation requires of a few milliseconds in order to perform channel estimation and time-frequency synchronization operations. Overheads can reduce peak data rate by 30% already with 2 RF channels and 50% with 4 RF channels. Thus, the number of RF channels that can be bundled per RF-Mux is also limited. The strategies to decrease the capacity overheads should focus on reducing the required number of symbols to perform channel estimation as well as the tuning time. Time interleaving is a core element that should be properly configured to extend data across the RF-Mux. The limited amount of memory for time de-interleaving also restricts the maximum bit rate per service. In some cases a memory size of 2^{19} cells (as that specified for DVB-T2 and most of MODCODs in ATSC 3.0) is insufficient to allow transmitting high data rate services. A memory size of 2^{20} cells and a maximum frame length of 300 ms could be enough in order not to decrease service data rate below 20 Mbps.

CB implementation involves that data is simultaneously received from several RF channel. For practical reasons, CB is limited to work with two RF channels since allocating more than two tuners at the receiver equipment is not currently foreseen. The data to be transmitted could be processes in a single modulator. However, this would require doubling processing capability. In practice, a big data rate stream is split into several sub-streams, according to the number of RF channels. Each sub-stream feeds a modulator input. Receiver must re-join the data to decode the service. The implementation of CB would permit the possibility to use TFS with two tuners to combine more than two RF channels, as an election of the operator.

6.1.5 Network Deployment Recommendations

A proper network deployment with TFS and CB enables exploiting the increased RF performance and capacity gains. The investigations carried out lead to the following network deployment recommendations:

- Harmonized coverage between operators can be achieved by the averaging of the imbalances between low level RF channels and high level channels.
- All RF channels can be potentially used but important gains are already achievable with the aggregation of 2-4 RF channels.
- Transport Stream data encapsulation should be centralized (e.g. by means of a gateway). Synchronization data should be inserted so that frames are broadcast at the same time at different stations (regardless the type of network: MFN or SFN).
- Repeaters and regenerators should operate over the complete RF-Mux instead of over single RF channels.
- Legislation update towards an effective separation between RF resources and broadcaster capacity is desirable for the efficient use of TFS and CB.
- The introduction of ANP strategies with TFS may allow for the implementation of a tighter frequency reuse from e.g. $\eta = 7$ to $\eta = 4$ what can guarantee the existing number of active RF channels even after the release of the second digital dividend.

6.2 Future Research Topics

6.2.1 MIMO with TFS or CB

State-of-the-art DTT standards such as DVB-T2 have already approached the theoretical capacity limits of single-antenna systems. The implementation of two antennas at the transmitter and receiver sides (2-by-2 MIMO) basically doubles the capacity per RF channel by transmitting two streams over the same bandwidth with different polarizations. MIMO is adopted in DVB-NGH [103], to exploit its benefits in mobile and portable scenarios, and ATSC 3.0, to enable increased data rates by spatial multiplexing.

The compatibility of TFS and CB with MIMO should be thoroughly studied since MIMO already requires two tuners at the receiver. The cost feasibility of such a system needs to be evaluated to minimize the number of required tuners per RF channel, in particular with CB. Single-tuner TFS could work

with MIMO, thus not requiring more than two tuners. Regarding performance, MIMO could benefit from TFS and CB since the negative effects of the frequency and directional variations of the cross-polar antenna diagrams could be smooth.

6.2.2 Layer Division Multiplexing with Multi-RF Technologies

Layer Division Multiplexing (LDM) [104] is adopted in the next-generation US DTT standard ATSC 3.0 to enable the efficient provision of services for fixed and mobile reception by means of multiple signal layers with a different power level, using the complete time and frequency resources. ATSC 3.0 implementes two-layers, each one can be configured with a desired robustness and capacity to address mobile reception (UL, Upper Layer) and fixed roof-top reception (LL, Lower Layer). Reception of the LL is possible when UL has been demodulated and cancelled from the received signal. The requirements for reducing receiver complexity imposes a trade-off between the optimum configurations of both layers since they share some BICM blocks such as the TI. Whereas the lower layer requires a low carrier spacing (i.e. high FFT mode) and a low-dense PP, mobile reception (UL) requires a high carrier spacing (i.e. low FFT mode) and a high-dense PP to cope with the time variability of the signal and the inter-carrier interferences produced by the mobility of the receiver.

The performance of TFS and CB could be studied in connection with pedestrian and indoor reception. The additional frequency diversity could be useful to compensate the lack of time diversity in slow time-varying channels when the system is configured to obtain high capacity in the LL. In addition, implementation aspects should be investigated to enable an optimum inter-RF frequency interleaving of the encoded data in both layers. This is particularly important with the common TI approach adopted in ATSC 3.0.

6.2.3 Inter-RF FI with LPLT Network Topologies

DTT networks have traditionally been deployed by means of HPHT topologies. The hypothetical evolution of the DTT platform towards a converged broadband-broadcast network using also a Low-Power Low-Tower (LPLT) topology has been considered in several studies [105, 106]. The investigations reveal a high potential for increasing spectral efficiency although the cost of such networks is the main drawback. The use of TFS and ANP, in particular, could lead to even higher gains in spectral efficiency due to the potential reduction of interferences coming from signal of close co-channel transmitter stations which may suffer a high degree of correlation due to their short distances.

Appendix A

Measurement Campaigns Details

The measurement data used in the characterization of the imbalances between RF channels in the UHF band are provided by Teracom, the Swedish DTT operator. Two sets of measurement data are available involving outdoor and indoor reception. Outdoor measurements are from 6 different transmitter areas is Sweden. The purpose of the measurement campaign was to collect data from different stations for network planning issues. Indoor measurements are taken at different buildings in Stockholm (Sweden) in order to investigate the variations in the received signal level for indoor reception. The characteristics of the two sets of measurements are detailed next.

A.1 Outdoor Measurements

Data from six different transmitter areas are provided. At the time of the measurements only four frequencies were transmitted per site. The measurements were done mobile at 3 m using an omni-directional receiving antenna. The measured values have been calibrated in order to remove the gain variation of the measurement antenna. For service planning the effective antenna gain, antenna gain including the feeder loss, is set to be constant.

The six stations are labelled with letters to A to F. Figure A.1 depicts the DTT station in the surroundings of Stockholm area. A measurement route within the Vastervik transmitter area is shown. For each transmitter area a set of measurements is collected for the 4 active RF channels. The level is provided as the relative level for each frequency, in dB, to the total level of

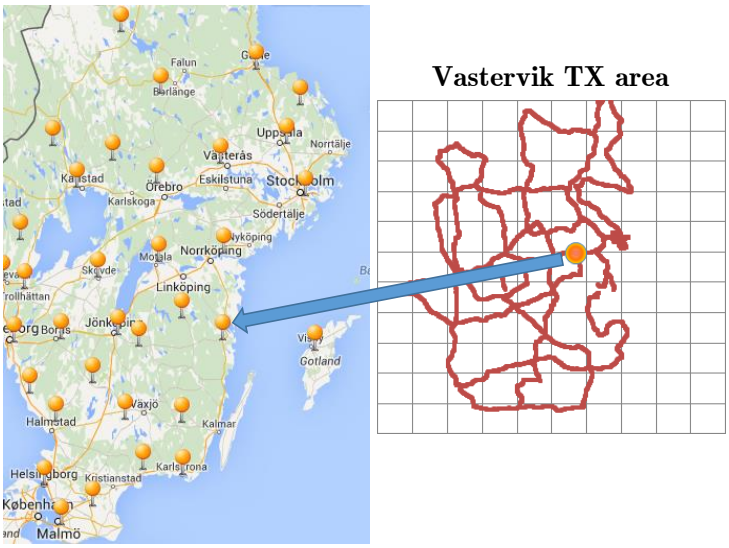

Figure A.1: Map of Sweden with the location of the transmitter station of the Teracom network and plot of a measurement trace corresponding to Vastervik transmitter area. Source: Teracom.

all four frequencies (0 dB). The different signal levels at each frequency where recorded in a cyclic manner for the 4 RF channels in each location. The number of samples per measured area is: A-27000, B-30000, C-58000, D-41000, E-6000 and F-56000.

A.2 Indoor Measurements

Received signal levels were measured for six operational multiplexers in the Stockholm area in four residential flats (homes). The level of the six multiplexes is registered at the same time and point by point along a path of some meters in each house. The distance between two measurements was 5 cm or 2 cm. An the length of the paths is in the range 2 to 4 meters. 2 cm is preferred in some situations due to fast fading effects. In total ten paths have been measured. Eight out of the ten measured paths were performed with a resolution of 2 cm. The total number of measured points is around 1400. The levels of the six frequencies are measured in addiction to a seventh signal from a signal generator used for receiving antenna position indication. This indicates the

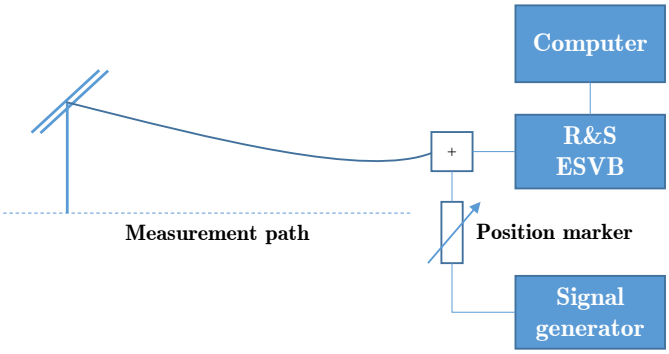

Figure A.2: Indoor measurement equipment.

time periods for the move of the measuring antenna to the next measurement point.

Measurement equipment

Figure A.2 presents the equipment set up for the measurement campaign. The signal level is measured with a Rohde & Schwarz level meter ESVB.

The measurement antenna was mounted on a carbon fiber tripod. Antenna height is 1.3 meter. Receiving antenna is a broadband dipole antenna. The dipole antenna was always mounted with its front towards the direction of the measurement path. Measured antenna pattern is provided in Figure A.3. Maximum antenna gain for the dipole antenna is 0.5 dBi at 490 MHz and 1.0 dBi at 740 MHz.

Transmitter network and receiver locations

The DTT signal in Stockholm area is provided by two transmitters operating in SFN. The main station is 'Nacka' and there is an additional fill in station 'Marieberg'. The location of the station and the measured houses is depicted in Figure A.4. ERP is 0.1 kW in Marieberg and 100 kW in Nacka. Antenna heigh is 80 m and 300 m, respectively. The small station only influences the reception in location 1, which is situated 2.8 km from Marieberg and 8.4 km from Nacka. At this location, the measured field strength from Nacka is aproximately 20 dB stronger than from Marieberg. The buildings are all made of concrete and the characteristics of the measurement data are described next:

- **Dannemoragatan** is a 5 floor building located 8.4 km far from Marieberg.

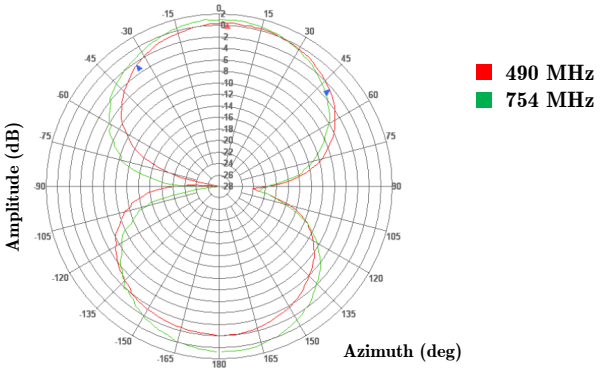

Figure A.3: Receiver antenna diagram.

Figure A.4: Situation of the measured houses and the Nacka and Marieberg stations.

  - Moa A (Small bed room). Path length: 3.2 m. Srep size: 2 cm.
  - Moa B (Small bed room). Path length: 3.2 m. Step size: 2 cm.
  - Vard (Living room). Path length: 4 m. Step size: 5 cm.
  - Sov (Master bedroom). Path length: 3.5 m. Step size: 2 cm.
  - Kök (Kitchen). Path length: 3.5 m. Step size: 5 cm.

- **Ystadvägen** is a 2 floor row building located 3.7 km from Nacka.
  - Vard 1 (Living room). Path length: 3.5 m. Step size: 2 cm.
  - Vard 2 (Living room). Path length: 3.5 m. Step size: 2 cm.

Table A.1: RF-Muxes involved in gain calculation

RF-Mux	CH23	CH42	CH50	CH53	CH55	CH56
6	-	-	X	X	X	X
14	-	X	X	X	-	X
30	X	X	X	X	-	-
33	X	X	X	-	-	X

- **Edvin Adolphssons väg** is a 5 floor semi-closed building situated 13 km from Nacka and has a metal window.
  - Vard 1 (Living room). Path length: 2 m. Step size: 2 cm.
  - Vard 2 (Living room). Path length: 2 m. Step size: 2 cm.
- Näsbydalsvägen (the 16 floor tower block), have a metal surface and is 16 km far from the transmitter.
  - Vard 1 (Living room). Path length: 3.5 m. Step size: 2 cm.

There is no direct signal from the transmitter except for Näsbydalsvägen. Home in Näsbydalsvägen is most far from the transmitter, but the received signal level is the highest. This flat is situated on the 13th floor and the transmitter antenna is visible from a room adjacent to the one in which the measurements were performed. Despite the high measured signal level the possibility to receive digital TV is not stable.

The operational network in Stockholm area involve six RF channels (23, 42, 50, 53, 55 and 56). The study of the coverage gain is performed over 4 different frequency allocations with channel separations of 6, 14 , 30 and 33. The four groups of four frequencies used in the calculation are given in Table A.1.

APPENDIX A. MEASUREMENT CAMPAIGNS DETAILS

Appendix B

Physical Layer and Network Planning Simulations

The methodology approach of this dissertation comprises the use of a physical layer simulator and a network planning simulator to assess the performance gains of multi-RF aggregation technologies.

The Institute of Telecommunications and Multimedia Applications of the Universitat Politècnica de València has developed simulators based on the DVB-T2, DVB-NGH and ATSC 3.0[1] standards. These physical layer simulators, which have been cross-check during the standardization processes of the related standards, permit the evaluation of the DTT physical layer concepts under realistic channel conditions. On the other hand, a network planning simulator has been expressly developed for the evaluation of the network planning gains by inter-RF FI and ANP.

B.1 Physical Layer OFDM-based Simulators

A general overview of the simulators is depicted in Figure B.1.

The simulators, which are developed in MATLAB® are implemented following the specifications in [26] and [27]. This section describes the structure,

[1]The ATSC 3.0 standardization process is still ongoing. However, most of the blocks of the DVB-T2 and DVB-NGH standards are reused in ATSC 3.0. Thus, the basic results of the simulations will also apply to this new standard.

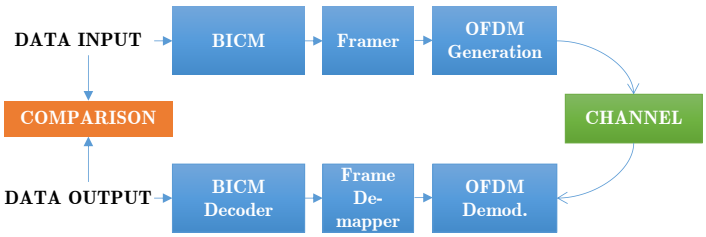

Figure B.1: OFDM-based simulator chain.

characteristics and parameters of the simulator. The main blocks in the transmitter correspond to the BICM module where the LDPC FEC words are bit-interleaved, mapped to cells, and interleaved by means of a cell interleaver (on a FEC word level) and a time interleaver (on a group of FEC words level). If rotated constellations are implemented, the proper rotated QAM mapping and the I/Q component interleaver are also part of the chain. The frame mapper module implementes the frame builder and the frequency interleaver. The OFDM generation module only implements the IFFT and GI insertion operations.

The simulator inputs are frames which size is defined according to the number of FEC words within and the chosen modulation. Every frame is processed through the BICM which converts the coded data into constellation cells. The frame mapper reshapes the data in a matrix of N OFDM symbols each one containing K orthogonal subcarriers. Frequency interleaving takes place after this operation. Finally, OFDM modulation takes place. Note that for simplification pilot insertion is not used. Ideal channel estimation is implemented. The receiver implements the related operation in the reverse order.

The simulations with inter-RF FI are conducted using a TFS approach in which a time-interleaved frame is divided in parts according to the number of RF channels to be simulated. The time interleaver duration is taken into account as:

$$T_{TI} = T_{OFDMsymb} \cdot N_{OFDMsymb}$$

$$N_{OFDMsymb} = \lfloor \frac{\frac{FEC_{length}}{M} \cdot N_{FECBlocks\_TIBlock}}{N_{activecarriers}} \rfloor$$

where

- $T_{OFDMsymb}$ is the OFDM symbol duration given by $T_{OFDMsymb} = T_U \cdot (1 + GI)$

- $N_{OFDMsymb}$ is the number of OFDM symbols required for the chosen BICM parameters
- T_U is the useful OFDM symbol duration
- FEC_{length} is the FEC block length, in bits
- $N_{FECBlocks\_frame}$ is the number of interleaved FEC blocks in the frame
- $N_{activecarriers}$ is the number of active carriers for the selected FFT size

The following numerical example shows how the frame duration is selected for these parameters: FEC_{length} = 64800, M = 2 (QPSK), $N_{FECBlocks\_frame}$ = 16, FFT_{size} = 16k ($N_{activecarriers}$ = 13632), GI = 1/16 BW = 6 MHz (T_{sample} = 7/48 μs).

$$N_{OFDMsymb} = \lfloor \frac{\frac{64800}{2} \cdot 16}{13632} \rfloor = 39 \text{ symbols}$$

$$T_{OFDMsymb} = 16 \cdot 1024 \cdot \frac{7}{48} \cdot \left(1 + \frac{1}{16}\right) = 2.583 \text{ ms}$$

$$T_{TI} = 2.583 \text{ ms} \cdot 39 \text{ symbols} = 99 \text{ ms}$$

Inter-RF FI Emulation

Performance evaluation with inter-RF FI is made by comparing the performance of the transmission across the RF-Mux channel with respect to the transmission over the RF channel with the worst C/N condition since the worst RF channel is the one that limits the reception of the complete service offering.

The time domain signal containing information of a time-interleaved frame is filtered across an emulated RF-Mux channel. Figure B.2 depicts a simple diagram of the transmitted and received data of the frame. The received data is evenly affected by the conditions of as many RF channels as those which are part of the RF-Mux (in the figure RF_1, RF_2, RF_3 and RF_4).

The characteristics of each RF channel in the emulated RF-Mux channel are set according to the C/N imbalances derived from the model presented in Section 3.3. Only the mean value of the imbalances is taken into account for simplicity. The variability among locations could also be considered in order to simulate the performance of inter-RF FI over a large number of locations what would imply at the expense of more time-demanding simulations.

For the given set of RF channels in the RF-Mux, the corresponding signal strength imbalance among the frequencies is calculated referred to the lowest

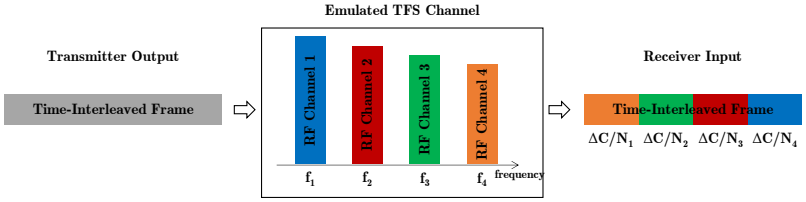

Figure B.2: Scheme of the emulation of the RF-Mux channel.

Table B.1: RF channel imbalance (dB)

RF_1 (503 MHz)	RF_2 (533 MHz)	RF_3 (563 MHz)	RF_4 (593 MHz)
0	1.10	2.15	3.15

frequency (the lowest frequency gets an imbalance of 0 dB) according to the following equation:

$$\mu_{f_i} = -44 \cdot \log_{10}\left(\frac{f_i}{f_{worst}}\right)$$

With this, the C/N of RF_2, RF_3 and RF_4 are below the C/N of RF_1. RF_4 is considered as the worst RF channel (see Table B.1).

The variability among locations is considered by means of the following method. For each pair of frequencies in the RF-Mux, a correlation matrix for the difference between the signal strength of these frequencies can be defined as:

$$\begin{pmatrix} 1 & \rho_{21} & \dots & \rho_{N_{RF},1} \\ \rho_{21} & 1 & \dots & \rho_{N_{RF},1} \\ \dots & \dots & \dots & \dots \\ \rho_{N_{RF},1} & \rho_{N_{RF},2} & \dots & 1 \end{pmatrix}$$

where ρ_{ij} is the corresponding correlation factor for frequencies f_i and f_j. The correlation factor is derived from the variance of the difference of two random variables as:

$$\sigma^2_{X-Y} = \sigma^2_X + \sigma^2_Y - 2\rho\sigma_X\sigma_Y$$

Assuming that $\sigma_X = \sigma_Y = 1$, then:

$$\rho_{ij} = 1 - \frac{\sigma^2_{X-Y}}{2}$$

According to the proposed RF imbalance model, σ^2_{X-Y} is estimated by σ^2_{FS}.

N_{RF} correlated arrays of samples can be obtained for the simulation from the same number of independent initial arrays L_i $N(0,1)$ as follows:

$$\begin{pmatrix} L'_1 \\ L'_2 \\ \dots \\ L'_{N_{RF}} \end{pmatrix} = chol(\mathbf{P}) \cdot \begin{pmatrix} L_1 \\ L_2 \\ \dots \\ L_{N_{RF}} \end{pmatrix} + \begin{pmatrix} \mu_1 \\ \mu_2 \\ \dots \\ \mu_{N_{RF}} \end{pmatrix}$$

where L'_i are the N_{RF} new sequences that integrate the effect of the corresponding RF channel, $chol(\mathbf{P})$ is a lower triangular matrix as a result of the Cholesky factorization of the matrix $\mathbf{P}$, and μ_i is the mean value calculated for each frequency.

B.2 Network Planning Simulations

As stated in Chapter 4, an hexagon-based network planning simulator is used to assess the potential gains of Inter-RF FI and ANP over classical deployments. This section explains those methodology characteristics which were not fully covered in the aforementioned chapter.

Receiver antenna properties

The receiver antenna diagram weighs the interference contributions according to the angular (azimuth φ) direction between the main station and the co-channel stations. ITU-R BT.419 [59] recommends the values for antenna discrimination for fixed reception to be used in frequency planning. , $Q(\varphi)$, relative to the direction of main response for broadcast reception to be used for frequency planning, as depicted in Figure B.3. With this antenna, cross-polar discrimination (XPD) is set to $Q(\forall\varphi)$ = -16 dB, independently of direction[2].

Propagation-related aspects

The land propagation model used for calculating the received field strength at the worst point in the cell is the ITU Recommendation ITU-R P.1546 [65] which defines the received electrical field strength at a certain distance given ERP, effective antenna height, frequency, receiver antenna height, terrain type and percentage of time.

[2]Directional and polarization discrimination performance will be worse when using omni-directional antennas for portable indoor or mobile reception as identified in [79] where XPD is found to be in the range between -7 dB and -12 dB.

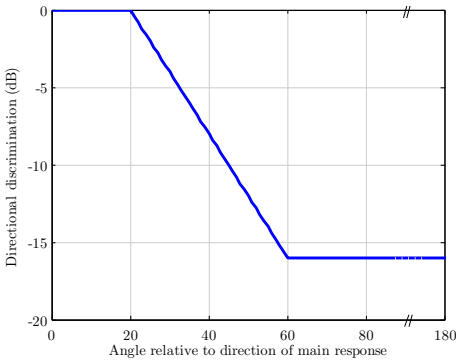

Figure B.3: Characteristics of directivity of the receiving antennas in UHF band according to ITU-R BT.419 [59]. Antenna discrimination relative to direction of main response, $Q(\varphi)$. Valid for signals of vertical or horizontal polarization.

The local received power from transmitter i is given by the deterministic field strength from [65] and additional terms for frequency-independent but directional-dependent shadow fading and for frequency-dependent fading (independent of transmitter).

Shadow fading is modelled as an independent log-normal random variable (i.e. Gaussian distribution in dB with standard deviation 5.5 dB and 0 dB mean) for each transmitter station [65] defined as $\{F_0, F_1 ... F_{N_I}\}$ with N_I being the number of CCI stations. The shadowing components of the signals from different transmitters are assumed to be correlated for similar propagation paths (since they are affected by the same obstacles). A site-to-site cross correlation coefficient (ρ_c) is modelled according to the angle-of-arrival difference ($\phi \in [0, \pi]$) and the ratio between the propagated path lengths ($\frac{D_1}{D_2}$) by equation B.1 [107]. The angle-of-arrival is assumed to be equal to the transmitter direction (i.e. multipath effects are not taken into account).

$$\rho_c = \begin{cases} \sqrt{\frac{D_1}{D_2}} & for \quad 0 \leq \phi \leq \phi_T \\ \left(\frac{\phi_T}{\phi}\right)^{\zeta} \cdot \sqrt{\frac{D_1}{D_2}} & for \quad \phi_T \leq \phi \leq \pi \end{cases} \tag{B.1}$$

D_1 represent the distance to the closest transmitter. ϕ_T is an angle threshold defined as $\phi_T = 2\sin^{-1}\frac{r_c}{2D_1}$, where r_c represents the serial shadowing correlation distance. The exponent ζ accounts for the height and shapes of the terrain and buildings. The parameters are set to $\zeta = 0.3$ and $r_c = 300$ m [107].

Shadow fading is assumed to be frequency independent. Thus all TFS frequencies originating from a particular site are assumed to have the same shadow fading realisation.

Shadow fading for the different transmitter stations is calculated as:

$$Y_i = \sqrt{\rho_c} \cdot F_0 + \sqrt{1 - \rho_c} \cdot F_i \tag{B.2}$$

where F_0 represents the receiver-position-dependent fading component and F_i models the station-dependent component [108].

Real transmitting antennas introduce a sort of frequency dependent fading, since the real antenna diagram typically varies significantly with frequency and direction. Also the effects of the wave propagation (multipath) and the positioning of the antenna are frequency dependent. All these effects are modelled as a frequency-dependent fading with 2 dB standard deviation. This supposes a conservative approach according to the results presented in [55] on RF channel imbalances.

For the given network and frequency reuse pattern, co-channel stations positions are calculated. The point inside the centre hexagon (for MFN) or centre cluster (for a network of SFN clusters) with the lowest capacity (lowest C/(N+I)) is taken as the worst location for Non-TFS. For inter-RF FI, the one with the lowest capacity taking into account the C/(N+I) of all RF-Mux frequencies is taken.

Note that the receiver antenna is pointed towards the centre of the cell in the case of a pure MFN and towards the transmitter station which provides the highest C/(N+I) within an SFN cluster.

C/(N+I) is computed assuming the field strength for the 50% of time for the wanted signal [65]. The path losses from all transmitters with significant interference contributions are calculated. The three first co-channel transmitter rings are taken into account for cluster size equal 1 (pure MFN case). For cluster size 7, the first tier of clusters is considered. For the large area SFN calculation the number of interfering cells is computed according to the weighting function given by Equation 4.7. In all cases, adding more co-channel transmitters do not cause significant changes in the NSE calculation.

A realistic model for time correlation is unfortunately not well-established. Three particular cases are studied: a maximum-conservative case with 100% correlation and in the other end two variants of uncorrelated cases. For the fully-correlated case (C) received field strength for all stations and frequencies is assumed to reach their 1% time value at the same time, i.e. with 100% correlation. In this case, the total interference, for this percentage of time, is the sum of the individual interferences' peak values (worst-case). For the uncorrelated case U1, a random statistical distribution ($T = 10000$ values) of field strength values from the curves in [65] is calculated by fitting Gaussian

distributions in the range 1% to 10% and 10% to 50% percentage of time. With this, individual transmitters reach their different field strength values at independent points in time, i.e. their sum is typically much lower than in the worst case scenario. In this case, the frequencies transmitted in the same station are considered to be fully-correlated. With the uncorrelated case U2, all signals are assumed to be uncorrelated regardless their frequency and location. Although real signals are neither fully-correlated nor uncorrelated, the extreme cases are studied as a means to investigate the boundaries of the spectral efficiencies under analysis. ITU-R P.1406 Recommendation states that the correlation in mean received field strength from different stations mainly depends on the position of the sources. Signals coming from opposite directions are mainly uncorrelated whereas a high degree of correlation exists for co-sited sources [72].

At the top of each field strength realization, as described above, log-normal fading distribution with $K = 100000$ realizations is applied to the wanted and interfering signals by means of a Monte-Carlo simulation.

Payload capacity overheads

Payload capacity overheads due to GI+PP (Guard Interval and Pilot Pattern) in MFN and SFN configurations are considered since they reduce payload capacity values. A typical MFN network configured with DVB-T2 32k GI 1/128 PP7 presents a GI+PP payload capacity overhead of 2.04%. An SFN cluster with 7 transmitters and transmitter distance 60 km can be configured with the same mode but GI 1/8 PP2, in both 6 MHz and 8 MHz channel bandwidth, to withstand maximum SFN delay. This GI+PP configuration leads to 19.67% payload capacity overhead. With this GI configuration, those co-channel transmitters situated outside a cluster are taken as pure interfering stations. For the case of a large area SFN, the selected GI is 19/128 PP2, the maximum permitted by DVB-T2, which leads to an overhead of 21.49%. According to [81], in this study FFT time window is assumed to be synchronized to the strongest received signal within the SFN since the antenna is positioned towards the main contributing station.

Network Planning Simulator

The following method is applied to calculate the network spectral efficiency in the worst point of the cell or cluster of cells:

1. A pattern of co-channel transmitters is calculated according to the selected reuse pattern.

2. The received field strength in the worst point[3] of the cell is calculated for the center cell and from the co-channel cells.

3. Antenna discrimination is applied to co-channel transmitters according to the angle of arrival with respect to the direction of the wanted transmitter.

4. Log-Normally distributed slow fading, with zero mean and a standard deviation of 5.5 dB is generated, for $N = 100000$ samples. The fading is the same across all RF channels for each transmitter.

5. Log-Normally distributed fast fading, with zero mean and a standard deviation 2 dB, is generated with $N = 100000$ samples. The fading is specific to each frequency for each transmitter.

6. The fading values are added to the respective field strength of each transmitter.

7. The C/I is calculated according to the network type: MFN of SFN.

8. Spectral efficiency is calculated for each sample. If inter-RF FI is used, the mean spectral efficiency across the RF-Mux is calculated for each sample. The nth percentile of the mean is calculated.

[3]The worst location for a reuse pattern is found by running the above simulation for all locations within the cell.

APPENDIX B. PHYSICAL LAYER AND NETWORK PLANNING SIMULATIONS

Appendix C

VHF and UHF Propagation Models

Path loss attenuation estimation in broadcast systems is generally based on accurate point-to-area or point-to-point prediction models. Point-to-area models are intended to provide a general estimate of radio propagation based on the general characteristics of different environments which are described from measurement campaigns. Point-to-point models estimate path loss from specific data of the environment within the link between transmitter and receiver.

C.1 ITU-R P.525 Recommendation

The basic propagation loss, which serves as the initial point for several models, is based on the free space propagation model. Its main reference is the ITU-R P.525 Recommendation [63]. This model takes the form of the free space loss equation for an isotropic antenna. The equation that describes the path loss (L_{p_n}) for a given frequency f_n is as follows:

$$L_{p_n}[dB] = 32.44 + 20 \cdot \log_{10}(d) + 20 \cdot \log_{10}(f_n)$$

where d (km) is the path distance between transmitter and receiver.

The model considers a clear (without obstructions) path and provides the propagation loss at a given distance and frequency.

C.2 ITU-R P.529 Recommendation

The empirical Okumura-Hata model [109] defines a series of equations for calculating the path loss for different scenarios which are derived from measurement campaigns carried out in Tokyo, Japan, by Okumura [110]. The initial measurements have been validated by a large number of measurements in different scenarios. The basic model estimates the median attenuation relative to free space, as a function of distance (d, 1 to 20 km), transmitter height (h_{tx}, 30 to 200 m), receiver height (h_{rx}, 1 to 10 m), frequency (f_n, 150 to 1500 MHz), and corrections factors according to urban, suburban and open area (rural) environments. The model was extended to frequencies up to 2000 MHz by COST 231 [111]. An extension of the Hata model to longer distance (20 to 100 km) was also developed within ITU-R in the ITU-R P.529 model [64]. Other corrections were also applied by the US National Telecommunications Industry Association (NTIA) to cover a larger range of input parameters to extend the range to 300 km, the antenna height to 2500 m and the frequency to 1500 MHz.

Focusing on broadcasting applications, the P.529 model takes urban areas as a reference point and applies correction factors for considering other types of environment. Urban areas correspond to a city or a large town with buildings and houses of two or more floors. It is also representative of larger villages with close houses and trees. A correction term is applied depending on the size of the city (medium-small or large cities). The suburban category represents a village scattered by trees and houses, with some obstacles near the receiving antenna. The rural area or open area category represents an area in which there are no tall trees or buildings in path such as a farm land, rice fields or open fields. The equations of the model for different environments are the following:

- Urban Area

$$\begin{aligned} L_{p_n} &= 69.55 + 26.16 \cdot \log_{10}(f_n) - 13.82 \cdot \log_{10}(h_{tx}) - \\ &\quad - a(h_{rx}) + (44.9 - 6.55 \cdot \log_{10}(h_{tx}))(\log_{10}(d))^{b_n} - K_n \end{aligned}$$

$$b_n = \begin{cases} 1 & \text{if } d < 20 \\ 1 + (0.14 + 0.000187 \cdot f_n + 0.00107 \cdot h'_{tx})(\log_{10}(\frac{d}{20}))^{0.8} & \text{if } d \geq 2 \end{cases}$$

$$h'_{tx} = \frac{h_{tx}}{1 + 0.000007 \cdot h_{tx}^2}$$

  - Correction for Medium-Small cities

$$a(h_{rx}) = (1.1 \log_{10}(f_n) - 0.7) \cdot h_{rx} - (1.56 \cdot \log_{10}(f_n) - 0.8)$$

– Correction for Large cities

$$a(h_{rx}) = \begin{cases} 8.29 \cdot (\log_{10}(1.54 \cdot h_{rx}))^2 - 1.10 & \text{if } f_n < 300 \text{ MHz} \\ 3.2 \cdot (\log_{10}(11.75 \cdot h_{rx}))^2 - 4.97 & \text{if } f_n \geq 300 \text{ MHz} \end{cases}$$

- Sub-Urban

$$K_n = 2 \cdot (\log_{10}(f_n))^2 + 5.4$$

- Rural

$$K_n = 4.78 \cdot (\log_{10}(f_n))^2 + 18.33 \cdot \log_{10}(f_n) + 40.49$$

C.3 ITU-R P.1546 Recommendation

The ITU-R P.1546 [65] is the standard propagation model for VHF and UHF recommended by ITU. It replaces the older ITU-R P.370 recommendation [112]. The model is based on empirical curves derived from field-strength measurements taken over years covering different environments. The curves are provided for frequencies between 30 MHz to 3 GHz, distances ranging 10 to 1000 km, for effective antenna transmitter heights between 37.5 and 1200 m, and receiving antennas at 10 m height. The curves provide field strength (dBμV/m) values calculated for 1 kW ERP. It should be noted that the field strength values provided by the model represent values exceeded by a certain amount of time (i.e. 50%, 10% or 1%). Propagation above three different environments is considered: land, cold sea (linked to the Atlantic Ocean) and warm sea (linked to the Mediterranean Sea).

Due to the restrictions derived from the measurements, which would make the model only applicable to a certain amount of scenarios, interpolation equations are given to fit a wider range of input parameters. From the frequency-dependency perspective, whereas the curves are given for 100 MHz, 600 MHz and 2000 MHz, the following interpolation method makes it possible to calculate received field strength for other frequencies in-between.

$$E_{f_n} = \begin{cases} E_{100} + (E_{600} - E_{100}) \frac{\log_{10}(\frac{f_n}{100})}{\log_{10}(6)} & \text{if } f_n < 600 \text{ MHz} \\ E_{600} + (E_{2000} - E_{600}) \frac{\log_{10}(\frac{f_n}{600})}{\log_{10}(\frac{10}{3})} & \text{if } f_n \geq 600 \text{ MHz} \end{cases}$$

Finally, it is possible to convert the estimated field strength to equivalent path loss by the following equation:

$$L_{p_n} = 139.3 - E_{f_n} + 20 \cdot \log_{10}(f_n) \tag{C.1}$$

C.4 Other Models and Recommendations

There exist other models in the bibliography which take other assumptions into account that, in most cases, are path specific. The ITU-R P.526 takes into account propagation by diffraction caused by obstacles on the way from the transmitter to the receiver. However, a similar behaviour is expected for frequencies in the same band. In [113] a propagation model for UHF and VHF bands is derived from measurements but it is frequency independent. A recent ITU model has also been published in ITU-R P.1812 Recommendation [114] which present a powerful tool for path specific path loss estimation taking into account multiple factors influencing propagation between transmitter and receiver. The Longley-Rice model, or Irregular Terrain Model, was developed in the 1960s and is supported by the NTIA [66]. The model is based on measurement data between 20 MHz to 40 GHz, at distances from 1 to 2000 km and at antenna heights between 0.5 m and 3 km. The input parameters of the model also include the properties of the terrain ground curvature, subsoil, as well as climate.

References

[1] R. Beutler, *Digital Terrestrial Broadcasting Networks*, ser. Lecture Notes in Electrical Engineering. Springer, 2009, vol. 23. [Online]. Available: http://dx.doi.org/10.1007/978-0-387-09635-3

[2] "Roadmap for the Evolution of DTT - A bright Future for TV," Digital Television Action Group (DIGITAG), Tech. Rep., 2015.

[3] G. Faria, "The Magics of Terrestrial Digital Television (DVB-T)," in *Asia Pacific Broadcasting Union (ABU) - 38th General Assembly 2001*, June 2011, pp. 1–6.

[4] C. Shannon, "A mathematical theory of communication," *Bell system technical journal*, vol. 27, pp. 379–423 and 623–656, 1948.

[5] I. Eizmendi, M. Velez, D. Gomez-Barquero, J. Morgade, V. Baena-Lecuyer, M. Slimani, and J. Zoellner, "DVB-T2: The Second Generation of Terrestrial Digital Video Broadcasting System," *IEEE Transactions on Broadcasting*, vol. 60, no. 2, pp. 258–271, June 2014.

[6] C. Nour and C. Douillard, "Rotated QAM Constellations to Improve BICM Performance for DVB-T2," in *Spread Spectrum Techniques and Applications, 2008. ISSSTA '08. IEEE 10th International Symposium on*, Aug 2008, pp. 354–359.

[7] D. Gomez-Barquero, Ed., *Next Generation Mobile Broadcasting*. CRC Press, March 2013.

[8] D. Gomez-Barquero, C. Douillard, P. Moss, and V. Mignone, "DVB-NGH: the Next Generation of Digital Broadcast Services to Handheld Devices," *IEEE Transactions on Broadcasting*, vol. 60, no. 2, pp. 246–257, 2014.

[9] A. Ligeti, "Single frequency network planning," Ph.D. dissertation, Kungliga Tekniska högskolan, 1999.

[10] "Digital Dividend: Insights for Spectrum Decisions," ITU, Tech. Rep., Aug 2012.

[11] J. Zander and P. Mähönen, "Riding the data tsunami in the cloud: myths and challenges in future wireless access," *IEEE Communications Magazine*, vol. 51, no. 3, pp. 145–151, March 2013.

[12] "Cisco Visual Networking Index: Global Mobile Data Traffic Forecast Update 2014-2019 White Paper," Tech. Rep., Feb 2015.

[13] "Spectrum Requirements for Broadcasting Services in preparation for WRC-15," EBU, Recommendation 136, 2012.

[14] D. Gomez-Barquero and W. Caldwell, "Broadcast Television Spectrum Incentive Auctions in the U.S.: Trends, Challenges and Opportunities," *IEEE Communications Magazine*, vol. 53, no. 7, July 2015.

[15] P. Lamy, "Results of the Work of the High Level Group on the Future Use of the UHF band (470-790 MHZ)," Report to the European Commission, 2012.

[16] T. O'Leary, E. Puirefagut, and W. Sami, "GE06 - overview of the second session (RRC-06) and the main features for broadcasters," *EBU Technical Review*, p. 20, October 2006.

[17] G. J. Sullivan, J. Ohm, W.-J. Han, and T. Wiegand, "Overview of the High Efficiency Video Coding (HEVC) Standard," *IEEE Transactions on Circuits and Systems for Video Technology*, vol. 22, no. 12, pp. 1649–1668, 2012.

[18] T. K. Tan, M. Mrak, V. Baroncini, and N. Ramzan, "HEVC Verification Test Results," MPEG, Tech. Rep. JCTVC-Q0204, 2014.

[19] J. Forney, G., "Burst-Correcting Codes for the Classic Bursty Channel," *IEEE Transactions on Communication Technology*, vol. 19, no. 5, pp. 772–781, October 1971.

[20] W. Zou and Y. Wu, "COFDM: an overview," *IEEE Transactions on Broadcasting*, vol. 41, no. 1, pp. 1–8, Mar 1995.

[21] J. D. Parsons, *The Mobile Radio Propagation Channel*. John Wiley & Sons, Ltd, 2001.

[22] D. Gozalvez, J. Lopez-Sanchez, D. Gomez-Barquero, J. J. Gimenez, and N. Cardona, "Combined Time and Space Diversity: Mobile Reception in DVB-T and DVB-T2 Systems," *IEEE Vehicular Technology Magazine*, vol. 7, no. 4, pp. 114–121, Dec 2012.

[23] J. Boutros and E. Viterbo, "Signal Space Diversity: A Power and Bandwidth Efficient Diversity Technique for the Rayleigh Fading Channel," *IEEE Transactions on Information Theory*, vol. 44, no. 4, pp. 1453–1467, 1998.

[24] D. Gozalvez, J. J. Gimenez, D. Gomez-Barquero, and N. Cardona, "Rotated Constellations for Improved Time and Frequency Diversity in DVB-NGH," *IEEE Transactions on Broadcasting*, vol. 59, no. 2, pp. 298–305, June 2013.

[25] J. J. Gimenez, E. Stare, S. Bergsmark, and D. Gomez-Barquero, "Time Frequency Slicing for Future Digital Terrestrial Broadcasting Networks," *IEEE Transactions on Broadcasting*, vol. 60, no. 2, pp. 227–238, June 2014.

[26] *Frame structure channel coding and modulation for a second generation digital terrestrial television broadcasting system (DVB-T2)*, ETSI Std. EN 302 755, Rev. V1.3.1, April 2012.

[27] *Next Generation broadcasting system to Handheld, physical layer specification (DVB-NGH)*, Digital Video Broadcasting Std. DVB Bluebook A160, November 2012.

[28] J. J. Gimenez, E. Stare, S. Bergsmark, and D. Gomez-Barquero, "Time Frequency Slicing for the Next Generation Mobile Broadcasting Standard DVB-NGH," in *International Broadcasting Convention (IBC)*, 2013.

[29] M. Makni, J. Robert, and E. Stare, "Performance analysis of time frequency slicing," in *Electronic Media Technology (CEMT), 14th ITG Conference on*, 2011, pp. 1–6.

[30] J. Morgade, P. Angueira, J. A. Arenas, A. Basterra, D. de la Vega, D. Plets, and W. Joseph, "A software based dvb-t2 time frequency slicing evaluation framework," in *Broadband Multimedia Systems and Broadcasting (BMSB), 2013 IEEE International Symposium on*, June 2013, pp. 1–5.

[31] J. Zoellner, J. Robert, M. Makni, L. Stadelmeier, and N. Muhammad, "A power efficient framing structure for a next generation mobile broadcast

system," in *Broadband Multimedia Systems and Broadcasting (BMSB), 2011 IEEE International Symposium on*, June 2011, pp. 1–6.

[32] C. B. Woodworth, M. J. Karol, Z. J. Haas, and R. D. Gitlin, "Spectrally efficient universal time slots using time-frequency-code slicing," in *Personal, Indoor and Mobile Radio Communications, 1994. Wireless Networks - Catching the Mobile Future., 5th IEEE International Symposium on*, vol. 3, Sep 1994, pp. 1009–1013 vol.3.

[33] A. Batra, J. Balakrishnan, G. R. Aiello, J. R. Foerster, and A. Dabak, "Design of a multiband OFDM system for realistic UWB channel environments," *IEEE Transactions on Microwave Theory and Techniques*, vol. 52, no. 9, pp. 2123–2138, Sept 2004.

[34] A. Batra, J. Balakrishnan, and A. Dabak, "Multi-band OFDM: a new approach for UWB," in *Circuits and Systems, 2004. ISCAS '04. Proceedings of the 2004 International Symposium on*, vol. 5, May 2004, pp. V–365–V–368 Vol.5.

[35] J. Balakrishnan, A. Batra, and A. Dabak, "A multi-band OFDM system for UWB communication," in *Ultra Wideband Systems and Technologies, 2003 IEEE Conference on*, Nov 2003, pp. 354–358.

[36] M. P. Wylie-Green, P. A. Ranta, and J. Salokannel, "Multi-band OFDM UWB solution for IEEE 802.15.3a WPANs," in *Advances in Wired and Wireless Communication, 2005 IEEE/Sarnoff Symposium on*, April 2005, pp. 102–105.

[37] *High rate ultra wideband PHY and MAC standard*, ETSI Std. ECMA-368, December 2005.

[38] K. Pedersen, F. Frederiksen, C. Rosa, H. Nguyen, L. Garcia, and Y. Wang, "Carrier aggregation for LTE-advanced: functionality and performance aspects," *IEEE Communications Magazine*, vol. 49, no. 6, pp. 89–95, June 2011.

[39] R. Chandra, R. Mahajan, T. Moscibroda, R. Raghavendra, and P. Bahl, "A Case for Adapting Channel Width in Wireless Networks," in *ACM SIGCOMM*. Association for Computing Machinery, Inc., August 2008.

[40] M. Arslan, K. Pelechrinis, I. Broustis, S. Singh, S. Krishnamurthy, S. Addepalli, and K. Papagiannaki, "ACORN: An Auto-Configuration Framework for 802.11n WLANs," *IEEE/ACM Transactions on Networking*, vol. 21, no. 3, pp. 896–909, June 2013.

[41] J. Fang, K. Tan, Y. Zhang, S. Chen, L. Shi, J. Zhang, Y. Zhang, and Z. Tan, "Fine-Grained Channel Access in Wireless LAN," *IEEE/ACM Transactions on Networking*, vol. 21, no. 3, pp. 772–787, June 2013.

[42] L. Cao, L. Yang, and H. Zheng, "The Impact of Frequency-Agility on Dynamic Spectrum Sharing," in *New Frontiers in Dynamic Spectrum, 2010 IEEE Symposium on*, April 2010, pp. 1–12.

[43] Y. Yuan, P. Bahl, R. Chandra, T. Moscibroda, and Y. Wu, "Allocating Dynamic Time-Spectrum Blocks in Cognitive Radio Networks," in *Mobile Ad Hoc Networking and Computing (MobiHoc)*. Association for Computing Machinery, Inc., September 2007. [Online]. Available: http://research.microsoft.com/apps/pubs/default.aspx?id=73430

[44] J. Park, P. Pawelczak, P. Gronsund, and D. Cabric, "Analysis Framework for Opportunistic Spectrum OFDMA and Its Application to the IEEE 802.22 Standard," *IEEE Transactions on Vehicular Technology*, vol. 61, no. 5, pp. 2271–2293, Jun 2012.

[45] S. Joshi, P. Pawelczak, D. Cabric, and J. Villasenor, "When Channel Bonding is Beneficial for Opportunistic Spectrum Access Networks," *IEEE Transactions on Wireless Communications*, vol. 11, no. 11, pp. 3942–3956, November 2012.

[46] "Frequency and network planning aspects of DVB-T2," European Broadcasting Union, Tech. Rep. 3384, Nov 2013.

[47] J. Morgade Prieto, "Methods for Improving the Digital Terrestrial Broadcasting Spectrum Efficiency in UHF Bands," Ph.D. dissertation, Universidad del Pais Vasco/Euskal Herriko Unibersitatea, 2014.

[48] G. Baruffa, M. Femminella, F. Mariani, and G. Reali, "Protection Ratio and Antenna Separation for DVB-T/LTE Coexistence Issues," *IEEE Communications Letters*, vol. 17, no. 8, pp. 1089–7798, 2013.

[49] M. Fuentes, C. Garcia-Pardo, E. Garro, D. Gomez-Barquero, and N. Cardona, "Coexistence of digital terrestrial television and next generation cellular networks in the 700 mhz band," *IEEE Wireless Communications*, vol. 21, no. 6, pp. 63–69, December 2014.

[50] M. Rezaei, I. Bouazizi, and M. Gabbouj, "Statistical Time-Frequency Multiplexing of HD Video Traffic in DVB-T2," *International Journal of Digital Multimedia Broadcasting*, vol. 2009, p. 12, 2009.

[51] E. Stare, "Improved Spectral Efficiency by Time Frequency Slicing and Advanced Network Planning," in *International Broadcasting Convention (IBC)*, 2013.

[52] G. Caire, G. Taricco, and E. Biglieri, "Bit-Interleaved Coded Modulation," *IEEE Transactions on Information Theory*, vol. 44, no. 3, pp. 927–946, May 1998.

[53] D. Gozalvez, "Combined time, frequency and space diversity in multimedia mobile broadcasting systems," Ph.D. dissertation, Universitat Politècnica de València, 2012.

[54] *Implementation guidelines for a second generation digital terrestrial television broadcasting system (DVB-T2)*, ETSI Std. TS 102 831, Rev. V1.2.1, Aug 2012.

[55] J. J. Gimenez, D. Gozalvez, D. Gomez-Barquero, and N. Cardona, "Statistical model of signal strength imbalance between RF channels in DTT network," *Electronics Letters*, vol. 48, no. 12, pp. 731–732, 2012.

[56] H. Himmanen, "Studies on channel models and channel characteristics for mobile broadcasting," in *Broadband Multimedia Systems and Broadcasting, 2008 IEEE International Symposium on*, 2008, pp. 1–9.

[57] "Transmitting antenna characteristics at VHF and UHF," ITU, Recommendation ITU-R BT.1195-1, 2013.

[58] Teracom, "Dependence of TFS gain with antenna height and type," DVB Technical Module, Tech. Rep. DVB TM-T20331, 2007.

[59] "Directivity and polarization discrimination of antennas in the reception of television broadcasting," ITU, Recommendation ITU-R BT.419-3.

[60] "Radiation pattern characteristics of UHF television receiving antennas," ITU, Tech. Rep. ITU-R BT.2138.

[61] M. Waddell, "TVWS Opportunities. Evaluating Coexistence Parameters," in *3rd IEEE BTS GOLD Workshop. Broadcasting in the IP Era*, May 2014.

[62] A. W. Graham, N. C. Kirkman, and P. M. Paul, *The Mobile Environment Part 1: Propagation Mechanisms and Modelling.* John Wiley & Sons, Ltd, 2006, pp. 37–71. [Online]. Available: http://dx.doi.org/10.1002/9780470059128.ch4

[63] "Calculation of free-space attenuation," ITU, Recommendation ITU-R P.525-2, 1994.

[64] "Prediction methods for the terrestrial land mobile service in the VHF and UHF bands," ITU, Recommendation ITU-R P.529-3, 1999.

[65] "Method for point-to-area predictions for terrestrial services in the frequency range 30 MHz to 3 000 MHz," ITU, Recommendation ITU-R P.1546-5, 2013.

[66] G. Hufford, A. Longley, and W. Kissick, "A Guide to the Use of the ITS Irregular Terrain Model in the Area Prediction Mode," NTIA, Tech. Rep. 82-100, 2012.

[67] "Technical criteria of Digital Video Broadcasting Terrestrial (DVB-T) and Terrestrial Digital Audio Broadcasting (T-DAB) allotment planning," European Conference of Postal and Telecommunications Administrations (CEPT), Tech. Rep. 049, 2004.

[68] "Attenuation in vegetation," ITU, Recommendation ITU-R P.833-8, 2013.

[69] "Digital sound broadcasting to vehicular, portable and fixed receivers using terrestrial transmitters in the UHF/VHF bands," ITU, Recommendation ITU-R BS.1203-1, 1994.

[70] J. A. Green and I. R. Pullen, "Building penetration loss measurements for digital audio broadcasting (DAB)," in *IET Conference Proceedings*, 1995.

[71] D. Plets, W. Joseph, L. Verloock, E. Tanghe, L. Martens, E. Deventer, and H. Gauderis, "Influence of building type on penetration loss in uhf band for 100 buildings in flanders," in *Antennas and Propagation Society International Symposium, 2008. AP-S 2008. IEEE*, July 2008, pp. 1–4.

[72] "Propagation effects relating to terrestrial land mobile and broadcasting services in the VHF and UHF bands," ITU, Recommendation ITU-R P.1406-1, 2007.

[73] J. A. Arenas, U. Gil, D. Plets, P. Angueira, W. Joseph, and L. Martens, "Statistical analysis of field strength location variability for uhf multimedia broadband services," *IEEE Antennas and Wireless Propagation Letters*, vol. 11, pp. 34–36, 2012.

[74] J. A. Nelder and R. Mead, "A Simplex Method for Function Minimization," *Computer Journal*, 1965.

[75] J. J. Gimenez, D. Gomez-Barquero, C. Garcia-Pardo, and N. Cardona, "Time Frequency Slicing coverage gain modeling for future broadcasting networks," in *Telecommunications (ICT), 2014 21st International Conference on*, May 2014, pp. 181–185.

[76] M. Rezaei, I. Bouazizi, and M. Gabbouj, "Statistical Time-Frequency Multiplexing of HD Video Traffic in DVB-T2," *International Journal of Digital Multimedia Broadcasting*, vol. 2009, p. 12, 2009.

[77] J. J. Gimenez, E. Stare, S. Bergsmark, and D. Gomez-Barquero, "Advanced network planning for time frequency slicing (tfs) toward enhanced efficiency of the next-generation terrestrial broadcast networks," *IEEE Transactions on Broadcasting*, vol. 61, no. 2, June 2015.

[78] J. Zander, S.-L. Kim, M. Almgren, and O. Queseth, *Radio Resource Management for Wireless Networks*. Norwood, MA, USA: Artech House, Inc., 2001.

[79] R. Vaughan, "Polarization diversity in mobile communications," *IEEE Transactions on Vehicular Technology*, vol. 39, no. 3, pp. 177–186, Aug 1990.

[80] "Benefits and Limitations of Single Frequency Networks (SFN) for DTT," EBU, Recommendation Tech Report 016, 2012.

[81] R. Brugger and D. Hemingway, "OFDM Receivers. Impact on Coverage of Inter-Symbol Interference and FFT Window Positioning," EBU, Tech. Rep. Jul, 2003.

[82] "SFN frequency planning and network implementation with regard to T-DAB and DVB-T," EBU, Recommendation Tech Report 024, 2013.

[83] "Report from ad-hoc group B/CAI-FM24 to B/MDT & FM PT24 on spectrum requirements for DVB-T implementation," European Broadcasting Union, Tech. Rep. 023, Oct 2013.

[84] D. Plets, W. Joseph, P. Angueira, J. A. Arenas, L. Verloock, and L. Martens, "On the Methodology for Calculating SFN Gain in Digital Broadcast Systems," *IEEE Transactions on Broadcasting*, vol. 56, no. 3, pp. 331–339, Sept 2010.

[85] C. Tunc, A. Altintas, and V. Ertürk, "Examination of existent propagation models over large inhomogeneous terrain profiles using fast integral equation solution," *IEEE Transactions on Antennas and Propagation*, vol. 53, no. 9, pp. 3080–3083, Sept 2005.

[86] P. Siebert, T. Van Caenegem, and M. Wagner, "Analysis and Improvements of Zapping Times in IPTV Systems," *IEEE Transactions on Broadcasting*, vol. 55, no. 2, pp. 407–418, June 2009.

[87] O. Jeon, R. Fox, and B. Myers, "Analog AGC Circuitry for a CMOS WLAN Receiver," *IEEE Journal of Solid-State Circuits*, vol. 41, no. 10, pp. 2291–2300, Oct 2006.

[88] J. Balakrishnan, A. Batra, and A. Dabak, "A multi-band OFDM system for UWB communication," in *Ultra Wideband Systems and Technologies, 2003 IEEE Conference on*, Nov 2003, pp. 354–358.

[89] D. Landstrom, S. Wilson, J.-J. van de Beek, P. Odling, and P. Borjesson, "Symbol time offset estimation in coherent OFDM systems," *IEEE Transactions on Communications*, vol. 50, no. 4, pp. 545–549, Apr 2002.

[90] Z. Y. Choi and Y. H. Lee, "Frame synchronization in the presence of frequency offset," *IEEE Transactions on Communications*, vol. 50, no. 7, pp. 1062–1065, Jul 2002.

[91] B. Park, H. Cheon, C. Kang, and D. Hong, "A novel timing estimation method for OFDM systems," *IEEE Communications Letters*, vol. 7, no. 5, pp. 239–241, May 2003.

[92] B. Chen, "Maximum likelihood estimation of OFDM carrier frequency offset," *IEEE Signal Processing Letters*, vol. 9, no. 4, pp. 123–126, April 2002.

[93] P. Ciblat and E. Serpedin, "A fine blind frequency offset estimator for OFDM/OQAM systems," *IEEE Transactions on Signal Processing*, vol. 52, no. 1, pp. 291–296, Jan 2004.

[94] H. Minn, V. Bhargava, and K. Letaief, "A robust timing and frequency synchronization for OFDM systems," *IEEE Transactions on Wireless Communications*, vol. 2, no. 4, pp. 822–839, July 2003.

[95] G. Santella, "A frequency and symbol synchronization system for OFDM signals: architecture and simulation results," *IEEE Transactions on Vehicular Technology*, vol. 49, no. 1, pp. 254–275, Jan 2000.

[96] K. Shi and E. Serpedin, "Coarse frame and carrier synchronization of OFDM systems: a new metric and comparison," *IEEE Transactions on Wireless Communications*, vol. 3, no. 4, pp. 1271–1284, July 2004.

[97] J.-J. van de Beek, M. Sandell, and P. Borjesson, "ML estimation of time and frequency offset in OFDM systems," *IEEE Transactions on Signal Processing*, vol. 45, no. 7, pp. 1800–1805, Jul 1997.

[98] M.-H. Hsieh and C.-H. Wei, "A low-complexity frame synchronization and frequency offset compensation scheme for OFDM systems over fading channels," *IEEE Transactions on Vehicular Technology*, vol. 48, no. 5, pp. 1596–1609, Sep 1999.

[99] B. Park, H. Cheon, E. Ko, C. Kang, and D. Hong, "A blind OFDM synchronization algorithm based on cyclic correlation," *IEEE Signal Processing Letters*, vol. 11, no. 2, pp. 83–85, Feb 2004.

[100] H. Bolcskei, "Blind estimation of symbol timing and carrier frequency offset in wireless OFDM systems," *IEEE Transactions on Communications*, vol. 49, no. 6, pp. 988–999, Jun 2001.

[101] F. Gini and G. Giannakis, "Frequency offset and symbol timing recovery in flat-fading channels: a cyclostationary approach," *IEEE Transactions on Communications*, vol. 46, no. 3, pp. 400–411, Mar 1998.

[102] E. Machet, "Plenary Session 2: Regulatory and Licensing Models for DTT Summary of the answers to the questionnaire," in *32nd EPRA Meeting, Belgrade*, 2010.

[103] D. Vargas, D. Gozalvez, D. Gomez-Barquero, and N. Cardona, "MIMO for DVB-NGH, the next generation mobile TV broadcasting," *IEEE Communications Magazine*, vol. 51, no. 7, pp. 130–137, 2013.

[104] J. Montalban, "Solutions for New Terrestrial Broadcasting Systems Offring Stationary and Mobile Services Simultaneously," Ph.D. dissertation, Universidad del Pais Vasco/Euskal Herriko Unibertsitatea, 2014.

[105] D. Gomez-Barquero, "Cost efficient provisioning of mass mobile multimedia services in hybrid cellular and broadcasting systems," Ph.D. dissertation, Universitat Politècnica de València, 2009.

[106] L. Shi, E. Obregon, K. W. Sung, J. Zander, and J. Bostrom, "Cell TV. On the Benefit of TV Distribution Over Cellular Networks: A Case Study," *IEEE Transactions on Broadcasting*, vol. 60, no. 1, pp. 73–84, March 2014.

[107] S. R. Saunders and A. Aragon Zavala, *Antennas and Propagation for Wireless Communication Systems*, 2nd ed. New York, NY, USA: John Wiley & Sons, Inc., 2007.

[108] R. Fraile, J. F. Monserrat, J. Gozalvez, and N. Cardona, "Mobile radio bi-dimensional large-scale fading modelling with site-to-site cross-correlation," *European Transactions on Telecommunications*, vol. 19, no. 1, pp. 101–106, 2008.

[109] M. Hata, "Empirical formula for propagation loss in land mobile radio services," *IEEE Transactions on Vehicular Technology*, vol. 29, no. 3, pp. 317–325, Aug 1980.

[110] Y. Okumura, E. Ohmori, T. Kawano, and K. Fukuda, "Field strength and its variability in the vhf and uhf land mobile radio service," *Rev. Elec. Commun. Lab.*, vol. 16, no. 9, pp. 825–873, 1968.

[111] "Digital Mobile Radio: Towards Future Generation Systems," Final Report of the COST 231 Project, Tech. Rep., 1998.

[112] "VHF and UHF propagation curves for the frequency range from 30 MHz to 1 000 MHz. Broadcasting services," ITU, Recommendation ITU-R P.370-7, 1995.

[113] C. Perez-Vega and J. M. Zamanillo, "Path-loss model for broadcasting applications and outdoor communication systems in the vhf and uhf bands," *IEEE Transactions on Broadcasting*, vol. 48, no. 2, pp. 91–96, Jun 2002.

[114] "A path-specific propagation prediction method for point-to-area terrestrial services in the VHF and UHF bands," ITU, Recommendation ITU-R P.1812-3, 2013.